Development of Diethylamine Modified Electrode for the Determination of Paracetamol, Tramadol and Uric acid

by

Bulbul Chowdhury

A thesis submitted in partial fulfillment of the requirements for the degree of
Master of Science in Chemistry

Khulna University of Engineering & Technology
Khulna 9203, Bangladesh.

March 2018

Declaration

This is to certify that the thesis work entitled “Development of Diethylamine Modified Electrode for the Determination of Paracetamol, Tramadol and Uric acid” has been carried out by Bulbul Chowdhury in the Department of Chemistry, Khulna University of Engineering & Technology, Khulna, Bangladesh. The above thesis work has not been submitted anywhere for the award of any degree or diploma.

Signature of Supervisor

Signature of Candidate

Acknowledgements

The author is extremely indebted to the Almightily Allah for the successful completion of the research work and the preparation of this dissertation.

The author expresses his deepest sense of gratitude and indebtedness to his respective and honorable supervisor **Dr. Md. Abdul Motin**, Professor, Department of Chemistry, Khulna University of Engineering & Technology, Khulna for providing me the opportunity of working under his kind supervision. He had helped me at each and every point of the thesis work with his dedication, comments, suggestions and guidance which put me on the right path to fulfill the requirement, without which this situation was impossible to overcome. I learnt a lot of things from him, not only the academic knowledge, but also the way of research. This will be precious wealth in all my future academic life. Our communication is always flexible and efficient. He also friendly supported me a lot in my daily life which I am truly comprehended.

The author also expresses his deepest sense of gratitude to his respective and honorable teacher **Dr. Mohammad Hasan Morshed**, Professor and Head, Department of Chemistry, Khulna University of Engineering & Technology, Khulna for cooperation of successful completion of the research work.

Again the author bestows thanks to his respective teacher **Md. Abdul Hafiz Mia**, Assistant Professor, Department of Chemistry, Khulna University of Engineering & Technology, Khulna for his lucid cooperation and necessary advice during the period of study.

The author feels proud to express his sincere appreciation and indebtedness to his parents, family members who always blessed, inspired and sacrificed a lot in the long process of building his academic career which can never be repaid.

Bulbul Chowdhury

Abstract

Paracetamol (PA) and Tramadol (TD) are very important drugs for the treatment of common diseases such as cold, fever, headache etc. They are co-exist in some tablets. Uric acid (UA) is the primary end product of purine metabolism. UA also exists in biological fluids such as blood and urine. A modified electrode has been developed using diethylamine (DEA) as a trifunctional electrochemical sensor for simultaneous detection of UA, PA and TD. Cyclic voltammetry (CV), differential pulse voltammetry (DPV) and UV-Vis. spectroscopy were used as detection techniques.

In this work, glassy carbon (GC), gold (Au) and platinum (Pt) electrodes were used as the working electrode. The electrodes were modified with DEA by applying continuous potential cycle for 15 scans at a range of -0.5 to 1.5 V. Then the electrodes were activated in phosphate buffer solution (PBS) (pH 7) by applying continuous potential cycle for 10 scans at a range of -0.5 V to 1.5 V. A ternary solution of UA, PA and TD was prepared and the CV and DPV were taken at the modified (GC, Au and Pt) electrodes. It is seen that the performance of modified GC electrode is better than the modified Au and Pt electrodes.

The influence of pH has been studied by varying pH from 3 to 9. The detection is mostly favorable at pH 7. The effect of different scan rates has been discussed and the variation of peak current plotted against square root of scan rate. The peak currents increase proportionally with increasing square root of scan rates indicates the electrochemical processes are controlled by diffusion process.

The effects of bare and modified GC electrode on single, binary and ternary solution of UA, PA and TD have been studied. CVs of the single solution of UA, PA and TD at bare GC electrode shows the oxidation peaks at 0.34V, 0.46V and 0.94V respectively. But at modified GC electrode it shows the oxidation peaks at 0.27V, 0.38V and 0.81V. At bare GC electrode, the ternary mixture of UA, PA and TD shows two oxidation peaks at 0.41V and 0.93V. But DEA modified GC electrode shows three separated and well defined oxidation peaks at 0.27V, 0.38V and 0.81V. The peak intensity of DEA modified

electrodes are higher compared with the bare GC electrode. Similar behavior have been observed in the DPV technique.

Quantitative analysis of UA, PA and TD have been carried out by DPV using DEA modified GC electrode in a single, binary and ternary solution. In every case, the peak currents of UA, PA and TD increase linearly with increasing their concentrations over the range of 0.5-2.5 mM. The DEA modified GC electrode shows good selectivity and strong anti-interference activity for the determination of UA, PA and TD in binary and ternary mixture with excellent results. The limit of detection (LoD) has been calculated by signal-to-noise (S/N=3) ratio. In simultaneous detection, the LoD for UA, PA and TD are 1.95 μmol L^{-1}, 1.45 μmol L^{-1} and 1.26 μmol L^{-1} respectively at DEA modified GC electrode. The sensitivity of UA, PA and TD are 52.08 μA/mM/cm^2, 62.25 μA/mM/cm^2 and 33.67 μA/mM/cm^2 respectively at DEA modified GC electrode.

DEA modified GC electrode has been successfully used for the quantitative determination of UA, PA and TD in some commercial tablets of different pharmaceutical companies of Bangladesh and biological fluids. The results have been valided by UV-Vis spectroscopic method and pathological report. The amount of PA and TD in some well-established pharmaceutical (Beximco, ACI, Square, Incepta, ACME etc) tablet samples have been found approximately same with compared to the labeled value. But the amount of PA, TD have been found less with compared to the labeled value in the tablets of some pharmaceutical companies (Opsonin, Renata, General, etc). Simultaneous detection of UA, PA and TD is not possible by UV-Vis spectroscopic method due to their very close absorbance maxima. The single determination of PA, TD and UA in tablet and blood samples by DEA modified GC electrode is very consistent with the determination of PA, TD and UA by UV-Vis spectroscopic method and pathological method in the same samples. Thus it is suggested that the DEA modified sensor may be used in the pharmaceutical industry and pathology for the determination of PA, TD and UA.

Contents

LIST OF TABLES

LIST OF FIGURES

CHAPTER I

Introduction

1.1 General

Electroanalytical chemistry, also known as electroanalysis, lies at the interface between analytical science and electrochemistry. It is concerned with the development, characterization and application of chemical analysis methods employing electrochemical phenomena. It has major significance in modern analytical science, enabling measurements of the smallest chemical species, right up to the macromolecules of importance in modern biology. The history of electrochemical sensors starts basically with the development of the glass electrode [1]. It is preferable to consider electroanalytical chemistry as that area of analytical chemistry and electrochemistry in which the electrode is used as a probe, to measure something that directly or indirectly involves the electrode [2].

Electroanalytical techniques are concerned with the interplay between electricity & chemistry, namely the measurement of electrical quantities such as current, potential or charge and their relationship to chemical parameters such as concentration [3-5]. These methods are a class of techniques in analytical chemistry which study an analyte by measuring the potential (volts) and/or current (amperes) in an electrochemical cell containing the analyte. These methods can be broken down into several categories depending on which aspects of the cell are controlled and which are measured. The three main categories are potentiometry (the difference in electrode potentials is measured), coulometry (the cell's current is measured over time), and voltammetry (the cell's current is measured while actively altering the cell's potential).

The use of electrical measurements for analytical purposes has found large range of applications including environmental monitoring, industrial quality control & biomedical analysis. In particular, electrochemical sensors and detectors are very attractive in the fields

of environmental conservation and industrial analysis. A typical chemical sensor is a device that transforms chemical information in a selective and reversible way, ranging from the concentration of a specific sample component to total composition analysis, into an analytically useful signal. The interest in electrochemical sensors continues unabated today, stimulated by the wide range of potential applications. Their impact is most clearly illustrated in the widespread use of electrochemical sensors seen in daily life, where they continue to meet the expanding need for rapid, simple and economic methods of determination of numerous analytes [6-8]. Electrochemical sensors have attractive qualities, which can boast the following advantages:

1) low detection and determination limits,
2) high sensitivity,
3) relative simplicity and rapidity,
4) wide spectrum of the analyte (especially drug compounds),
5) insignificant effect of the matrix (from endogenous substances in biological media or from excipients in pharmaceutical dosage forms),
6) low cost of equipment.

Recent advances in electrochemical sensor technology will certainly expand the scope of these devices towards a wide range of organic and inorganic contaminants and will facilitate their role in field analysis. These advances include the introduction of modified or ultra-microelectrodes, the design of highly selective chemical or biological recognition layers, of molecular devices or sensor arrays, and developments in the areas of micro fabrication, computerized instrumentation and flow detectors [9-11].

1.2 Chemically modified electrodes

Chemically modified electrodes (CMEs) comprise a relatively modem approach to electrode systems a wide spectrum of basic electrochemical investigations, including the relationship of heterogeneous electron transfer and chemical reactivity to electrode surface chemistry, electrostatic phenomena at electrode surfaces, and electron and ionic transport phenomena in polymers, and the design of electrochemical devices and systems for applications in chemical sensing, energy conversion and storage, molecular electronics, electrochromic displays, corrosion protection, and electro-organic syntheses. Compared

with other electrode concepts in electrochemistry, the distinguishing feature of a CME is that a generally quite thin film (from a molecular monolayer to perhaps a few micrometers-thick multilayer) of a selected chemical is bonded to or coated on the electrode surface to endow the electrode with the chemical, electrochemical, optical, electrical, transport, and other desirable properties of the film in a rational, chemically designed manner [12].

The range of electrode surface properties includes, but is more diverse than, that of ion-selective electrodes (ISEs) which also involve, in their highest forms, rational design of the phase-boundary, partition and transport properties of membranes on or between electrodes. While CMEs can operate both voltammetrically and potentiometrically, they are generally used voltammetrically, a redox (electron transfer) reaction being the basis of experimental measurement or study, whereas ISEs are generally used in potentiometric formats where a phase-boundary potential (interfacial potential difference) is the measured quantity [13]. Gas-sensing electrodes (e.g., for CO_2, NH_3, NOx) are also potentiometrically based [14] although the oxygen electrode, which functions amperometrically, is an exception [15]. Chemically sensitive field effect transistors (CHEMFETs) are basically non-faradaic electrode systems in which electric field variations in the semiconductor gate region control the magnitude of the source drain current [16].

1.3 General methods of modification of electrodes

The concept of chemically modified electrodes (CMEs) is one of the exciting developments in the field of electroanalytical chemistry. Many different strategies have been employed for the modification of the electrode surface. The motivations behind the modifications of the electrode surface are: (i) improved electrocatalysis, (ii) freedom from surface fouling and (iii) prevention of undesirable reactions competing kinetically with the desired electrode process [17]. The increasing demand for it has led to the development of a rapid, simple and non-separation method for the simultaneous determination of compounds where the CMEs have emerged as an efficient and versatile approach, and have attracted considerable attention over the past decades due to its advantages in terms of reduced costs, automatic and fast analysis, high sensitivity and selectivity [18-20]. There are numerous techniques that may be used to modify electrode surfaces. Among various CMEs, polymer-modified electrodes (PMEs) are promising approach to determination. Some modification processes are-

Covalent Bonding: This method employs a linking agent (e.g. an organosilane) to covalently attach one of several monomolecular layers of the chemical modifier to the electrode surface [21].

Drop-Dry Coating (or solvent evaporation): A few drops of the polymer, modifier or catalyst solution are dropped onto the electrode surface and left to stand to allow the solvent to dry out [22].

Dry-Dip Coating: The electrode is immersed in a solution of the polymer, modifier or catalyst for a period sufficient for spontaneous film formation to occur by adsorption. The electrode is then removed from solution and the solvent is allowed to dry out [23].

Composite: The chemical modifier is simply mixed with an electrode matrix material, as in the case of an electron-transfer mediator (electrocatalyst) combined with the carbon particles (plus binder) of a carbon paste electrode. Alternatively, intercalation matrices such as certain Langmuir-Blodgett films, zeolites, clays and molecular sieves can be used to contain the modifier [24].

Spin-Coating (or Spin-Casting): it is also called spin casting; a droplet of a dilute solution of the polymer is applied to the surface of a rotating electrode. Excess solution is spun off the surface and the remaining thin polymer film is allowed to dry. Multiple layers are applied in the same way until the desired thickness is obtained. This procedure typically produces pinhole-free thin films for example; oxide xerogel film electrodes prepared by spin-coating a viscous gel on an indium oxide substrate [25].

Electrodeposition: In this technique the electrode is immersed in a concentrated solution ($\sim 10^{-3}$ $molL^{-1}$) of the polymer, modifier or catalyst followed by repetitive voltammetry scans. The first and second scans are similar, subsequent scans decrease with the peak current. For example, electrochemical deposition of poly (o-toluidine) on activated carbon fiber [26].

Electropolymerization: A solution of monomer is oxidized or reduced to an activated form that polymerizes to form a polymer film directly on the electrode surface. This

procedure results in few pinholes since polymerization would be accentuated at exposed (pinhole) sites at the electrode surface. Unless the polymer film itself is redox active, electrode passivation occurs and further film growth is prevented.

In this technique the electrode is immersed in a polymer, modifier or catalyst solution and layers of the electropolimerized material builds on the electrode surface. Generally, the peak current increases with each voltammetry scan such that there is a noticeable difference between the first and final scans indicating the presence of the polymerized material. For example, electropolymerization of aniline on platinum electrode perturbations.

1.4 Sensor

The development of chemical and biological sensors is currently one of the most active areas of analytical research. Sensors are small devices that incorporate a recognition element with a signal transducer. Such devices can be used for direct measurement of the analyte in the sample matrix [27]. Chemical sensors have been widely used in applications such as critical care, safety, industrial hygiene, process controls, product quality controls, human comfort controls, emissions monitoring, automotive, clinical diagnostics, home safety alarms, and, more recently, homeland security. In these applications, chemical sensors have resulted in both economic and social benefits. A useful definition for a chemical sensor is ‘‘a small device that as the result of a chemical interaction or process between the analyte and the sensor device, transforms chemical or biochemical information of a quantitative or qualitative type into an analytically useful signal” [28]. The biosensors can be defined in terms of sensing aspects, where these sensors can sense biochemical compounds such as biological proteins, nucleotides and even tissues.

1.5 Types of chemical sensors

Chemical sensors are categorized into the following groups according to the transducer type.

1.5.1 Optical sensor

It relies on an optical transducer for signal measurement. In optical sensors there is a spectroscopic measurement associated with the chemical reaction. Normally it involve a two phase system in which the reagents are immobilized in or on a solid substrate such as a membrane which changes color in the presence of a solution of the analyte. Optical sensors are often referred to as 'optodes' and the use of optical fibres is a common feature. Absorbance, reflectance and luminescence measurements are used in the different types of optical sensors.

1.5.2 Mass sensitive sensor

These make use of the piezoelectric effect and include devices such as the surface acoustic wave (SAW) sensor and are particularly useful as gas sensors. They rely on a change in mass on the surface of an oscillating crystal which shifts the frequency of oscillation. The extent of the frequency shift is a measure of the amount of material adsorbed on the surface.

1.5.3 Heat sensitive sensor

Chemical reactions produce heat and the quantity of the heat produced depends on the amounts of the reactants. Thus, the measurement of heat of reaction can be related to the amount of a particular reactant. Measurements of the heats of reaction form the basis of the field of calorimetry and this has provided a class of chemical sensors which has gained considerable importance. Calorimetric sensors, like all other chemical sensors, have a region where a chemical reaction takes place and a transducer which responds to heat.

There are three classes of calorimetric sensors which are of particular importance. The first uses a temperature probe such as a thermistor as the transducer to sense the heat involved in a reaction on its surface. The second class of calorimetric sensors is referred to as catalytic sensors and is used for sensing flammable gases. The third class is called thermal conductivity sensors and this sense a change in the thermal conductivity of the atmosphere

in the presence of a gas. This is the basis of the thermal conductivity detector which has been used for many years in gas chromatography [29].

1.5.4 Electrochemical sensor

Electrochemical sensors, in which an electrode is used as the transducer element, represent an important subclass of chemical sensors. Electrochemical sensors are essentially an electrochemical cell which employs a two or three electrode arrangement. Electrochemical sensor measurement can be made at steady-state or transient. The applied current or potential for electrochemical sensors may vary according to the mode of operation, and the selection of the mode is often intended to enhance the sensitivity and selectivity of a particular sensor.

Depending on the exact mode of signal transduction, electrochemical sensors can use a range of modes of detection such as potentiometric, voltammetric and conductimetric. Each principle requires a specific design of the electrochemical cell. Potentiometric sensors are very attractive for field operations because of their high selectivity, simplicity and low cost. They are, however, less sensitive and often slower than their voltammetric counterparts. Examples of transduction techniques include:

- Potentiometric – The measurement of the potential at zero current. The potential is proportional to the logarithm of the concentration of the substance being determined.

- Voltammetric – Increasing or decrease the potential that is applied to a cell until the oxidation or reduction of the analyte occurs. This generates a rise in current that is proportional to the concentration of the electroactive potential. Once the desired stable oxidation/reduction potential is known, stepping the potential directly to that value and observing the current is known as amperometry.

- Conductiometric – Observing changes in electrical conductivity of the solution [30].

The selection and development of an active material is a challenge. The active sensing materials may be of any kind as whichever acts as a catalyst for sensing a particular analyte or a set of analytes. The recent development in the modified electrode sensors has paved the way for large number of new materials and devices of desirable properties which have useful functions for numerous electrochemical sensor and biosensor applications [31].

1.6 Determination of compounds by modified electrode sensor

The determination of analytes is an interesting subject in electroanalytical chemistry. The increasing demand for it has led to the development of a rapid, simple and non-separation method for the determination of analytes where the chemically modified electrodes (CMEs) have emerged as an efficient and versatile approach and have attracted considerable attention over the past decades due to its advantages in terms of reduced costs, automatic and fast analysis, high sensitivity and selectivity [32-33]. This type of chemically modified electrode sensors are well known for the measurement of multiple analytes in a mixture.

In this work, a novel modified electrode sensor is developed using DEA (Diethylamine) as a trifunctional electrochemical sensor for the determination of Paracetamol (PA), Tramadol (TD) and Uric acid (UA). These compounds (PA and UA) go through redox reaction on the electrode surface within the same potential range which causes an overlapping oxidation peak at bare electrode. The electro activeness of such compounds depends upon the pH of the medium, nature of the electrode and active moiety present in their structures.

1.7 Prospect of Modified Electrode Sensor for the Determination of PA, TD and UA

PA, TD and UA have a basic structures that might be electrochemically oxidized at a gold, platinum or carbon electrodes [34-36]. But so many difficulties were existed to simultaneously determine PA, TD and UA. The major difficulty is that the voltammetric peaks corresponding to oxidation/reduction of PA and UA are, in many cases, highly overlapped [37]. At bare Glassy Carbon and other available electrodes PA, TD and UA are detectable quantitatively if they are investigated individually. But when investigated simultaneously one in presence of other, in spite of giving corresponding peaks they give a

broad overlapped peak resulting from all the drugs. This is why modification of electrode is necessary to get corresponding, non-overlapped peaks. Recently, an enormous amount of research has been devoted to the development of new chemically modified electrodes for monitoring PA, TD and UA. Among various chemically modified electrodes, polymer-modified electrodes (PMEs) are promising approach to detect PA, TD and UA. Polymer-modified electrodes prepared by electropolymerization have received extensive interest in the detection of analytes because of their selectivity, sensitivity and homogeneity in electrochemical deposition, strong adherence to electrode surface and chemical stability of the films. Selectivity of PMEs as a sensor can be attained by different mechanisms such as size exclusion, ion exchange, hydrophobicity interaction and electrostatic interaction [38-41].

1.7.1 Paracetamol

Paracetamol (PA) known as acetaminophen or N-acetyl-p-amino or N-(4-hydroxyphenyl) phenol is a mild analgesic, antipyretic agent and also a non-steroidal anti-inflammatory drug [42]. Paracetamol is part of the class of drugs known as "aniline analgesics"; it is the only such drug still in use today [43]. It is not considered as nonsteroidal anti-inflammatory drugs (NSAIDs) because it does not exhibit significant anti-inflammatory activity (it is a weak Cyclooxygenase (COX) inhibitor) [44-45]. This is despite the evidence that paracetamol and NSAIDs have some similar pharmacological activity [46].

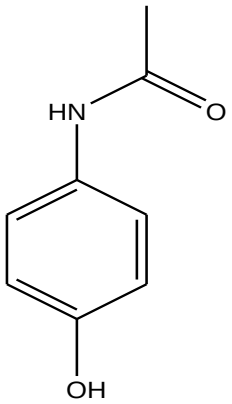

Figure 1.3: Paracetamol

1.7.2 Uses of Paracetamol

Paracetamol is a medicine used to treat pain and fever. It is typically used for mild to moderate pain. There is poor evidence for fever relief in children. It is often sold in combination with other ingredients such as in many cold medications [47-48]. In combination with opioid pain medication, paracetamol is used for more severe pain such as cancer pain and after surgery. It is typically used either by mouth or rectally but is also available intravenously [49].

1.7.3 Uric Acid (UA)

Uric acid is a heterocyclic compound of carbon, nitrogen, oxygen, and hydrogen with the formula $C_5H_4N_4O_3$. It forms ions and salts known as urates and acid urates, such as ammonium acid urate. UA is a diprotic acid with pK_{a1} = 5.4 and pK_{a2} = 10.3. It is a product of the metabolic breakdown of purine nucleotides. The water solubility of UA and its alkali metal and alkaline earth salts is low. In humans and higher primates, uric acid is the final oxidation (breakdown) product of purine metabolism and is excreted in urine. In humans, about 70% of daily uric acid disposal occurs via the kidneys, and in 5–25% of humans, impaired renal (kidney) excretion leads to hyperuricemia.

Extreme abnormalities of UA levels indicate symptoms of several diseases, such as gout, hyperuricemia, leukemia, pneumonia, and Lesch-Nyhan [50-51].

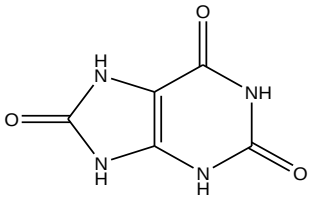

Figure 1.3: Uric Acid

1.7.4 Uses of Uric Acid

Uric acid may be a marker of oxidative stress, and may have a potential therapeutic role as an antioxidant. On the other hand, like other strong reducing substances such as ascorbate, uric acid can also act as a pro oxidant. Thus, it is unclear whether elevated levels of uric

acid in diseases associated with oxidative stress such as stroke and atherosclerosis are a protective response or a primary cause. For example, some researchers propose hyperuricemia-induced oxidative stress is a cause of metabolic syndrome. On the other hand, plasma uric acid levels correlate with longevity in primates and other mammals. This is presumably a function of urate's antioxidant properties [52- 53].

1.7.5 Tramadol (TD)

Tramadol, (1R,2R)-2-[(dimethylamino)methyl]-1-(3-methoxyphenyl)cyclohexanol, is a synthetic monoamine uptake inhibitor and centrally acting analgesic, used for treating moderate to severe pain and it appears to have actions at the μ-opioid receptor as well as the noradrenergic and serotonergic systems[54].

Tramadol (TD) is a centrally acting analgesic that was first introduced in Germany in 1977. Today it has become the most prescribed opioid worldwide [55]. It is generally said to be devoid of many of the serious adverse effects of traditional opioid receptor agonists such as the risk for respiratory depression [56] and drug dependence [57]. Based on this, in contrast to other opioids, the abuse potential of tramadol is considered to be either low or absent [58]. Hence, tramadol is the only clinically available non-scheduled opioid [59] however recently reported results of post-marketing surveillance and case reports [60] have shown that tramadol abuse and tramadol related fatalities have been noted. Its overall analgesic efficacy is comparable to that achieved using equianalgesic doses of morphine or alfentanil.

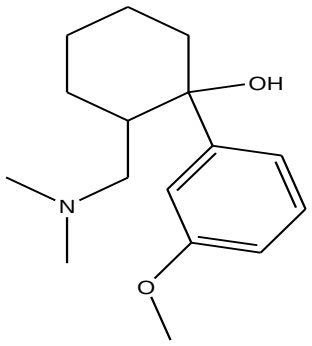

Figure 1.4: Tramadol

1.7.6 Uses Tramadol

Tramadol a medicine used for treating moderate to severe pain and it appears to have actions at the μ-opioid receptor as well as the noradrenergic and serotonergic systems [61]. Considering complementary mechanisms of action of two anal- gesics, combining these drugs as a fixed tablet, tramadol 37.5 mg, enhance the analgesic effectiveness, reduce the side effects and also increase the drug compliance and provide effective analgesia in patients with moderate to severe acute pain and those with chronic painful conditions characterized by intermittent exacerbations of pain [62-64].

1.7.7 Diethylamine (DEA)

Diethylamine is an organic compound with the formula $(CH_3CH_2)_2NH$. It is a secondary amine. It is a flammable, weakly alkaline liquid that is miscible with most solvents. It is a colorless liquid, but commercial samples often appear brown due to impurities. It has a strong ammonia-like odor.

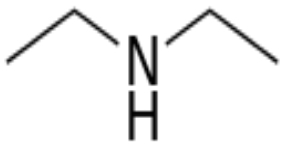

Figure 1.4: Diethylamine

Diethylamine is manufactured by the alumina-catalyzed reaction of ethanol and ammonia. It is obtained together with ethylamine and triethylamine. It is used in the production of corrosion inhibitor N, N-diethylaminoethanol, by reaction with ethylene oxide. It is also a precursor to a wide variety of other commercial products. Diethylamine can be used in the production of LSD and therefore it is strictly monitored in the U.S. Diethylamine has low toxicity, but the vapor causes transient impairment of vision [65].

1.7.8 Uses Diethylamine

The applications of Diethylamine are varied. Diethylamine is used in the production of pesticides. It is used in a mixture for the production of DEET which goes into the repellents that are found readily in supermarkets for general use. It is also mixed with other chemicals to form Diethylaminoethanole, which is used mainly as a corrosion inhibitor in water treatment facilities as well as production of dyes, rubber, resins, and pharmaceuticals. Apart from the aforementioned, Diethylamine is also used in manufacture of basic chemicals and pharmaceuticals [66].

1.8 Electrochemistry as an analytical tool

Electrochemistry has become a powerful tool to study widely for solving the different problem in the arena of organic chemistry, biochemistry, material science, environmental science etc. Many natural and biochemical processes have redox nature. Their redox mechanisms can be easily established based on the experiment in voltammetry. For example, cyclic voltammetry is the most widely used modern electro-analytical method available for the mechanistic probing study of redox system.

1.9 Electrical double layer

Electroanalytical studies are centered on electrode, which is considered as a probe in the electrolyte. An electrode can only donate or accept electrons from a species that is present in a layer of solution that is immediately adjacent to the electrode. Thus, this layer may have a composition that differs significantly from that of the bulk of the solution. Let us consider the structure of the solution immediately adjacent to that electrode. Immediately after impressing the potential, there will be a momentary surge of current, which rapidly decays to zero if no reactive species is present at the surface of the electrode. This current is a charging current that creates an excess of negative charge at the surface of the two electrodes. As a consequence of ionic mobility, however, the layers of solution immediately adjacent to the electrodes acquire an opposing charge. This effect is illustrated in Figure 1.5. The surface of the metal electrode is shown as having an excess of positive charge as a consequence of an applied positive potential. The charged solution layer

consists of two parts: (1) a compact inner layer (d_0 to d_1), in which the potential decreases linearly with distance from the electrode surface and (2) a diffuse layer (d_1 to d_2), in which the decrease is exponential. This assemblage of charge at the electrode surface and in the solution adjacent to the surface is termed as electrical double layer.

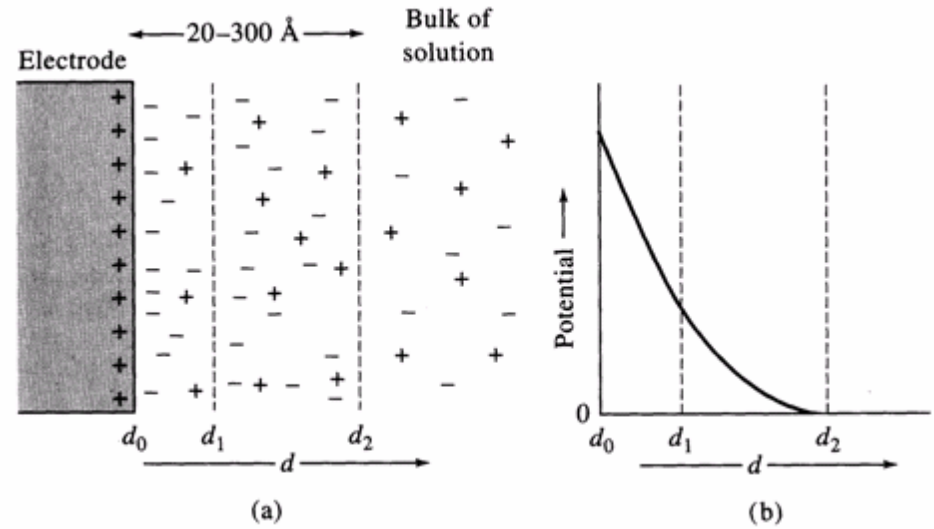

Figure 1.5: Electrical double layer formed at electrode surface as a result of an applied potential

1.10 Faradaic and nonfaradaic currents

Two types of processes can conduct currents across an electrode/solution interface. One involves a direct transfer of electrons via an oxidation reaction at one electrode and a reduction reaction at the other. Processes of this type are called faradaic processes because they are governed by Faraday's law, which states that the amount of chemical reaction at an electrode is proportional to the current; the resulting currents are called faradaic currents. Under some conditions a cell will exhibit a range of potentials where faradaic processes are precluded at one or both of the electrodes for thermodynamic or kinetic reasons. Here, conduction of continuous alternating currents can still take place. With such currents, reversal of the charge relationship occurs with each half cycle, as first negative and then positive ions are attracted alternately to the electrode surface. Electrical energy is consumed and converted to heat by friction associated with this ionic movement. Thus, each electrode surface behaves as one plate of a capacitor, the capacitance of which may be

large. The capacitive current increases with frequency and with electrode area; by controlling these variables, it is possible to arrange conditions such that essentially all the alternating current in a cell is carried across the electrode interface by this nonfaradaic process [67].

Current in voltammetric experiment is a measure of the rate of the electrode process. When an electrode is placed in an electrolyte solution, different processes may occur. Steps involved in an electrode reaction are (Figure 1.6**)**.

1) Mass transfer of species between bulk solution and the electrode surface.
2) Heterogeneous electron transfer at the electrode/solution interface.
3) Chemical reactions, either preceding or following electron transfer.
4) Surface reactions such as adsorption, desorption and electrodeposition-dissolution [68].

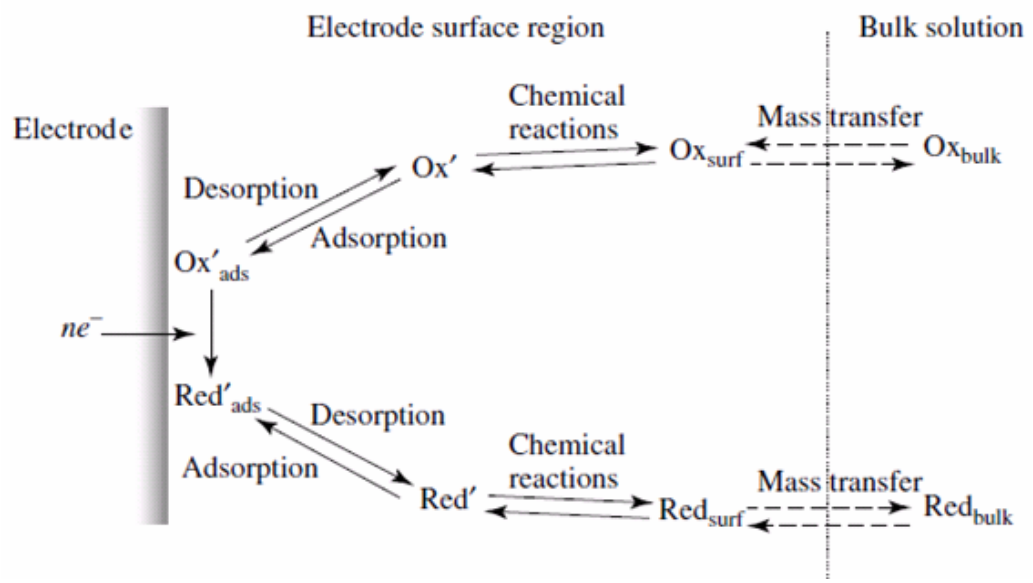

Figure 1.6: Typical steps involved in an electrode reaction

1.11 Mass transfer process in voltammetry

The movement of the electro-active substance through solution is referred as mass transfer at the electrode surface. In electrochemical systems, there are different types of mass transfer system by which a substance may be transferred to the electrode surface from bulk solution. Depended on the experimental conditions, any of these or more than one might be operating in a given experiment system.

A reacting species may be brought to an electrode surface by three types of mass transfer processes:

- Migration
- Diffusion
- Convection

1.11.1 Migration

Migration refers to movement of a charge particle in a potential field. It occurs by the movement of ions through a solution as a result of electrostatic attraction between the ions and the electrodes. In general, most electrochemical experiment it is unwanted but can be eliminated by the addition of a large excess of supporting electrolytes. In the electrolysis solution, ions will move towards the charged electrode that means cations to the cathode and anions to the anode. This motion of charged particle through solution, induced by the charges on the electrodes is called migration [69]. This charge movement constitutes a current. This current is called migration current. The fraction of the current carried by a given cation and anion is known as its transport number. The larger the number of different kinds of ions in a given solution, the smaller is the fraction of the total charge that is carried by a particular species. Electrolysis is carried out with a large excess of inert electrolyte in the solution so the current of electrons through the external circuit can be balanced by the passage of ions through the solution between the electrodes, and a minimal amount of the electroactive species will be transported by migration. Migration is the movement of charged species due to a potential gradient. In voltammetric experiments, migration is undesirable but can be eliminated by the addition of a large excess of supporting electrolytes in the electrolysis solution. The effect of migration is applied zero by a factor of fifty to hundred ions excess of an inert supporting electrolyte.

1.11.2 Diffusion

The movement of a substance through solution by random thermal motion is known as diffusion. Whereas a concentration gradient exists in a solution, that is the concentration of a substance, is not uniform throughout the solution. There is a driving force for diffusion of the substance from regions of high concentration to regions of lower concentration. In any

experiment in which the electrode potential is such that the electron transfer rate is very high, the region adjacent to the electrode surface will become depleted of the electro-active species, setting up a concentration in which this species will constantly be arriving at the electrode surface by the diffusion from points further away [70]. The one kind of mode of mass transfer is diffusion to an electrode surface in an electrochemical cell. The rate of diffusion is directly proportional to the concentration difference. When the potential is applied, the cations are reduced at the electrode surface and the concentration is decreased at the surface film. Hence a concentration gradient is produced. Finally, the result is that the rates of diffusion current become larger.

1.11.3 Convection

By mechanical way reactants can also be transferred to or from an electrode. Thus forced convection is the movement of a substance through solution by stirring or agitation. This will tend to decrease the thickness of the diffuse layer at an electrode surface and thus decrease concentration polarization. Natural convection resulting from temperature or density differences also contributes to the transport of species to and from the electrode [71]. At the same time a type of current is produced. This current is called convection current. Removing the stirring and heating can eliminate this current. Convection is a far more efficient means of mass transport than diffusion. These three kinds of mass transfer processes are shown in Figure 1.7.

In this research work, various electrochemical techniques such as cyclic voltammetry (CV), differential pulse voltammetry (DPV) along with UV-visible Spectrophotometry were used for the qualitative and quantitative determination of PA, TD and UA.

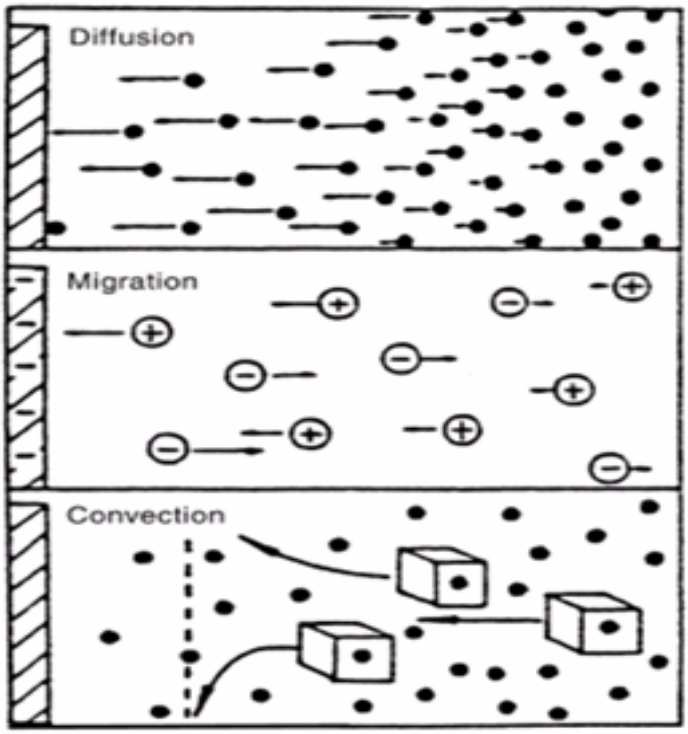

Figure 1.7: Modes of mass transfer

1.12 Objectives of the research work (Within 150 words):

The purposes of this research work are to develop electrochemically modified electrode for the detection of PA, TD and UA qualitatively and quantitatively. The specific objectives of this research work are-

i) To develop Diethylamine (DEA) modified GC, Au and Pt electrodes,

ii) To compare the behavior of PA, TD and UA at bare and DEA modified electrodes,

iii) To recognize the most favorable condition (such as pH and scan rate) for the separation of PA, TD and UA,

iv) To determine the quantity of PA and TD individually and simultaneously in tablet samples of some Bangladeshi industry and UA in known sample such as human urine and blood serum.

CHAPTER II

Literature Review

Many analytical techniques have been described for the simultaneous determination of PA, TD and PA, UA such as spectrophotometry, high-performance liquid chromatography and electrochemical methods. Among them, electrochemical method based on modified electrode sensor has attracted more attention for their high sensitivity, simplicity, reproducibility, on site monitoring and low cost.

Wang et al., 2008, constructed a glassy carbon electrode modified with hexacyanoferrate lanthanum (LaHCF) and was characterized by cyclic voltammetry (CV) and electrochemical impedance spectrum (EIS). The LaHCF modified glassy carbon electrode showed good catalytic character on uric acid (UA) and was used to detect uric acid and ascorbic acid (AA) simultaneously. The DPV peak currents increased linearly on the UA in the range of 2.0×10^{-7} to 1.0×10^{-4} mol/L with the detection limit (signal-to-noise ratio was 3) for UA 1.0×10^{-7} mol/L. The proposed method showed excellent selectivity and stability, and the determination of UA and AA simultaneously in urine was satisfactory [72].

Yang et al., 2009, synthesized a Polypyrrole (PPy) nanotubes by chemical oxidative polymerization of pyrrole within the pores of polycarbonate membrane using the technology of diffusion of solutes. An amperometric uric acid sensor based on PPy NEEs has been developed and used for determination of uric acid in human serum samples. The electrode can direct response to uric acid at potential of 0.60V vs. SCE with wide linear range of 1.52×10^{-6} to 1.54×10^{-3} M. The detection limit was 3.02×10^{-7} M. This sensor was used to determine uric acid in real serum samples. PPy NEEs is thought of as a good application in the foreground [73].

Sadikoglu et al., 2012, prepared a stable modified glassy carbon electrode based on poly (*p*-aminobenzene sulfonic acid) (*p*-ABSA) film by electrochemical polymerization technique in phosphate buffer solution (PBS) (pH 7.0) and its electrochemical behavior were studied by cyclic voltammetry (CV). The polymer film-modified electrode was used for the dermination of uric acid (UA). The modified glassy carbon electrode had an excellent response and specificity for the electrocatalytic oxidation of UA in PBS (pH 7.0). A linear calibration curve for DPV analysis was constructed in the uric acid concentration range 1×10^{-5} M to 1×10^{-4} M. Limit of detection (LOD) and limit of quantification (LOQ) at *p*-ABSA modified electrode were obtained as 1.125×10^{-6} M and 3.750×10^{-6} M, respectively. This electrode was used for UA determinations in human urine samples satisfactorily [74].

Babaei et al., 2011, constructed a modified electrode based on a multi-walled carbon nanotube-modified glassy carbon electrode (MWCNTs/GCE) for the sensitive simultaneous determination of paracetamol and tramadol in pharmaceutical preparations and biological fluids. The measurements were carried out by the application of differential pulse voltammetry (DPV), cyclic voltammetry (CV) and chronoamperometry (CA) methods. Application of the DPV method demonstrated that in phosphate buffer (pH 7.5) there was a linear relationship between the oxidation peak current and the concentration of PA over the range 0.5 µmol L^{-1} to 210 µmol L^{-1}. A similar linear correlation between oxidation peak current and concentration was observed for TD over the range of 2 µmol L^{-1} to 300 µmol L^{-1}. The analytical performance of this sensor has been evaluated for detection of PA and TD in human serum, human urine and some pharmaceutical preparations with satisfactory results [75].

Garrett et al., 2010, constructed a modified electrode based on Multiwalled Carbon Nanotube/Chitosan Composite for the determination of Paracetamol (PA) and Uric acid (UA). The measurements were carried out using differential pulse voltammetry (DPV), cyclic voltammetry (CV) and chronoamperometry (CA). DPV measurements showed a linear relationship between oxidation peak current and concentration of PA and UA in phosphate buffer (pH 7) over the concentration range 2 mM to 250 mM, and 10 mM to 400 mM, respectively. The analytical performance of this sensor has been evaluated for detection of PA and UA in human serum and human urine with satisfactory results [76].

Shahrokhian et al., 2011, for the determination of paracetamol in the presence of Codeine and Ascorbic acid using MWCNT/Hydroquinone Sulfonic Acid-overoxidized poly pyrole modified Glassy carbon electrode was prepared. In comparison to the bare glassy carbon electrode, a considerable shift in the peak potential together with an increase in the peak current was observed for AC on the surface of oppy/MWCNT/GCE, which can be related to the enlarged microscopic surface area of the electrode. The effect of the experimental conditions on the electrode response, such as types of counter ion, pyrole and counter ion concentration, potential and number of cycles in the polymerization procedure, amount of MWCNT, and the pH, were investigated. Under the optimized conditions, the calibration curve was obtained over two concentration ranges of 2×10^{-7}–6×10^{-6} M and 4×10^{-5} – 1×10^{-4}M of AC with a linear correlation coefficient (R_2) of 0.9959 and 0.9947 respectively. The estimated detection limit (3σ) for AC was obtained as 5×10^{-8} M. The developed method was successfully applied to analyze the pharmaceutical preparations of AC, and a recovery of 95% with a relative standard deviation of 0.98% was obtained for AC [77].

Yuehua et al., 2016, constructed a glassy carbon electrode modified with Poly (L-lysine)/ graphen oxide (GO) and was characterized by differential pulse voltammetry (DPV). The PLL/GO modified glassy carbon electrode showed good catalytic character on uric acid (UA) and was used to detect uric acid and dopamine (DA) simultaneously. The DPV peak currents increased linearly on the UA in the range of 2.0×10^{-7} to 1.0×10^{-4} mol/L with the detection limit (signal-to-noise ratio was 3) for UA 1.0×10^{-7} mol/L. The proposed method showed excellent selectivity and stability, and the determination of UA and DA simultaneously in urine was satisfactory [78].

Nie et al., 2013, constructed an electrode modified with poly(3,4-ethylenedioxy-thiophene) (PEDOT) and β-cyclodextrin functionalized single-walled carbon nanotubes (β-CD-SWCNT) composite for the simultaneous determination of folic acid (FA) and uric acid (UA) under coexistence of ascorbic acid (AA). The modified electrode combined the features of PEDOT and SWCNT, which hold excellent conductivity, low cost and high surface areas for working as an efficient electron-mediator for FA and UA in the presence of AA. The differential pulse voltammetry (DPV) data showed that the obtained anodic peak currents were linearly proportional to concentration in the range of 1-1000 μM with a

detection limit (S/N = 3) of 0.8 µM for FA and in the range of 0.1-500 µM and with a detection limit of 0.07 µM for UA. Moreover, the proposed sensor was successfully employed for the determination of FA and UA in spiked human urine samples with satisfactory results [79].

Chitravathi et al., 2016, prepared a modified glassy carbon electrode based on poly (Nile blue) and its electrochemical behavior were studied by cyclic voltammetry (CV). The polymer film-modified electrode was used for the determination of Paracetamol (PA), Tramadol (TD) and Caffeine (CAF). The modified glassy carbon electrode had an excellent response and specificity for the electrocatalytic oxidation of PA, TD and CAF in PBS (pH 7.0). It showed good sensitivity and selectivity in a wide linear range from 2.0×10^{-7} to 1.62×10^{-5} M, 1.0×10^{-4} M and 8.0×10^{-7} to 2.0×10^{-5} M with detection limits of 0.08, 0.5 and 0.1 µM for PA, TD and CAF [80].

Ghorbani et al., 2010, a sensitive and selective electrochemical sensor was fabricated via the drop-casting of carbon nanoparticles (CNPs) suspension onto a glassy carbon electrode (GCE). The application of this sensor was investigated in simultaneous determination of acetaminophen (ACE) and tramadol (TRA) drugs in pharmaceutical dosage form and ACE determination in human plasma. In order to study the electrochemical behaviors of the drugs, cyclic and differential pulse voltammetric studies of ACE and TRA were carried out at the surfaces of the modified GCE (MGCE) and the bare GCE. An optimum electrochemical response was obtained for the sensor in the buffered solution of pH 7.0 and using 2 µL CNPs suspension cast on the surface of GCE. Using differential pulse voltammetry, the prepared sensor showed good sensitivity and selectivity for the determination of ACE and TRA in wide linear ranges of 0.1–100 and 10–1000 µM, respectively. The resulted detection limits for ACE and TRA was 0.05 and 1 µM, respectively. The CNPs modified GCE was successfully applied for ACE and TRA determinations in pharmaceutical dosage forms and also for the determination of ACE in human plasma [81].

Jingkun et al., 2013, a sensitive and selective sensor based on poly(3,4-ethylenedioxy-thiophene) (PEDOT) and β-cyclodextrin functionalized single-walled carbon nanotubes (β-CD-SWCNT) composite was fabricated for the determination of folic acid (FA) and uric

acid (UA) under coexistence of ascorbic acid (AA). Voltammetric techniques separated the anodic peaks of FA and UA with activation overpotential, and the interference from AA was effectively excluded from FA and UA determination. The differential pulse voltammetry (DPV) data showed that the obtained anodic peak currents were linearly proportional to concentration in the range of 1-1000 µM with a detection limit (S/N = 3) of 0.8 µM for FA and in the range of 0.1-500 µM and with a detection limit of 0.07 µM for UA. It also presented superior reproducibility and long-term stability, as well as high selectivity. Moreover, the proposed sensor was successfully employed for the determination of FA and UA in spiked human urine samples with satisfactory results [82].

Hathoot et al., 2013, Modified platinum electrode based on the poly 8-(3-acetylimino-6-methyl-2, 4-dioxopyran)-1aminonaphthalene (PAMDAN) film was prepared by electrochemical polymerization technique. The modified electrode showed electrocatalytic activity toward tramadol (TD) oxidation in acidic aqueous solution. It was demonstrated that Pt electrode modified by PAMDAN film (PAMDAN/Pt modified electrode) could be used for TD detection using cyclic voltammetry (CV) and square wave voltammetry (SWV) techniques. This modified electrode was quite effective not only for detecting TD, but also for simultaneous determination of TD and dopamine (DA) in a mixture with satisfactory results [83].

Ensafi et al., 2011, N-(3,4-dihydroxyphenethyl)-3,5-dinitrobenzamide modified multiwall carbon nanotubes paste electrode was constructed and used as a voltammetric sensor for oxidation of penicillamine (PA), uric acid (UA) and tryptophan (TP). In a mixture of PA, UA and TP, those voltammograms were well separated from each other with potential differences of 300, 610, and 310 mV, respectively. The peak currents were linearly dependent on PA, UA and TP concentrations in the range of 0.05–300, 5–420, and 1.0–400 µmol L^{-1}, with detection limits of 0.021, 2.0, and 0.82 µmol L^{-1}, respectively. The modified electrode was used for the determination of those compounds in real samples [84].

From the above literature review, it is seen that the determination of PA, TD and UA individually or in a binary mixture or in a ternary mixture using Diethylamine modified electrode sensor was not reported previously. Most of the work for the determination of

PA, TD and UA has been done individually or binary using carbon nanotube or carbon paste electrodes.

In this work, Diethylamine modified electrode sensor has been developed for the determination of PA, TD and UA. Diethylamine has choosen as the sensing material because Diethylamine is a promising material regarding its low cost and availability, high sensitivity and selectivity. The modification process of glassy carbon electrode with Diethylamine is easy compared with the carbon paste electrodes. This modified electrode sensor can also be applicable for the determination of these compounds in tablet samples (PA and TD) and real samples (UA).

CHAPTER III

Experimental

The electrochemical behavior of Paracetamol (PA), Tramadol (TD) and Uric acid (UA) in buffer solution at various pH has been investigated using cyclic voltammetry (CV) and differential pulse voltammetry (DPV) at Glassy carbon (GC), Gold (Au) and Platinum (Pt) electrode. The sensitivity of electrode reactions has been improved by modifying the electrodes with Diethylamine. DPV has also been employed for the quantitative estimation of PA, TD and UA in known sample and real sample such as tablets, blood and urine sample. The instrumentation is given details in the following sections. The source of different chemicals, instruments and methods are briefly given below.

3.1 Chemicals

Analytical grade chemicals and solvents have been used in electrochemical synthesis and analytical work. The used chemicals were-

Sl. No.	Chemicals	Molecular formula	Molar mass	Reported purity	Producer
1.	Paracetamol	$C_8H_9NO_2$	151.163	99.5%	Loba Chemie Pvt. Ltd., India
2.	Tramadol	$C_{16}H_{25}NO_2$	263.412	99%	Loba Chemie Pvt. Ltd., India
3.	Uric Acid	$C_5H_4N_4O_3$	168.11	99%	Damstadt, Germany
4.	Diethylamine	$C_4H_{11}N$	73.14	99.5%	E-Merck, Germany
5.	Glacial Acetic Acid	CH_3COOH	60.05	99.5%	Loba Chemie Pvt. Ltd., India

Sl. No.	Chemicals	Molecular formula	Molar mass	Reported purity	Producer
6.	Sodium Acetate	$CH_3COONa.3H_2O$	136.08	99%	Merk Specialities Pvt. Ltd., India
7.	Potassium Chloride	KCl	74.60	99%	E-Merck, Germany
8.	Sodium Di-hydrogen Orthophosphate	$NaH_2PO_4.2H_2O$	156.01	98%	Loba Chemie Pvt. Ltd., India
9.	Di-sodium Hydrogen Orthophosphate	$Na_2HPO_4.2H_2O$	177.99	97%	Loba Chemie Pvt. Ltd., India
10.	Sodium Hydroxide	NaOH	40.0	97%	E-Merck, Germany
11.	Sodium Bicarbonate	$NaHCO_3$	84.0	99%	E-Merck, Germany

3.2 Equipments

During this research work the following instruments were used-

- The electrochemical studies (CV, DPV) were performed with a computer controlled potentiostats/ galvanostats (µstat 400, Drop Sens, Spain)
- A Pyrex glass micro cell with 26eflon cap
- Glassy carbon (GC)/ Gold (Au)/ Platinum (Pt) as working electrode (BASi, USA)
- Ag/AgCl as reference electrode (BASi, USA)
- Liquid micro size (0.05µm) polishing alumina (BAS Inc. Japan)
- Pt wire as counter electrode (Local market, Dhaka, Bangladesh)
- A HR 200 electronic balance with an accuracy of ± 0.0001g was used for weighting and
- A pH meter (pH Meter, Hanna Instruments, Italy) was employed for maintaining the pH of the solutions.
- The UV-Vis spectroscopic analysis was performed by a computer controlled spectrophotometer (Thermo Scientific, USA).

3.3 Cyclic Voltammetry (CV)

There are many well developed electro-analytical techniques are used for the study of electrochemical reactions. Among these we have selected the CV technique to study and analyze the redox reactions occurring at the polarizable electrode surface. This technique provides suitable information to understand the mechanism of electron transfer reaction of the compounds as well as the nature of adsorption of reactants or products on the electrode surface. CV is often the first experiment performed in an electrochemical study. CV consists of imposing an excitation potential nature on an electrode immersed in an unstirred solution and measuring the current and its potential ranges varies from a few millivolts to hundreds of millivolts per second in a cycle. This variation of anodic and cathodic current with imposed potential is termed as voltammogram [85].

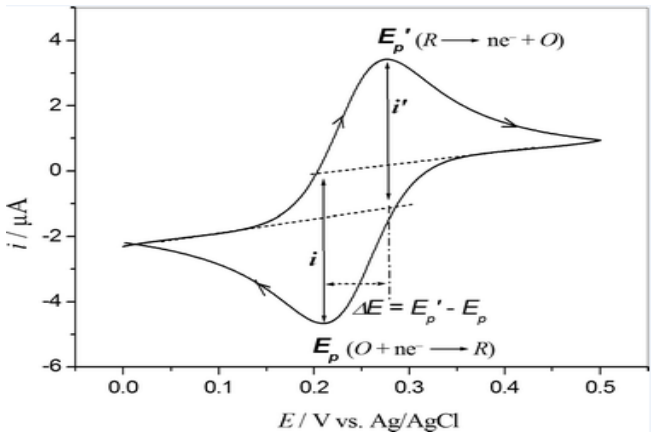

Figure 3.1: The expected response of a reversible redox couple during a single potential cycle

This technique is based on varying the applied potential at a working electrode in both forward and reverse directions while monitoring the current. Simply stated, in the forward scan, the reaction is $O + e^- \rightarrow R$, R is electrochemically generated as indicated by the cathodic current. In the reverse scan, $R \rightarrow O + e^-$, R is oxidized back to O as indicated by the anodic current. The CV is capable of rapidly generating a new species during the forward scan and then probing its fate on the reverse scan. This is a very important aspect of the technique [86].

In CV the current function can be measured as a function of scan rate. The potential of the working electrode is controlled vs a reference electrode such as Ag/AgCl electrode.

The electrode potential is ramped linearly to a more negative potential and then ramped is reversed back to the starting voltage. The forward scan produces a current peak for any analyte that can be reduced through the range of potential scan. The current will increase as the current reaches to the reduction potential of the analyte [87].

The current at the working electrode is monitored as a triangular excitation potential is applied to the electrode. The resulting voltammogram can be analyzed for fundamental information regarding the redox reaction. The potential at the working electrode is controlled vs a reference electrode, Ag/AgCl (standard NaCl) electrode. The excitation signal varies linearly with time. First scan positively and then the potential is scanned in reverse, causing a negative scan back to the original potential to complete the cycle. Signal on multiple cycles can be used on the scan surface. A cyclic voltammogram is plot of response current at working electrode to the applied excitation potential.

3.4 Important features of CV

An electrochemical system containing species 'O' capable of being reversibly reduced to 'R' at the electrode is given by,

$$O + ne^- = R \quad \text{.....3.1}$$

Nernst equation for the system is

$$E = E^0 + \frac{0.059}{n} \log \frac{C_0^s}{C_R^s} \quad \text{.....3.2}$$

Where,

E = Potential applied to the electrode

E^0 = Standard reduction potential of the couple versus reference electrode

n = Number of electrons in Equation (3.1)

C_0^s = Surface concentration of species 'O'

C_R^s = Surface concentration of species 'R'

A redox couple that changes electrons rapidly with the working electrode is termed as electrochemically reverse couple. The relation gives the peak current i_{pc}

$$i_{pc} = 0.4463\ nFA\ (D\alpha)^{1/2}C \quad \text{.....3.3}$$

$$\alpha = \left(\frac{nFv}{RT}\right) = \left(\frac{nv}{0.026}\right)$$

Where,

i_{pc} = peak current in amperes

F= Faraday`s constant (approximately 96500)

A = Area of the working electrode in cm^2

v= Scan rate in volt/ sec

C= Concentration of the bulk species in mol/L

D= Diffusion coefficient in cm^2 /sec

In terms of adjustable parameters, the peak current is given by the Randless- Sevcik equation,

$$i_{pc}=2.69\times10^5\times n^{3/2}AD^{1/2}Cv^{1/2} \quad \ldots\ldots\ldots\ldots\ldots\ldots\ldots 3.4$$

The peak potential E_p for reversible process is related to the half wave potential $E_{1/2}$, by the expression,

$$E_{pc} = E_{1/2} - 1.11\left(\frac{RT}{nF}\right), \quad \text{at } 25^0\text{C} \ldots\ldots\ldots\ldots\ldots\ldots 3.5$$

$$E_{pc} = E_{1/2} - \left(\frac{0.0285RT}{n}\right)\ldots\ldots\ldots\ldots\ldots\ldots\ldots\ldots 3.6$$

The relation relates the half wave potential to the standard electrode potential

$$E_{1/2} = E^0 - \frac{RT}{nF}\ln\frac{f_{red}}{f_{ox}}\left(\frac{D_{ox}}{D_{ox}}\right)^{1/2}$$

$$E_{1/2} = E^0 - \frac{RT}{nF}\ln\left(\frac{D_{ox}}{D_{red}}\right)^{1/2} \quad \ldots\ldots\ldots\ldots\ldots\ldots\ldots 3.7$$

Assuming that the activity coefficient f_{ox} and f_{red} are equal for the oxidized and reduced species involved in the electrochemical reaction.

From Equation (3.6), we have,

$$E_{pa} - E_{pc} = 2.22\left(\frac{RT}{nF}\right) \text{at } 25^0\text{C}\ldots\ldots\ldots\ldots\ldots\ldots\ldots 3.8$$

$$\text{Or, } E_{pa} - E_{pc} = \left(\frac{0.059}{n}\right) \quad \text{at } 25^0\text{C}\ldots\ldots\ldots\ldots\ldots\ldots 3.9$$

This is a good criterion for the reversibility of electrode process. The value of i_{pa} should be close for a simple reversible couple,

$$i_{pa}/i_{pc} = 1 \text{…….3.10}$$

And such a system $E_{1/2}$ can be given by,

$$E_{1/2} = \frac{E_{pa} + E_{pc}}{2} \text{…….3.11}$$

For irreversible processes (those with sluggish electron exchange), the individual peaks are reduced in size and widely separated, Totally irreversible systems are characterized by a shift of the peak potential with the scan rate [88];

$$E_p=E^0-(RT/\alpha n_aF)[0.78-\ln(k^0/(D)^{1/2})+\ln(\alpha n_aF\alpha/RT)^{1/2}] \text{……..3.12}$$

Where α is the transfer coefficient and n_a is the number of electrons involved in the charge transfer step. Thus E_p occurs at potentials higher than E^0, with the over potential related to k^0 (standard rate constant) and α. Independent of the value k^0, such peak displacement can be compensated by an appropriate change of the scan rate. The peak potential and the half-peak potential (at 25^0 C) will differ by 48/ αn mV. Hence, the voltammogram becomes more drawn-out as αn decreases.

The peak current, given by

$$i_p=(2.99\times10^5)n(\alpha n_a)^{1/2}ACD^{1/2}v^{1/2} \text{……...3.13}$$

is still proportional to the bulk concentration , but will be lower in height (depending upon the value of α) . Assuming α = 0.5, the ratio of the reversible–to–irreversible current peaks is 1.27 (i.e. the peak current for the irreversible process is about 80% of the peak for a reversible one). For quasi-reversible systems (with $10^{-1}>k^0>10^{-5}$ cm/s) the current is controlled by both the charge transfer and mass transport. The shape of the cyclic voltammogram is a function of the ratio k^0 $(\pi vnFD/RT)^{1/2}$. As the ratio increases, the process approaches the reversible case. For small values of it, the system exhibits an irreversible behavior. Overall, the voltammograms of a quasi-reversible system are more drawn out and exhibit a larger separation in peak potential compared to a reversible system.

Unlike the reversible process in which the current is purely mass transport controlled, currents due to quasi-reversible process are controlled by a mixture of mass transport and charge transfer kinetics [89, 90]. The process occurs when the relative rate of electron transfer with respect to that of mass transport is insufficient to maintain Nernst equilibrium at the electrode surface.

3.5 Pulse methods

The basis of all pulse techniques is the difference in the rate of decay of the charging and the faradaic currents following a potential step (or pulse). The charging current decays considerably faster than the faradaic current. A step in the applied potential or current represents an instantaneous alteration of the electrochemical system. Analysis of the evolution of the system after perturbation permits deductions about electrode reactions and their rates to be made. The potential step is the base of pulse voltammetry. After applying a pulse of potential, the capacitive current dies away faster than the faradic one and the current is measured at the end of the pulse. This type of sampling has the advantage of increased sensitivity and better characteristics for analytical applications. At solid electrodes there is an additional advantage of discrimination against blocking of the electrode reaction by adsorption [91]. Three of these pulse techniques are widely used.

- Normal Pulse Voltammetry (NPV)
- Differential Pulse Voltammetry (DPV)
- Square Wave Voltammetry (SWV)

In this research work differential pulse voltammetry was used for the quantitative determination of PA, TD and UA.

3.6 Differential Pulse Voltammetry (DPV)

Differential pulse voltammetry (DPV) is a technique in which potential is applied after certain period of time and measures the resulting faradic current as a function of applied potential either in oxidation or reduction. It is designed to minimize background charging currents. The waveform in DPV is a sequence of pulses, where a baseline potential is held for a specified period of time prior to the application of a potential pulse. Current is sampled just prior to the application of the potential pulse. The potential is then stepped by a small amount (typically < 100 mV) and current is sampled again at the end of the pulse. The potential of the working electrode is then stepped back by a lesser value than during the forward pulse such that baseline potential of each pulse is incremented throughout the sequence.

By contrast, in normal pulse voltammetry the current resulting from a series of ever larger potential pulse is compared with the current at a constant 'baseline' voltage. Another type of pulse voltammetry is square wave voltammetry, which can be considered a special type of differential pulse voltammetry in which equal time is spent at the potential of the ramped baseline and potential of the superimposed pulse. The potential wave form consists of small pulses (of constant amplitude) superimposed upon a staircase wave form [92]. Unlike NPV, the current is sampled twice in each pulse Period (once before the pulse, and at the end of the pulse), and the difference between these two current values is recorded and displayed.

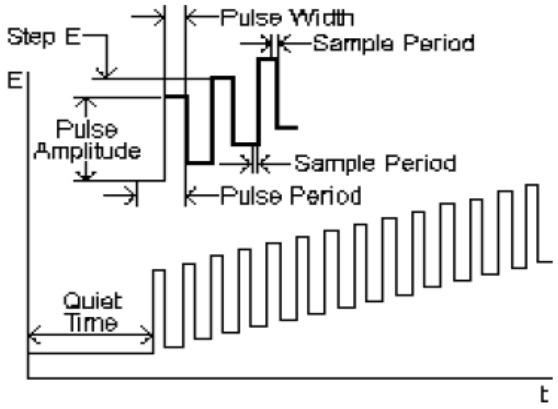

Figure 3.2: Scheme of application of potential

3.7 Important features of DPV

Differential pulse voltammetry has following important features in this work:

i) Current is sampled just prior to the application of the potential pulse.

ii) DPV help to improve the sensitivity of the detection and the resolution of the voltammogram.

3.8 Computer Controlled Potentiostats (for CV and DPV experiment)

Potentiostats/ Galvanostats (µStat 400, DropSens, Spain) is the main instrument for voltammetry, which has been applied to the desired potential to the electrochemical cell (i.e. between a working electrode and a reference electrode), and a current-to-voltage converter, which measures the resulting current, and the data acquisition system produces the resulting voltammogram.

3.9 Electrochemical Cell

An electrochemical cell is a device capable of either generating electrical energy from chemical reactions or facilitating chemical reactions through the introduction of electrical energy [93]. A typical electrochemical cell consists of the sample dissolved in a solvent, an ionic electrolyte, and three (or sometimes two) electrodes (Figure 3.3). These are reference electrode (RE), working electrode (WE), and counter electrode (CE) (also called the secondary or auxiliary electrode). The applied potential is measured against the RE, while the CE closes the electrical circuit for the current to flow. The experiments are performed by a potentiostat that effectively controls the voltage between the RE and WE, while measuring the current through the CE (the WE is connected to the ground). Cells (sample holders) come in a variety of sizes, shapes, and materials. The type used depends on the amount and type of sample, the technique, and the analytical data to be obtained. The material of the cell (glass, Teflon, polyethylene) is selected to minimize reaction with the sample. In this investigation three electrodes electrochemical cell has been used. It has advantages over two electrodes cell because of using 3rd electrode. It reduces the solvent resistance and ensures that no electron transfer through the reference electrode.

Figure 3.3: The three electrode system consisting of a working electrode, a reference electrode and a counter electrode.

3.10 Electrodes

Three types of electrodes are used in this research:

i) Working electrodes are Glassy carbon (GC) electrode with 3.0 mm diameter disc, Gold (Au) & Platinum (Pt) electrode with 1.6 mm diameter disc.

ii) Ag/AgCl (standard NaCl) electrode used as reference electrode from BASi, USA

iii) Counter electrode is a Pt wire

The working electrode is an electrode on which the reaction of interest is occurring. The reference electrode is a half-cell having a known electrode potential and it keeps the potential between itself and the working electrode. The counter electrode is employed to allow for accurate measurements to be made between the working and reference electrodes.

3.11 Supporting electrolyte

The supporting electrolyte is an inert soluble ionic salt added to the solvent; generally in 10-fold or 100-fold excess over the concentration of the species being studied. The inertness meant here is the ability to avoid oxidation or reduction at the indicating or reference electrode during the course of the electrochemical measurements.

There are three functions of the supporting electrolyte. First, it carries most of the ionic current of the cell since its concentration is much larger than that of the other species in solution. Thus it serves to complete the circuit of the electrochemical cell and keep the cell resistance at a low value. Second, it maintains a constant ionic strength. This is necessary because the structure of the inter phase region should not change significantly if a reaction occurs there. A stable structure is created on the electrolyte side by adding a high concentration of an inert salt. Third, migration current observed is reduced by the presence of large excess of ions that are not electrochemically active at the potentials in use, because they can carry an ionic current without permitting its conversion into electronic, and hence net or measured, current at the electrodes.

3.12 Preparation of buffer solutions

Preparation of different kinds of buffer solution is discussed below:

Acetate Buffer Solution: To prepare acetate buffer (pH 3.0-5.0) solution definite amount of sodium acetate was dissolved in 0.5M acetic acid in a volumetric flask and the pH was measured. The pH of the buffer solution was adjusted by further addition of acetic acid and / or sodium acetate.

Phosphate Buffer Solution: Phosphate buffer solution (pH 6.0-8.0) was prepared by mixing a solution of 0.5M sodium dihydrogen ortho-phosphate ($NaH_2PO_4.2H_2O$) with a solution of 0.5M disodium hydrogen ortho-phosphate ($Na_2HPO_4.2H_2O$). The pH of the prepared solution was measured with pH meter.

Bicarbonate Buffer Solution: To prepare hydroxide buffer (pH 9.0-11.0) solution definite amount of sodium hydroxide was dissolved in 0.5M sodium bicarbonate in a volumetric flask. The pH of the prepared solution was measured with pH meter.

3.13 Electrode polishing

Materials may be adsorbed to the surface of a working electrode after each experiment. Then the current response will degrade and the electrode surface needs to clean. In this case, the cleaning required is light polishing with 0.05µm alumina powder. A few drops of polish are placed on a polishing pad and the electrode is held vertically and the polish rubbed on in a figure-eight pattern for a period of 30 seconds to a few minutes depending upon the condition of the electrode surface. After polishing the electrode surface is rinsed thoroughly with deionized water.

3.14 Preparation of modified electrodes

In this study, Glassy carbon (GC), Gold (Au) and Platinum (Pt) electrodes purchase from the BASi, USA are used as working electrode. Electrode preparation includes polishing and conditioning of the electrode. The electrode was polished with 0.05µm alumina

powder on a wet polishing cloth. For doing so a part of the cloth was made wet with deionized water and alumina powder was sprinkled over it. Then the electrode was polished by softly pressing the electrode against the polishing surface at least 10 minutes before modify. The electrode surface would look like a shiny mirror after thoroughly washed with deionized water. Diethylamine was weighted and kept in phosphate buffer solution (pH 7). Then it was placed on a magnetic stirrer and stirred for 3 minutes at room temperature. The freshly cleaned bare electrode was modified with Diethylamine by using CV technique. The potential was cycled for 15 scans at a range of -0.5 V to 1.5 V. Then the modified electrode was activated in PBS (pH 7) by applying continuous potential cycled for 10 scans at a range of 1.0 V to 2.0 V. Then the modified electrode was dried by nitrogen gas for 10 minutes. Then a thin layer of Diethylamine was appeared on the surface of the electrode.

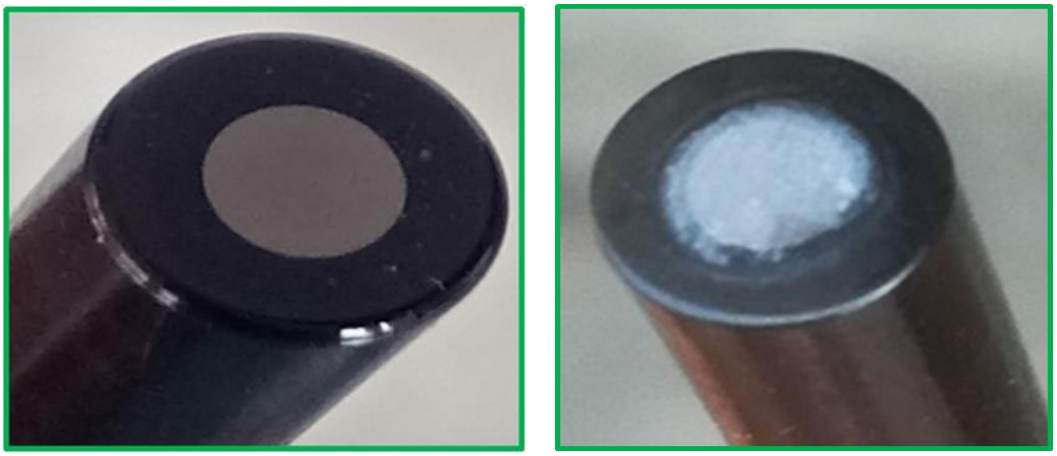

Bare GC electrode Diethylamine modified GC electrode

Figure 3.4: Bare and Diethylamine modified GC electrode

3.15 Preparation of Solutions

All standard solution of PA, TD and UA was prepared in 50ml 0.5M PBS (pH 7). Tablet samples are dissolved in 50ml 0.5M PBS (pH 7) with continues stirring by magnetic stirrer.

3.16 Removing Dissolved Oxygen from Solution

Dissolved oxygen can interfere with observed current response so it is needed to remove it. Experimental solution was indolent by purging for at least 5-10 minutes with 99.99% pure and dry nitrogen gas (BOC, Bangladesh). By this way, traces of dissolved oxygen were removed from the solution.

3.17 Experimental procedure

The electrochemical cell filled with solution 50mL of the experimental solution and the Teflon cap was placed on the cell. The working electrode together with reference electrode and counter electrode was inserted through the holes. The electrodes were sufficiently immersed. The solution system is deoxygenated by purging the nitrogen gas for about 10 minutes. The solution has been kept quiet for 10 seconds. After determination the potential window the voltammogram was taken at various scan rates, pH and concentrations from the Drop View Software.

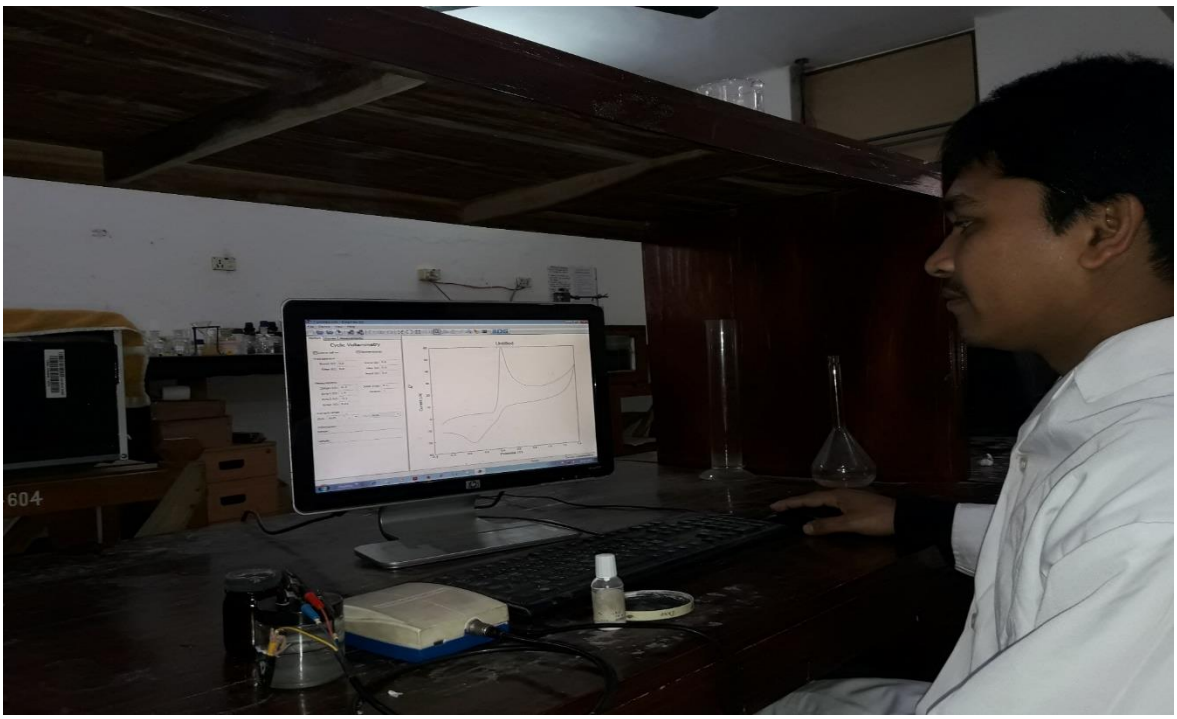

Figure 3.5: Experimental setup (Software controlled Potentiostats (μstat 400))

3.18 UV-Visible Spectrophotometry

In spectrometric analysis a source of radiation is used that extends into the ultraviolet region of the spectrum. The instrument employed for this purpose is a spectrophotometer. An optical spectrometer is an instrument possessing an optical system which can produce dispersion of incident electromagnetic radiation, and with which measurements can be made of the quantity of transmitted radiation at selected wavelength of the spectral range. A photometer is a device for measuring the intensity of transmitted radiation. When combined in the spectrophotometer the spectrometer and photometer are employed conjointly to produce a signal corresponding to the difference between the transmitted radiation of a reference material and that of a sample of selected wavelengths.

The essential parts of spectrophotometer are:

1. A source of radiant energy
2. A monochromator
3. Glass or silica cells for holding the solvent and for the solution under test
4. A device to receive of measure the beam or beam of radiant energy passing through the solvent or solution.

Lambert law states that when monochromatic light passes through a transparent medium, the rate of decrease in intensity with the thickness of the medium is proportional to the intensity of light [94]. This is equivalent to stating that the intensity of the emitted light decrease exponentially as the thickness of the absorbing medium increase arithmetically, or that any layer of given thickness of the medium absorbs the same fraction of the light incident upon it.

Beer studied the effect of concentration of the colored constituent in solution upon the light transmission. He found the same relation between transmission and concentration as Lambert had discovered between transmission and thickness of the layer. By combining both of the theories the final expression can be written as,

$$A = \log \frac{I_0}{I_t} = acl$$

Here, Io=intensity of the incident light; It=intensity of the transmitted light; A=Absorbance of the medium and l are dimensions of the cell.

Figure 3.6: UV-visible spectrophotometer

A computer controlled spectrophotometer (Thermo Scientific, USA) was used for UV-Vis experiment in a pair of quartz cells.

3.19 Standard deviation

In probability and statistics, the standard deviation of a probability distribution, random variable, or population or multiset of values is a measure of the spread of its values. It is usually denoted with the letter σ (lower case sigma). It is defined as the square root of the variance.

To understand standard deviation, keep in mind that variance is the average of the squared differences between data points and the mean. Variance is tabulated in units squared. Standard deviation, being the square root of that quantity, therefore measures the spread of data about the mean, measured in the same units as the data.

Said more formally, the standard deviation is the root mean square (RMS) deviation of values from their arithmetic mean. For example, in the population {4, 8}, the mean is 6 and

the deviations from mean are {-2, 2}. Those deviations squared are {4, 4} the average of which (the variance) is 4. Therefore, the standard deviation is 2. In this case 100% of the values in the population are at one standard deviation of the mean.

The standard deviation is the most common measure of statistical dispersion, measuring how widely spread the values in a data set. If the data points are close to the mean, then the standard deviation is small. As well, if many data points are far from the mean, then the standard deviation is large. If all the data values are equal, then the standard deviation is zero. [95].

3.20 Recovery percentage

Recovery percentage is an indication of a measurement that indicates the accuracy of a measurement or quantitative determination. The percentage of the recovered amount with response to amount taken is termed as recovery percentage as below-

$$\%\ of\ Recovery = \frac{amount\ found}{total\ amount\ taken} \times 100$$

CHAPTER IV

Results and Discussion

Cyclic voltammetry (CV) and differential pulse voltammetry (DPV) techniques have been used for investigating the electrochemical behavior of Paracetamol (PA), Tramadol (TD) and Uric Acid (UA) in presence of buffer solution by using bare and modified Glassy carbon (GC), Gold (Au) and Platinum (Pt) electrodes. In concordance with the experiment we have abstracted precious information considering electrochemical oxidations of PA, TD and UA which has been disputed elaborately in following section. DPV and UV-Vis spectroscopy have been used to quantitative estimation of PA and TD in this work.

4.1 Electrochemical behavior of PA, TD and UA at bare electrodes

4.1.1 Electrochemical behavior of PA, TD and UA at bare GC electrode

Figure 4.1 shows the cyclic voltammogram (CV) of the ternary solution of PA, TD and UA at bare GC electrode in Phosphate buffer solution (PBS) (pH 7). It shows two anodic peaks at 0.49 V and 0.87 V where three electroactive compounds present in the solution. It indicates that the bare GC electrode is unable to separate the individual oxidation peaks of PA, TD and UA by using CV technique.

Figure 4.2 shows the differential pulse voltammogram (DPV) of the ternary solution of PA, TD and UA at bare GC electrode in PBS (pH 7). It shows two peaks at 0.48 V and 0.97V where three electroactive compounds present in the solution. It also indicates that the bare GC electrode is unable to separate the individual oxidation peaks of PA, TD and UA by using DPV technique.

4.1.2 Electrochemical behavior of PA, TD and UA at bare Au electrode

Figure 4.3 shows the cyclic voltammogram (CV) of the ternary solution of PA, TD and UA at bare Au electrode in PBS (pH 7). It shows two oxidation peak at 0.59 V, 1.4V and two

reduction peak at 0.18 V, 0.43 V. It indicates that the bare Au electrode is unable to separate the individual oxidation peaks of PA, TD and UA by using CV technique.

Figure 4.4 shows the differential pulse voltammogram (DPV) of the ternary solution of PA, TD and UA at bare Au electrode in PBS (pH 7). It shows two peaks at 0.53 V and 0.96 V where three electroactive compounds present in the solution. It also indicates that the bare Au electrode is unable to separate the individual oxidation peaks of PA, TD and UA by using DPV technique.

4.1.3 Electrochemical behavior of PA, TD and UA at bare Pt electrode

Figure 4.5 shows the cyclic voltammogram (CV) of the ternary solution of PA, TD and UA at bare Pt electrode in Phosphate buffer solution (PBS) (pH 7). It shows only one anodic peaks at 0.53 V where three electroactive compounds present in the solution. It indicates that the bare Pt electrode is unable to separate the individual oxidation peaks of PA, TD and UA by using CV technique.

Figure 4.6 shows the differential pulse voltammogram (DPV) of the ternary solution of PA, TD and UA at bare Pt electrode in PBS (pH 7). It shows only one oxidation peaks at 0.51 V where three electroactive compounds present in the solution. It also indicates that the bare Pt electrode is unable to separate the individual oxidation peaks of PA, TD and UA by using DPV technique.

From the observations of the electrochemical behavior of PA, TD and UA in ternary solution it is clear that the bare electrodes (GC, Au and Pt) are unable to separate the individual oxidation peaks of PA, TD and UA. So, simultaneous determination of these three compounds in ternary mixture is not possible at bare electrodes by using the CV or DPV techniques.

4.2 Modification of GC electrode with Diethylamine (DEA) in PBS (pH 7)

In order to get response from UA, PA and TD in a mixture and to improve the selectivity of GC electrode, it was modified with DEA solution prepared in PBS (pH 7).

Figure 4.7 displays the continuous CVs of DEA thin film formation onto a bare GC in DEA solution over the potential range of –0.5 V to +1.5 V for 15 cycles at a scan rate of 0.2 V/s. As can be seen, the anodic currents increased and cathodic currents also increased, indicating the formation and growth of an electroactive layer on the GC electrode surface. After the twelve cycles, the increase of these peaks current tended to be stable. It is assumed that a uniform and thin film was present on the surface of GC electrode.

4.3 Electrochemical behavior of PA, TD and UA at DEA modified electrodes

4.3.1 Electrochemical behavior of PA, TD and UA at DEA modified GC electrode

Figure 4.8 shows the cyclic voltammogram (CV) of the ternary solution of PA, TD and UA at DEA modified GC electrode in PBS (pH 7). It shows three anodic peak at 0.37 V, 0.48 V and 0.91 V. It indicates that the modified GC electrode is able to separate the individual oxidation peaks of PA, TD and UA by using CV technique. But the peak of UA is very weak.

Figure 4.9 shows the differential pulse voltammogram (DPV) of the ternary solution of PA, TD and UA at DEA modified GC electrode in PBS (pH 7). It shows three peaks at 0.27 V, 0.38 V and 0.86 V where three electroactive compounds present in the solution. It indicates that the modified GC electrode is able to separate the individual oxidation peaks of PA, TD and UA by using DPV technique.

4.3.2 Electrochemical behavior of PA, TD and UA at DEA modified Au electrode

Figure 4.10 shows the cyclic voltammogram (CV) of the ternary solution of PA, TD and UA at modified Au electrode in PBS (pH 7). It shows one sharp anodic peak at 0.98 V and two small anodic peak at 0.27V and 0.49 V. It also shows two cathodic peak at 0.19V and 0.47V. It indicates that the modified Au electrode is able to separate the individual oxidation peaks of PA, TD and UA by using CV technique, but the current value is very low.

Figure 4.11 shows the differential pulse voltammogram (DPV) of the ternary solution of PA, TD and UA at modified Au electrode in PBS (pH 7). It shows four anodic peaks at 0.38 V, 0.49 V, 0.79 V and 1.1 V where 0.38 V , 0.49, 0.79 V indicate the oxidation peak of UA, PA, TD and 1.1 V indicates the overlapping peak of Au electrode with TD. It also indicates that the modified Au electrode is able to separate the individual oxidation peaks of PA, TD and UA by using DPV technique, but peak current is very low.

4.3.3 Electrochemical behavior of PA, TD and UA at DEA modified Pt electrode

Figure 4.12 shows the cyclic voltammogram (CV) of the ternary solution of PA, TD and UA at modified Pt electrode in PBS (pH 7). It shows only one anodic peak at 0.49 V. It indicates that the DEA modified Pt electrode is unable to separate the individual oxidation peaks of PA, TD and UA by using CV technique.

Figure 4.13 shows the differential pulse voltammogram (DPV) of the ternary solution of PA, TD and UA at DEA modified Pt electrode in PBS (pH 7). It shows three oxidation peaks at 0.40 V, 0.48 V and 0.89 V where three electroactive compounds present in the solution. It also indicates that the DEA modified Pt electrode is able to separate the individual oxidation peaks of PA, TD and UA by using DPV technique, but peak current is very low.

From the observations of the electrochemical behavior of PA, TD and UA in ternary solution it is clear that the bare electrodes (GC, Au, Pt and WBE.) are unable to separate the individual oxidation peaks of PA, TD and UA. So, simultaneous determination of these three compounds in ternary mixture is not possible at bare electrodes by using the CV or DPV techniques. DEA modified (GC and Au) electrodes are able to separate the individual peaks of PA, TD and UA using CV and DPV technique. But Au electrode give low peak current with respect to GCE.

4.4 Electrode selection

After analyzing CVs and DPVs for the electrochemical behavior of PA+TD+UA at DEA modified GC, Au and Pt electrodes (Figure 4.14 and Figure 4.15) it is clear that the

separation of the oxidation peaks as well as peak current of PA, TD and UA at DEA modified GC electrode is prominent than that of Au and Pt electrodes. For this concern, DEA modified GC electrode was selected to analysis the electrochemical behavior and quantitative determination of PA, TD and UA.

4.5 pH study

Figure 4.16 shows the cyclic voltammograms of the ternary mixture of PA, TD and UA in different buffer solution (pH 3, 5, 7 and 9). Figure 4.17 shows the differential pulse voltammogram (DPV) of the ternary solution of PA, TD and UA at DEA modified GC electrode. For the best consideration pH 7 was selected for the detection of PA, TD and UA in a ternary mixture. Because DEA modified GC electrode can properly separate ternary mixture of PA, TD and UA in PBS (pH 7).

4.6 Electrochemical Study

4.6.1 Cyclic voltammetric behavior of Paracetamol (PA) at bare GC electrode

Cyclic voltammogram of 2.5 mM PA in 0.5M PBS (pH 7) and only 0.5M PBS (pH 7) shows in Figure 4.18. The voltammogram of only 0.5M PBS (blue line) shows no oxidation peak at bare GC electrode. 2.5 mM PA (red line) shows one oxidation peak at 0.48 V and peak current is 65 µA. CV of PA in PBS shows small cathodic peak at bare GC electrode. This indicates that the redox process of PA at bare GC electrode is a quasi-reversible redox process.

4.6.2 Cyclic voltammetric behavior of Uric acid (UA) at bare GC electrode

Cyclic voltammogram of 2.5 mM UA in 0.5M PBS (pH 7) and only 0.5M PBS (pH 7) shows in figure 4.19. The voltammogram of only 0.5M PBS (blue line) shows no oxidation peak at bare GC electrode. 2.5 mM UA (red line) shows one oxidation peak at 0.38 V and peak current is 83 µA. CV of UA in PBS does not show any cathodic peak at bare GC electrode.

4.6.3 Cyclic voltammetric behavior of Tramadol (TD) at bare GC electrode

Cyclic voltammogram of 2.5 mM TD in 0.5M PBS (pH 7) and only 0.5M PBS (pH 7) shows in figure 4.20. The voltammogram of only 0.5M PBS (blue line) shows no oxidation peak at bare GC electrode. 2.5 mM TD (red line) shows one oxidation peak at 0.98 V and peak current is 33 µA. CV of TD in PBS does not show any cathodic peak at bare GC electrode.

4.6.4 Simultaneous detection of UA and PA at bare GC electrode using cyclic voltammetric technique

CV of 2.5 mM UA and 2.5 mM PA was taken for the simultaneous detection at bare GC electrode. The peaks of 2.5mM UA and 2.5mM PA was overlapped in the simultaneous voltammogram (Figure 4.21).

UA in PBS gives one anodic peak at +0.41 V. On the other hand PA gives anodic and cathodic peaks at +0.47 V and -0.1 V respectively. The binary mixture of UA and PA shows a single anodic peak was found at +0.49 V which is at high potential than the peaks for individual UA and PA. Small cathodic peak observed for the binary mixture of UA and PA at bare GC electrode. The anodic peaks in the binary mixture are the combined peak of both of the species which is due to the fouling effect. As both compounds are oxidized at a close potential their combined solution gives response as if a solution of double concentration. Bare GC electrode does not give separate peaks for simultaneous detection of UA and PA in their binary solution.

4.6.5 Simultaneous detection of PA and TD at bare GC electrode using cyclic voltammetric technique

CV of 2.5 mM PA and 2.5 mM TD was taken for the simultaneous detection at bare GC electrode (Figure 4.22). CV shows two anodic peaks at 0.51 V and 1.3 V. This indicates that the oxidation of PA and TD have a significant potential difference. From the individual CVs we can see that the oxidation peak at 0.49 V appeared for PA and 1.1 V is for TD.

4.6.6 Simultaneous detection of UA and TD at bare GC electrode using cyclic voltammetric technique

CV of 2.5 mM UA and 2.5 mM TD was taken for the simultaneous detection at bare GC electrode. CV shows two anodic peaks at 0.39 V and 1.3 V. This indicates that the oxidation of UA and TD have a significant potential difference (Figure 4.23). The peak at 0.39 V is for UA and at 1.3 V is for TD. Simultaneous determination of UA and TD at bare GC electrode possible but at DEA modified GC electrode they show a significant increase of current that is very important to determine the amount of UA an TD in a low concentration sample.

4.6.7 Simultaneous determination of UA, PA and TD at bare GC electrode using cyclic voltammetric technique

UA in PBS gives one anodic peak at +0.35 V, PA in PBS gives one anodic and one cathodic peaks at +0.46 V and -0.1 V respectively and TD in PBS gives one anodic peak at 1.2 V. Ternary mixture of UA, PA and TD in PBS, two anodic peak was found at +0.5 V and 1.3 V which is at higher potential than the individually oxidation potential of UA, PA and TD. No cathodic peak observed for the ternary mixture of UA, PA and TD at bare GC electrode (Figure 4.24). The anodic peaks of UA and PA in the ternary mixture are the combined peak of both of the species which is due to the fouling effect where TD gives an individual peak for the difference of oxidation potential compared to UA and PA. UA and PA are oxidized at a close potential their combined solution gives response as if a solution of double concentration. Bare GC electrode does not give separate peaks for simultaneous detection of UA, PA and TD in their ternary solution.

4.7 Cyclic voltammetric behavior of DEA solution at modified GC electrode

Cyclic voltammogram of PBS solution at DEA modified GC electrode shows in figure 4.25. DEA modified electrode in PBS solution shows no anodic or cathodic peak in the measurement potential of UA, PA and TD within -0.3 V to +1.4 V. It indicates that the deposited DEA film on GC electrode surface just enhance the signals of analytes without interfering with their oxidation potential and sensitivity.

4.8 Cyclic voltammetric behavior of UA at DEA modified GC electrode

Cyclic voltammogram of 2.5 mM UA in PBS (pH 7) solution and only PBS at DEA modified GC electrode shown in figure 4.26. There is no peak for PBS but a sharp and well defined peak is observed for UA at 0.28 V.

4.8.1 Comparison of the CV of UA at bare and DEA modified GC electrode

Figure 4.27 shows the comparison between the behaviors of UA at bare and DEA modified GC electrode. At bare GC electrode UA gives an anodic peak at 0.37 V having peak current 61 µA. But, at DEA modified GC electrode UA gives an anodic peak at 0.28 V having peak current 82 µA. It is clear that the anodic peak of UA at DEA modified GC electrode is sharper and well defined than that of bare GC electrode. The position of the anodic peak of UA at DEA modified GC electrode is shifted significantly and the currents are prominent than that of bare GC electrode.

4.8.2 Scan rate effect of UA at DEA modified GC electrode

The CVs of 2.5 mM UA in PBS (pH 7) at DEA modified electrode at different scan rates shown in figure 4.28. The scane rate and peak currents are represented in table 4.1.

From table 4.1 it is clear that the peak current of UA is gradually increased with the increased of scan rate. The peak current of UA increased with the increased of square root of scan rate ($v^{1/2}s^{-1/2}$) (Figure 4.29), the corresponding trend line is a straight line which does not passes through the origin indicates that the oxidation process of UA is an impurely diffusion controlled process.

4.8.3 Cyclic voltammetric behavior of PA at DEA modified GC electrode

Cyclic voltammogram of 2.5mM PA in PBS (pH 7) solution and only PBS at DEA modified GC electrode shown in figure 4.30. There is no peak for PBS but a sharp and well defined anodic and cathodic peak is observed for PA at 0.42 V and 0.17 V respectively.

4.8.4 Comparison of the CV of PA at bare and DEA modified GC electrode

Figure 4.31 shows the comparison between the behaviors of PA at bare and DEA modified GC electrode. At bare GC electrode PA gives an anodic and a cathodic peak at 0.51 V and -0.1 V having peak current 51 µA and 20 µA. But, at DEA modified GC electrode PA gives an anodic peak at 0.43 V having peak current 67 µA and a cathodic peak at 0.17 V having peak current 43 µA. It is clear that the anodic and cathodic peak of PA at DEA modified GC electrode is sharper and well defined than that of bare GC electrode. The position of the anodic peak of PA at DEA modified GC electrode is shifted significantly and the currents are prominent than that of bare GC electrode.

4.8.5 Scan rate effect of PA at DEA modified GC electrode

The CVs of 2.5 mM PA in PBS (pH 7) at different scan rates shown in figure 4.32 at DEA modified GC electrode. The scane rate and peak currents are represented in table 4.2.

From table 4.2 it is clear that the anodic and cathodic peak currents of PA is gradually increased with the increased of scan rate. The peak current of PA increased with the increased of square root of scan rate ($v^{1/2}s^{-1/2}$) (Figure 4.33), the corresponding trend lines are straight lines and they are not pass through the origin indicates that the redox process of PA is an impurely diffusion controlled process.

4.8.6 Cyclic voltammetric behavior of TD at DEA modified GC electrode

Cyclic voltammogram of 2.5mM TD in PBS (pH 7) solution and only PBS at DEA modified GC electrode shown in figure 4.34. There is no peak for PBS but a sharp and well defined peak is observed for TD at 1.3 V.

4.8.7 Comparison of the CV of TD at bare and DEA modified GC electrode

Figure 4.35 shows the comparison between the behaviors of TD at bare and DEA modified GC electrode. At bare GC electrode TD gives an anodic peak at 1.3 V having peak current 15 µA. But, at DEA modified GC electrode TD gives an anodic peak at 0.89 V having peak current 21 µA. It is clear that the anodic peak of TD at DEA modified GC electrode is sharper and well defined than that of bare GC electrode. The position of the anodic peak of TD at DEA modified GC electrode is shifted significantly and the currents are prominent than that of bare GC electrode.

4.8.8 Scan rate effect of TD at DEA modified GC electrode

The CVs of 2.5 mM TD in PBS (pH 7) at different scan rates shown in figure 4.36 at DEA modified GC electrode. The scane rate and peak currents are represented in table 4.3.

From table 4.3 it is clear that the peak current of TD is gradually increased with the increased of scan rate. The peak current of TD increased with the increased of square root of scan rate ($v^{1/2}s^{-1/2}$) (Figure 4.37), the corresponding trend line is a straight line which is not passed through the origin indicates that the oxidation process of TD is an impurely diffusion controlled process.

4.9 Simultaneous detection of UA, PA and TD at DEA modified GC electrode using CV

4.9.1 Simultaneous detection of PA and TD at DEA modified GC electrode using CV

CV of a binary mixture (2.5 mM) of PA and TD at bare GC and DEA modified GC electrode shows in figure 4.38. The CVs of PA, TD and the binary mixture (2.5 mM) of PA and TD in PBS at DEA modified GC electrode is shown in figure 4.39. For the mixture of PA and TD, there two peak were observed at +0.43 V and +1.3 V at bare GC electrode. But the peak of TD was not found as sharp as modified GC electrode performed. At DEA modified GC electrode, PA and TD gives two anodic peaks +0.41 V and +0.89 V respectively, and one cathodic peak at +0.17 V. From the positions of the anodic and

cathodic peaks it can be explained that the peaks of both PA and TD are separated at DEA modified GC electrode. The DEA modified GC electrode can separate the peaks of PA and TD when they are present in a mixture.

4.9.2 Simultaneous detection of UA and TD at DEA modified GC electrode using CV

CV of a binary mixture (2.5 mM) of UA and TD in PBS both at bare GC and DEA modified GC electrode shows in figure 4.40. The CVs of UA, TD and their binary mixture (2.5 mM) at DEA modified GC electrode shows in figure 4.41. At DEA modified GC electrode UA and TD shows two anodic peaks at +0.34 V and +1.2 V respectively. The peak currents of UA and TD are 83 µA and 35 µA. Binary mixture of UA and TD shows two peaks at +0.29 V and +0.89 V for their difference of oxidation potential. The peak currents of UA and TD were 60 µA and 24 µA at bare GC electrode. From the positions and currents of the peaks it can be explained that the peaks of both UA and TD are sharp and well defined at DEA modified GC electrode having peak current prominent than that of bare GC electrode. So DEA modified GC electrode can determine the amount of UA and TD accurately compared to bare GC electrode.

4.9.3 Simultaneous detection of UA and PA at DEA modified GC electrode using CV

CV of a binary mixture (2.5 mM) of UA and PA at bare GC and DEA modified GC electrode shows in figure 4.42. The CVs of UA, PA and their binary mixture (2.5 mM) at DEA modified GC electrode shows in figure 4.43. At DEA modified GC electrode the binary mixture of UA and PA shows one anodic peaks +0.42 V and a small peak at +0.34 which indicate the position of UA. Binary of UA and PA shows two oxidation peaks at +0.34 V and + 0.42 V for their difference of oxidation potential. From the positions and currents of the peaks it can be explained that the peaks of both UA and PA are sharp and well defined at DEA modified GC electrode having peak current prominent than that of bare GC electrode. So DEA modified GC electrode can determine the amount of UA and PA accurately compared to bare GC electrode.

4.9.4 Simultaneous detection UA, PA and TD ternary solution at DEA modified GC electrode using CV

CV of a ternary mixture (2.5 mM) of UA, PA and TD in PBS both at bare GC and DEA modified GC electrode shows in figure 4.44. The CVs of UA, PA and TD and their ternary mixture (2.5 mM) at DEA modified GC electrode shows in figure 4.45. At DEA modified GC electrode ternary mixture of UA, PA and TD shows three anodic peaks +0.34 V, +0.42 and +0.89 V respectively. In figure 4.45, the positions and currents of the peaks indicates that the DEA modified GC electrode can separate the peaks with good sensitivity compared to the bare GC electrode. So, DEA modified GC electrode can be used to simultaneous detection of UA, PA and TD in a ternary mixture.

4.10 Simultaneous detection of UA, PA and TD at DEA modified GC electrode using differential pulse voltammetric (DPV) technique

4.10.1 Simultaneous detection of UA and PA at DEA modified GC electrode using DPV

DPVs of a binary mixture (2.5 mM) of UA and PA at bare GC and DEA modified GC electrode shows in figure 4.46. The DPVs of UA, PA and their binary mixture (2.5 mM) at DEA modified GC electrode shows in figure 4.47. Binary mixture of UA and PA shows two anodic peaks at +0.27 V and +0.38 V respectively. For the mixture of UA and PA, there only one peak was observed at +0.49 V that was the overlapped peak of both UA and PA at bare GC electrode. In figure 4.47, the positions of the anodic peaks indicates that the peaks of both UA and PA are separated at DEA modified GC electrode. The DEA modified GC electrode can separate the peaks of UA and PA when they are present in a mixture using DPV technique.

4.10.2 Simultaneous detection of PA and TD at DEA modified GC electrode using DPV

DPVs of a binary mixture (2.5 mM) of PA and TD at bare GC and DEA modified GC electrode shows in figure 4.48. The DPVs of PA, TD and their binary mixture (2.5 mM) at DEA modified GC electrode shows in figure 4.49. At DEA modified GC electrode, binary

mixture of PA and TD shows two anodic peaks +0.38 V and +0.79 V respectively. The peak currents of PA and TD are 55 µA and 18 µA at DEA modified GC electrode. From the positions and currents of the peaks (Figure 4.49) it can be explained that the peaks of both PA and TD are sharp and well defined at DEA modified GC electrode having peak current prominent than that of bare GC electrode. So DEA modified GC electrode can determine the amount of PA and TD accurately compared to bare GC electrode using DPV technique.

4.10.3 Simultaneous detection of UA and TD at DEA modified GC electrode using DPV

DPV of a binary mixture (2.5 mM) of UA and TD at bare GC and DEA modified GC electrode shows in figure 4.50. The DPVs of UA, TD and their binary mixture (2.5mM) at DEA modified GC electrode shows in Figure 4.51. At DEA modified GC electrode binary mixture of UA and TD shows two anodic peaks +0.28 V and +0.81 V respectively. The peak currents of UA and TD are 70 µA and 16 µA. From the positions and currents of the peaks (Figure 4.51) it can be explained that the peaks of both UA and TD are sharp and well defined at DEA modified GC electrode having peak current prominent than that of bare GC electrode. So DEA modified GC electrode can determine the amount of UA and TD accurately compared to bare GC electrode using DPV technique.

4.10.4 Simultaneous detection UA, PA and TD at DEA modified GC electrode using DPV

DPV of a ternary mixture (2.5 mM) of UA, PA and TD in PBS both at bare GC and DEA modified GC electrode shows in figure 4.52. The DPVs of UA, PA and TD and their ternary mixture (2.5 mM) at DEA modified GC electrode shows in figure 4.53. At DEA modified GC electrode ternary mixture of UA, PA and TD shows three anodic peaks +0.27 V, +0.38 V and +0.810 V respectively. The peak currents of UA, PA and UA are 27 µA, 32 µA and 16 µA. For the mixture of UA, PA and TD, two peaks were observed at +0.50 V and +1.1 V respectively at bare GC electrode. In figure 4.53, the positions and currents of the peaks indicates that the DEA modified GC electrode can separate the peaks with high sensitivity compared to the bare GC electrode. So, DEA modified GC electrode can

be used to simultaneous detection (qualitative & quantitative) of UA, PA and TD in a ternary mixture using DPV technique.

4.11 Quantitative estimation of UA, PA and TD at DEA modified GC electrode in binary and ternary mixture

For the calculation sensitivity and detection limits of the analytes we need the surface area of DEA modified GC electrode. The surface area experiments are given below,

4.11.1 Electrode (modified with DEA) surface area calculation:

Figure 4.54 shows the CVs of potassium ferrocyanide in KCl solution and table 4.4 shows the peak current of potassium ferrocyanide at different scan rate at DEA modified GC electrode.

Electrode surface area was calculated Randles–Sevcik equation using ferrocyanide at different scan rate in 1M KCl solution.

In general, the peak current of diffusion controlled reversible or quasi-reversible electro - chemical reaction follows Randles–Sevcik equation

$$Ip = 0.4463nF\sqrt{\frac{nFD}{RT}}AC\sqrt{v} \quad \text{----------} \quad (1)$$

Where Ip: the peak current, n: the number of electrons, F: Faraday constant, T: the temperature in Kelvin, R: the gas constant, A: the surface area of the working electrode, D: the diffusion coefficient of the electroactive species, C: the bulk concentration of the electroactive species and *v*: the scan rate of voltammograms.

From Equation (1) we get,

$$Slope = 0.4463nF\sqrt{\frac{nFD}{RT}}AC$$

$$A = \frac{\text{Slope}}{0.4463nF\sqrt{\frac{nFD}{RT}}C}$$

From the curve (Figure 4.55) the value of slope is ~8.07×10^{-5} and the standard value of diffusion coefficient for ferricyanide in GCE is 1.52×10^{-6} cm^2/s. where concentration C = 2×10^{-6} mol/cm^3 so we get,

$$A = \frac{8.07\times10^{-5}}{0.4463\times1\times96500\sqrt{\frac{1\times96500\times 1.52\times10^{-6}}{8.314\times 298}}\times2\times10^{-6}}$$

A = 0.12 cm^2

Bare GC electrode (diameter = 3mm) has the surface area 0.071 cm^2. Surface area of DEA modified GC electrode is 0.12 cm^2 indicates that the surface area of GC electrode increased after modify.

4.11.2 Simultaneous quantitative estimation of UA and PA at DEA modified GC electrode

DPVs of simultaneous change of UA and PA (0.5-2.5 mM) shown in figure 4.56. Peak currents of UA and PA were increased linearly with the increase of their concentrations. The linear regression equation for UA and PA is Ip (UA) =20.87UA+16.80 (R^2= 0.990) and Ip (PA) =15.03PA+13.57 (R^2= 0.991) (Figure 4.57). The average current increase for UA and PA is 8.83 µA and 10.5 µA. The sensitivity was calculated for the binary mixture of UA and PA. The sensitivity of UA and PA are 73.5 µA/mM/cm^2 and 87.5 µA/mM/cm^2. Limit of detection (LoD) was calculated by signal to noise ratio (S/N=3). The LoD of UA and PA are 1.6 µmol L^{-1} and 1.14 µmol L^{-1}.

4.11.3 Simultaneous quantitative estimation of PA and TD at DEA modified GC electrode

DPVs of simultaneous change of PA and TD (0.5-2.5 mM) shown in figure 4.58. Peak currents of PA and TD were increased linearly with the increase of their concentrations. The linear regression equation for PA and TD is Ip (PA) =11.89PA+33.44 (R^2= 0.992) and Ip (TD) =3.562TD+4.121 (R^2= 0.980) (Figure 4.59). The average current increase for PA

and TD is 7.12 µA and 3.20 µA. The sensitivity was calculated for the binary mixture of PA and TD. The sensitivity of PA and TD are 59.33 µA/mM/cm^2 and 26.67 µA/mM/cm^2. Limit of detection (LoD) was calculated by signal to noise ratio (S/N=3). The LoD of PA and TD are 1.86 µmol L^{-1} and 2.05 µmol L^{-1}.

4.11.4 Simultaneous quantitative estimation of UA and TD at DEA modified GC electrode

DPVs of simultaneous change of UA and TD (0.5-2.5 mM) shown in figure 4.60. Peak currents of UA and TD were increased linearly with the increase of their concentrations. The linear regression equation for UA and TD is Ip (UA) =18.65UA+24.39 (R^2= 0.999) and Ip (TD) =3.216TD+3.97 (R^2= 0.992) (Figure 4.61). The average current increase for UA and TD is 9.25 µA and 2.77 µA. The sensitivity was calculated for the binary mixture of UA and TD. The sensitivity of UA and TD are 77.08 µA/mM/cm^2 and 23.08 µA/mM/cm^2. Limit of detection (LoD) was calculated by signal to noise (S/N=3) ratio. The LoD of UA and TD are 1.05 µmolL^{-1} and 2.22 µmolL^{-1} respectively.

4.12 Quantitative estimation of UA, PA and TD in ternary mixture at DEA modified GC electrode

4.12.1 Quantitative estimation of UA at constant PA+TD concentration at DEA modified GC electrode

DPV of the ternary mixture of UA, PA and TD at DEA modified GC electrode shown in figure 4.62 where concentration of PA and TD were kept constant and the concentration of UA was varied successively. Figure 4.63 shows the calibration curve for different concentrations of UA. This calibration curve can be used to determine UA in presence of PA and TD quantitatively in a ternary mixture. In case of UA the peak current increases with a linear regression equation Ip (UA) = 8.506UA+1.399 (R^2= 0.988).

4.12.2 Quantitative estimation of PA at constant UA+TD concentration at DEA modified GC electrode

DPV of the ternary mixture of UA, PA and TD at DEA modified GC electrode shown in figure 4.64 where concentration of UA and TD were kept constant and the concentration of PA was varied successively. Figure 4.65 shows the calibration curve for different concentrations of PA. This calibration curve can be used to determine PA in presence of UA and TD quantitatively in a ternary mixture. In case of PA the peak current increases with a linear regression equation Ip (PA) = 14.42PA-2.212 (R^2= 0.991).

4.12.3 Quantitative estimation of TD at constant UA+PA concentration at DEA modified GC electrode

DPV of the ternary mixture of UA, PA and TD at DEA modified GC electrode shown in figure 4.66 where concentration of UA and PA were kept constant and the concentration of TD was varied successively. Figure 4.67 shows the calibration curve for different concentrations of TD. This calibration curve can be used to determine TD in presence of UA and PA quantitatively in a ternary mixture. In case of TD the peak current increases with a linear regression equation Ip (TD) = 3.568TD+1.214 (R^2= 0.998).

4.12.4 Quantitative estimation of UA+PA at constant TD concentration at DEA modified GC electrode

DPV of the ternary mixture of UA, PA and TD in DEA modified GC electrode shown in figure 4.68 where concentration of TD was kept constant and the concentration of UA and PA was varied successively. Figure 4.69 shows the calibration curve for different concentrations of UA and PA. This calibration curve can be used to determine UA and PA in presence of TD quantitatively in a ternary mixture. In case of UA and PA the peak current increases with a linear regression equation Ip (UA) = 7.982UA+4.337 (R^2= 0.990) and Ip (PA) = 10.02PA+4.941 (R^2= 0.994).

4.12.5 Quantitative estimation of PA+TD at constant UA concentration at DEA modified GC electrode

DPV of the ternary mixture of PA, TD and UA in PBS at DEA modified GC electrode shown in figure 4.70 where concentration of UA was kept constant and the concentration of PA and TD was varied successively. Figure 4.71 shows the calibration curve for different concentrations of PA and TD. This calibration curve can be used to determine PA and TD in presence of UA quantitatively in a ternary mixture. In case of PA and TD the peak current increases with a linear regression equation Ip (PA) = 13.99PA+0.531 (R^2= 0.997) and Ip (TD) = 3.344TD+1.956 (R^2= 0.982) respectively.

4.12.6 Quantitative estimation of UA+TD at constant PA concentration at DEA modified GC electrode

DPV of the ternary mixture of PA, TD and UA in PBS at DEA modified GC electrode shown in figure 4.72 where concentration of PA was kept constant and the concentration of UA and TD was varied successively. Figure 4.73 shows the calibration curve for different concentrations of UA and TD. This calibration curve can be used to determine UA and TD in presence of PA quantitatively in a ternary mixture. In case of UA and TD the peak current increases with a linear regression equation Ip (UA) = 8.818UA+0.857 (R^2= 0.989) and Ip (TD) = 2.764TD+1.942 (R^2= 0.991).

4.12.7 Simultaneous quantitative estimation of UA, PA and TD at DEA modified GC electrode in a ternary mixture

DPV of the ternary mixture of the different concentrations of PA, TD and UA in PBS at DEA modified GC electrode shown in figure 4.74. The calibration curve for different concentrations of UA, PA and TD showed in figure 4.75. These calibration curve can be used to determine UA, PA and TD quantitatively in a ternary mixture. The anodic currents of UA, PA and TD increased linearly with increasing their concentrations over the range of 0.5-2.5mM. The linear regression equation of UA, PA and TD are Ipa = $6.374C_{UA}$ + 11.42 (R^2 = 0.981), Ipa = $7.144C_{PA}$ + 12.78 (R^2=0.990) and Ipa = $3.172C_{TD}$+ 2.128 (R^2 = 0.991),

respectively. The sensitivity of UA, PA and TD are 52.08 µA/mM/cm^2, 62.25 µA/mM/cm^2 and 33.67 µA/mM/cm^2 and detection limits are 1.95 µmol L^{-1}, 1.45 µmol L^{-1} and 1.26 µmol L^{-1} respectively.

The linear regression equations of the calibration curves for single concentration change, binary concentration change and ternary concentration changes are nearly equal, indicating that they do not interfere in the determination of each other. So, this modified electrode can be used to determine the target analytes (UA, PA and TD) individually, in a binary mixture and simultaneously in a ternary mixture.

4.13 Interference study

Figure 4.76 shows the DPV of the ternary solution of UA, PA and TD in the presence of aspirin, lysine, arginine, glycine, thiamine (vitamin B1), nicotinamide (vitamion B3), dopamine (DA) and glucose as interfering agents. From the voltammogram it is clear that the peak position of UA (0.27 V), PA (0.38 V) and TD (0.81 V) are not influenced by the interfering substances. The peak positions are remaining unchanged like they appeared when no interfering substances present (Figure 4.9). An oxidation peak appeared for dopamine at 0.18 V without interfering the peaks positions of UA, PA and TD. So, DEA modified GC electrode does not show any interference in the peak potential range of UA, PA and TD by the mentioned interfering substances.

4.14 Quantitative Analysis of real and tablet samples

Quantitative analysis in real (tablet and blood, human urine) samples were done by using this method. For each analyte recovery percentage (R %) and standard deviation (SD) was calculated to evaluate the consistency of the modified electrode sensor. The quantitative determination of each tablet samples was valided by UV-Vis method and the quantitative determination of UA in blood was valid by pathological report.

4.14.1 Quantitative analysis of paracetamol in standard and tablet samples

4.14.1.1 Quantitative analysis of standard PA

DPVs of different amount of standard PA in 50 mL PBS (pH 7) under optimum condition are shown in figure 4.77. Table 4.5 shows the current for different amount of PA. Figure 4.78 shows the calibration curve of PA with response to different amount. The regression equation for the calibration curve of PA is Ip = 1.453x+57.53 (R^2=0.988). This equation was used to determine the unknown amount in the real and tablet samples where, "Ip" is the current of the sample and "x" is the amount.

Table 4.6 shows the recovery percentage data of standard PA calculated from the regression equation of the calibration curve. The recovery percentage is found 98-102% indicates that the modified electrode has the ability to determine the amount of PA with high accuracy.

Table 4.7 shows the data of the determination of known 30 mg standard PA sample (5 times) for standard deviation calculation. The standard deviation was found ±0.2 mg. It is clear that the sensor can determine the amount with high consistency.

4.14.1.2 Determination of PA in tablet samples using DEA modified GC electrode

For each determination 1/25 parts of the tablet was dissolved in 50 mL of PBS (pH 7).

Calculation of the amount

Figure 4.79 shows the DPVs of PA containing tablets sample in 50 mL PBS (pH 7) and table 4.8 shows the current of tablet samples.

PA in ATP tablet

The linear regression equation of PA (Figure 4.78) is Ip = 1.4538x+57.533 where, "Ip" is the current of the PA in ATP and "x" is the amount.

For ATP the current found 86.25μA.

So, x= (86.25-57.533)/1.4538

= 19.75 mg in 1/25 parts of the tablet. [For each determination 1/25 parts of the tablet was dissolved in 50 mL of PBS (pH 7)].

So, total amount of PA in ATP tablet is 25×19.75= 493.87 mg.

Same calculation for every tablet samples. Table 4.9 shows amount of PA in different tablet samples.

4.14.1.3 Determination of PA in tablet samples using UV-Vis method

For each determination 1/6 parts of the tablet was dissolved in 1000 mL of PBS (pH 7).

Figure 4.80 shows the UV-Vis spectra of different concentrations of PA using PBS (pH 7) as solvent. Table 4.10 shows the absorbance for different concentrations of PA. Figure 4.81 shows the calibration curve of PA with response to different concentration. The regression equation for the calibration curve of PA is A = 0.0075x+0.045 (R^2=0.9912). This equation was used to determine the unknown amount in the real and tablet samples where, "A" is the absorbance of the sample and "x" is the amount.

Table 4.11 shows the quantitative determination of PA in different commercial tablets of different pharmaceuticals using UV-Visible technique with standard deviations. Each replicates were repeated by 4 times. Table 4.12 also shows the comparison of the determination of PA using UV-Visible technique with the determination of PA using DEA modified GC electrode.

The table 4.12 shows the amount of PA using DEA modified GC electrode in commercial samples are very close or nearly equal to the determination of PA using UV-Visible method. So, DEA modified GC electrode sensor can be used in pharmaceuticals to determine the actual quantity of PA in relevant tablets.

4.14.2 Quantitative analysis of tramadol in standard and tablet samples

4.14.2.1 Quantitative analysis of standard TD

DPVs of different amount of standard TD in 50 mL PBS (pH 7) under optimum condition are shown in figure 4.82. Table 4.13 shows the current for different amount of TD.

Figure 4.83 shows the calibration curve of TD with response to different amount. The regression equation for the calibration curve of TD is Ip = 0.412x+1.819 (R^2=0.991). This equation was used to determine the unknown amount in the real and tablet samples where, "Ip" is the current of the sample and "x" is the amount.

Table 4.14 shows the recovery percentage data of standard TD using the regression equation of the calibration curve. The recovery percentage is found 98-102% indicates that the sensor has the ability to determine the amount of TD with high consistency.

Table 4.15 shows the data of the determination of known 20 mg standard TD samples (5 times) for standard deviation calculation. The standard deviation was found ±0.3 mg. It is clear that the sensor can determine the amount with high consistency.

4.14.2.2 Determination of TD in tablet samples using DEA modified GC electrode

For the determination of Anadol 1/5 parts and 2/5 parts for others of the tablets were dissolved in 50 mL of PBS (pH 7).

Calculation of the amount

Figure 4.84 shows the DPVs of TD containing tablets sample in 50 mL PBS (pH 7) and table 4.16 shows the current of tablet samples.

TD in Anadol tablet

The linear regression equation of TD (Figure 4.83) is Ip = 0.4125x+1.8193 where, "Ip" is the current of the TD in anadol and "x" is the amount.

For Anadol the current found 9.97μA.

So, x= (9.97-1.8193)/0.4125

x= 19.76 mg in 1/5 parts of the tablet. [For the determination 1/5 parts of the tablet was dissolved in 50ml of PBS (pH 7)].

So, total amount of TD in Anadol tablet is 5×19.76= 98.80 mg.

Same calculation for every tablet sample. Table 4.17 shows the amount of TD in different commercial tablets of different pharmaceuticals.

4.14.2.3 Determination of TD in tablet samples using UV-Vis method

For determination of Anadol 1/10 parts and 1/5 parts for others of the tablets were dissolved in 1000 mL of PBS (pH 7).

Figure 4.85 shows the UV-Visible spectra of different concentrations of TD using PBS as solvent. Table 4.18 shows the absorbance for different concentrations of TD. Figure 4.86 shows the calibration curve of TD. The regression equation for the calibration curve of TD is A = 0.0035x+0.2016 (R^2=0.9902). This equation was used to determine the unknown amount in the real and tablet samples where, "A" is the absorbance of the sample and "x" is the amount.

Table 4.19 shows the quantitative determination of TD in different commercial tablets of different pharmaceuticals using UV-Visible technique with standard deviations. Each replicates were repeated by 4 times. Table 4.19 also shows the comparison of the determination of TD using UV-Visible technique with the determination of TD using DEA modified GC electrode.

The table 4.19 shows the amount of TD determined using DEA modified GC electrode in commercial samples are very close or nearly equal to the determination of TD using UV-Visible method. So, DEA modified GC electrode sensor can be used in pharmaceuticals to determine the actual quantity of TD in relevant tablets.

4.14.3 Simultaneous quantitative determination of Paracetamol and Tramadol in standard and combined tablet samples

4.14.3.1 Quantitative analysis of standard PA+TD at DEA modified GC electrode

DPVs of different amount of standard PA+TD in 50 mL PBS (pH 7) under optimum condition are shown in figure 4.87. Table 4.20 shows the peak current for different amount of PA and TD. Figure 4.88 shows the calibration curve of PA with response to different amount. The regression equation for the calibration curve of PA is IPA = 0.960x+36.90 (R^2=0.995). This equation was used to determine the unknown amount in the real and tablet samples where, "IPA" is the current of the sample and "x" is the amount of PA in

unknown PA+TD samples. Figure 4.89 shows the calibration curve of TD with response to different amount. The regression equation for the calibration curve of TD is ITD = 0.647x+1.573 (R^2=0.986). This equation was used to determine the unknown amount in the real and tablet samples where, "ITD" is the current of the sample and "x" is the amount of TD in unknown PA+TD samples.

Table 4.21 shows the recovery percentage data of standard TD using the regression equation of the calibration curve (Figure 4.89). The recovery percentage is found 98-109% indicates that the sensor can determine the amount of TD in PA+TD solution with high accuracy.

Table 4.22 shows the data of the determination of known 10 mg standard TD samples (5 times) for standard deviation calculation. The standard deviation was found ±0.4 mg. it is clear that the sensor can determine the amount with high consistency.

4.14.3.2 Simultaneous determination of PA+TD in tablet samples using DEA modified GC electrode

Figure 4.90 shows the DPVs of PA, TD containing tablets sample in 50 mL PBS (pH 7) and table 4.23 shows the current of tablet samples. Table 4.23 shows the amount of PA and TD in different commercial PA+TD containing tablets of different pharmaceuticals. Simultaneous determination of PA and TD in tablet samples are not valid by UV-Visible method because of the λ_{max} of PA (287.5 nm) and TD (280 nm) are very close and overlapped peak found for binary solution of PA and TD. So, simultaneous determination of PA and TD is not possible by UV-Visible method.

4.14.4 Quantitative analysis of UA in standard and blood sample

4.14.4.1 Quantitative analysis of standard UA

DPV of different amount of standard UA in 50mL PBS (pH 7) under optimum condition are shown in figure 4.91. Table 4.24 shows the peak current for different amount of UA. Figure 4.92 shows the calibration curve of UA with response to different amount. The regression equation for the calibration curve of UA is Ip = 26.327x-6.9388 (R^2=0.9936).

This equation is used to determine the unknown amount in the real samples where, "Ip" is the peak current of the sample and "x" is the amount of the sample.

Table 4.25 shows the recovery percentage data of standard UA using the regression equation of the calibration curve. The recovery percentage is found 96-110% indicates that the modified electrode has the ability to determine the amount of UA with high accuracy.

Table 4.26 shows the data of the determination of known 10 mg standard UA sample (5 times) for the standard deviation calculation. The standard deviation was found ±0.5mg. It is clear that the sensor can determine the amount with high consistency.

4.14.4.2 Determination of UA in blood and Urine sample using DEA modified GC electrode

For the determination of UA in blood sample 7.5mL blood sample was dissolved in 22.5 mL PBS (pH 7) and the solution was diluted for 4 times. Figure 4.93 shows the DPV of UA in the blood sample in PBS (pH 7) at scan rate 0.1V/s. Pathological report for the determination of UA in blood sample has been shown in figure 4.94.

Calculation of the amount of UA in Blood sample

The linear regression equation of UA (Figure 4.92) is Ip = 26.327x-6.9388 where, "Ip" is the peak current of the UA in blood sample and "x" is the amount. The peak current found for the blood sample was 5.51 μA.

So, X= (5.51+6.9388)/26.327

X= 0.473 [For the determination of UA 7.5mL blood was dissolved in 22.5mL PBS (pH 7)].

So, the amount of UA in 30 mL solution is 0.473×4= 1.89 and the total amount of UA in 100 mL or 1dl solution is (1.89×100)/30= 6.3 mg.

The amount of UA in the same blood sample was checked from a pathology. Table 4.27 shows the comparison among the amounts of UA determined by using DEA modified GC electrode with the amount of UA given by the pathological report and previously determined in our laboratory.

Calculation of the amount of UA in Urine sample

Urine was collected for 24 hours. Figure 4.95 shows the DPV of UA in urine sample in PBS (pH 7) at scan rate 0.1V/s. Normal level of uric acid excrete in urine (mg/24 hours) is 250-750 [96-97]. Table 4.28 shows the Comparison of the amount of UA determined by DEA modified GC electrode with normal uric acid level in the urine.

The linear regression equation of UA (Figure 4.92) is Ip = 26.327x-6.9388. The peak current found for the Urine sample was 31.64 μA.

So, X= (31.64+6.9388)/26.327

= 1.47 (For the determination of UA 20 mL Urine was dissolved in 30 mL PBS).

So, the amount of UA in 50 mL solution is 1.47×2.5= 3.68 and the total amount of UA first eight hours is (3.68×1150)/50= 84.64 mg. In this way UA in urine was calculated with distance eight hours. The total amount of UA in urine by 24 hours was (84.64+81.85+92.61) = 259.10 mg.

Table 4.1: Peak current (Ip) of 2.5 mM UA in PBS at DEA modified GC electrode at different scan rates.

Scan Rate (v/s)	Sq. root of scan rate ($v^{1/2}s^{-1/2}$)	Peak Current Ip (µA)
0.05	0.22	57.37
0.10	0.32	81.62
0.15	0.39	98.63
0.20	0.45	120.18
0.25	0.50	135.13

Table 4.2: Peak current (Ipa and Ipc) of 2.5 mM PA in PBS at DEA modified GC electrode at different scan rates.

Scan rate (v/s)	Sq. root of scan rate ($v^{1/2}s^{-1/2}$)	Ipa (µA)	Ipc (µA)
0.05	0.22	56.12	-18.93
0.10	0.32	78.72	-34.19
0.15	0.39	103.12	-48.18
0.20	0.45	125.08	-60.63
0.25	0.50	140.55	-69.64

Table 4.3: Peak current (Ip) of 2.5 mM TD in PBS at DEA modified GC electrode at different scan rates.

Scan Rate (v/s)	Sq. root of scan rate ($v^{1/2}s^{-1/2}$)	Peak Current Ip (µA)
0.05	0.22	41.56
0.10	0.32	55.62
0.15	0.39	66.44
0.20	0.45	74.11
0.25	0.50	81.72

Table 4.4: Peak current (Ipa and Ipc) of 2 mM Ferrocyanide in KCL at DEA modified GC electrode at different scan rates.

Scan rate (v/s)	Sq. root of scan rate ($v^{1/2}/s^{1/2}$)	Ipa (µA)	Ipc (µA)
0.05	0.22	19.42	-16.57
0.10	0.32	27.20	-25.82
0.15	0.39	32.43	-30.66
0.20	0.45	37.54	-35.72
0.25	0.50	42.24	-40.43

Table 4.5: Amount (mg) and peak current (Ip) of PA in PBS at DEA modified GC electrode.

Amount (mg)/ 50 mL	Current (µA)
10.00	69.76
15.00	80.01
20.00	86.91
25.00	96.77
30.00	101.52
35.00	108.29
40.00	113.88

Table 4.6: Recovery percentage of the determination of standard PA using DEA modified GC electrode.

Amount (mg)	Added (mg)	Total (mg)	Amount found (mg)	Recovery (%)
20	0	20	20.1	100.5
20	5	25	25.2	100.8
20	10	30	30.5	101.7
20	15	35	35.4	101.1
20	20	40	39.8	99.5

Table 4.7: Standard deviation of the determination of standard PA using DEA modified GC electrode.

Standard PA (mg)	Current (µA)	Amount found (mg)	Average value (mg)	Standard deviation (±mg)
30	101.87	30.3	30.0	0.2
30	102.06	30.6		
30	101.84	30.1		
30	101.35	29.6		
30	101.32	29.5		

Table 4.8: Peak Current (Ip) of PA in different tablet samples.

Tablet	Current (µA)
ATP	86.25
Fast	86.47
Pyralgin	86.21
Depyrin	86.52
Reset	86.56

Table 4.9: Amount found (mg) of PA in tablet samples of different pharmaceutical company using DEA modified GC electrode.

Tablets	Pharmaceutical name	Amount found (mg)	Labeled value (mg)
ATP	General	493.9	500.0
Fast	ACME	497.6	500.0
Pyralgin	Renata Ltd.	493.1	500.0
Depyrin	Delta Pharma	498.5	500.0
Reset	Incepta	499.2	500.0

Table 4.10: Concentration (ppm) and absorbance (A) of standard PA using UV-Vis method.

Concentration (ppm)	Absorbance (A)
40	0.252
50	0.339
60	0.419
70	0.512
80	0.623

Table 4.11: Determination of PA in different tablet samples using UV-Visible method.

Tablets	Pharmaceutical name	Observations No.	Absorbance (A)	Quantity (mg)	Average value ± SD (mg)	Labeled value (mg)
ATP	General	1	0.664	495.2	494.2 ±1.5	500.0
		2	0.664	495.2		
		3	0.661	492.8		
		4	0.662	493.6		
Fast	ACME	1	0.666	496.8	497.8 ±0.8	500.0
		2	0.667	497.6		
		3	0.669	499.2		
		4	0.667	497.6		
Pyralgin	Renata	1	0.659	492.9	493.5 ±1.4	500.0
		2	0.663	493.3		
		3	0.665	494.7		
		4	0.667	491.3		
Depyrin	Delta Pharma	1	0.674	502.6	500.9 ±0.5	500.0
		2	0.674	500.6		
		3	0.672	500.2		
		4	0.672	500.2		
Reset	Incepta	1	0.676	503.1	502.4 ±0.8	500.0
		2	0.674	502.5		
		3	0.659	501.7		
		4	0.662	502.3		

Table 4.12: Comparison of the amount of PA determined by DEA modified GC electrode sensor with UV-visible method

Tablets	Pharmaceutical name	Amount found by DEA modified GC electrode (mg)	Amount found by UV-Visible method (mg)	Labeled value (mg)
ATP	General	493.9 ±0.2	494.2±1.5	500.0
Fast	ACME	497.6 ±0.2	497.8±0.8	500.0
Pyralgin	Renata Ltd.	493.1±0.2	493.5±1.4	500.0
Depyrin	Delta Pharma	498.5±0.2	500.9±0.5	500.0
Reset	Incepta	499.2±0.2	502.4±0.8	500.0

Table 4.13: Amount (mg) and peak current (Ip) of TD in PBS at DEA modified GC electrode.

Amount (mg)/50 mL	Current (µA)
5.0	3.38
10.0	6.18
15.0	8.35
20.0	10.39
25.0	12.03
30.0	13.90

Table 4.14: Recovery percentage of the determination of standard TD using DEA modified GC electrode.

Amount (mg)	Added (mg)	Total (mg)	Amount found (mg)	Recovery (%)
20.0	0.0	20.0	20.4	102.0
20.0	5.0	25.0	24.8	99.2
20.0	10.0	30.0	30.1	100.3
20.0	15.0	35.0	35.6	101.7
20.0	20.0	40.0	39.7	99.3

Table 4.15: Standard deviation of the determination of standard TD using DEA modified GC electrode.

Standard TD (mg)	Current (µA)	Amount found (mg)	Average Value (mg)	Standard deviation (±mg)
20.0	10.44	20.2	20.1	0.3
20.0	10.42	20.1		
20.0	10.43	20.2		
20.0	10.39	19.9		
20.0	10.42	20.1		

Table 4.16: Current (Ip) of TD in different tablet samples.

Tablet	Current (µA)
Anadol	9.97
Tranal	9.64
Dolonil	9.83
Syndol	9.91
Lucidol	9.66

Table 4.17: Amount found (mg) of TD in tablet samples of different pharmaceutical companies using DEA modified GC electrode.

Tablets	Pharmaceutical name	Amount found (mg)	Labeled value (mg)
Anadol	Square	98.80 ±0.3	100.0
Tranal	Opsonin Pharma	47.40±0.3	50.0
Dolonil	ACME	48.55±0.3	50.0
Syndol	Health care	49.03±0.3	50.0
Lucidol	Beximco	47.52±0.3	50.0

Table 4.18: Concentration (ppm) and absorbance (A) of standard TD using UV-Vis method.

Concentration (ppm)	Absorbance (A)
80	0.301
120	0.426
160	0.513
200	0.621
240	0.773

Table 4.19: Determination of TD in different tablet samples using UV-Visible method

Tablets	Pharmaceutical name	Observations No.	Absorbance (A)	Quantity (mg)	Average value ±SD (mg)	Labeled value (mg)
Anadol	Square	1	0.238	104.0	99.75±1.5	100.0
		2	0.236	98.29		
		3	0.237	101.14		
		4	0.235	95.43		
Tranal	Opsonin	1	0.235	47.71	47.00±0.8	50.0
		2	0.235	47.71		
		3	0.234	46.28		
		4	0.234	46.28		
Dolonil	ACME	1	0.238	52.0	48.79±1.4	50.0
		2	0.236	49.15		
		3	0.234	46.28		
		4	0.235	47.71		
Syndol	Health care	1	0.237	50.57	50.22±0.5	50.0
		2	0.238	52.0		
		3	0.636	49.15		
		4	0.636	49.15		
Lucidol	Beximco	1	0.236	49.15	47.36±0.8	50.0
		2	0.234	46.28		
		3	0.234	46.28		
		4	0.235	47.71		

Table 4.20: Amount (mg) and peak current (Ip) of the binary solution of PA and TD in PBS at DEA modified GC electrode.

Amount (mg) of PA+TD	Current (μA)	
	Paracetamol	Tramadol
5+1	41.84	2.07
10+2	45.85	3.01
15+3	51.81	3.62
20+4	56.60	4.12
25+5	60.48	4.75

Table 4.21: Recovery percentage of the determination of standard TD in PA+TD binary solution using DEA modified GC electrode.

Amount (mg)	Added (mg)	Total (mg)	Amount found (mg)	Recovery (%)
5	0	5	4.9	98.0
5	2	7	7.1	101.4
5	4	9	9.1	101.1
5	6	11	10.9	99.0
5	8	13	13.2	101.5

Table 4.22: Standard deviation of the determination of standard TD in PA+TD binary solution using DEA modified GC electrode.

Standard TD (mg)	Current value (µA)	Amount found (mg)	Average value (mg)	Standard deviation (±mg)
10	21.73	9.9	10.0	0.4
10	21.96	10.0		
10	22.43	9.8		
10	23.50	10.2		
10	23.02	10.1		

Table 4.23: Amount found (mg) of PA and TD in PA+TD tablet samples of different pharmaceutical company using DEA modified GC electrode.

Tablet	Pharmaceutical name	Current (µA)		Amount of PA+TD found (mg)	PA+TD labeled value (mg)
		Paracetamol	Tramadol		
Napadol	Beximco	68.07	3.94	324.41+36.58	325+37.5
Acetram	Square	67.98	3.91	323.47+36.12	325+37.5
Resadol	Incepta	67.93	3.92	322.95+36.28	325+37.5

Table 4.24: Amount (mg) and peak current (Ip) of UA in PBS at DEA modified GC electrode

Amount (mg)	Peak current (Ip/µA)
0.5	7.11
0.7	11.30
0.9	16.09
1.1	21.48
1.3	26.70

Table 4.25: Recovery percentage of the determination of standard UA using DEA modified GC electrode

Amount (mg)	Added (mg)	Total (mg)	Amount found (mg)	Recovery (%)
5.0	0.0	5.0	5.1	102.0
5.0	2.5	7.5	7.3	97.3
5.0	5.0	10.0	10.2	102.0
5.0	7.5	12.5	12.7	101.6
5.0	10.0	15.0	14.8	98.7

Table 4.26: Determination of the standard deviation of standard UA using DEA modified GC electrode

Standard UA (mg)	Peak current (Ip/µA)	Amount found (mg)	Average value (mg)	Standard deviation (±mg)
10	76.79	10.8	10.1	0.5
10	76.37	10.6		
10	74.77	9.2		
10	75.14	9.7		
10	74.86	10.2		

Table 4.27: Comparison of the amount of UA determined by DEA modified GC electrode sensor with Pathological report.

Sample	Amount found by DEA modified GC electrode (mg/dl)	Pathological report (mg/dl)
Blood	6.3	6.2

Table 4.28: Determination the total amount of UA in urine (mg/24).

Sample	Amount found by DEA modified GC electrode (mg/24 hours)	Normal uric acid level in the urine (mg/24 hours)
Urine	259.10	250-750

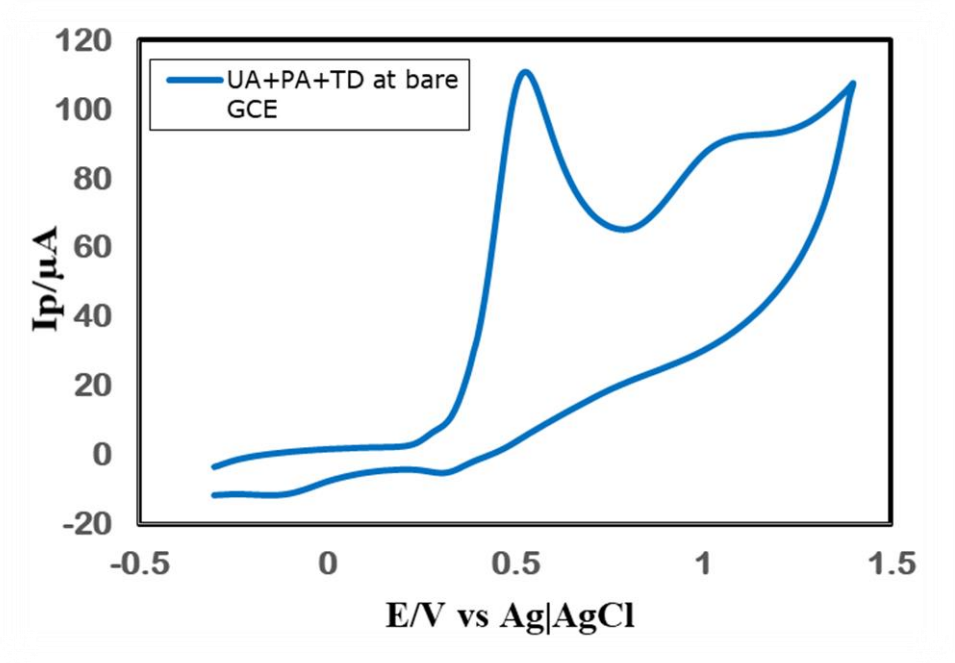

Figure 4.1: Cyclic voltammogram (CV) of 2.5 mM UA+ 2.5 mM PA+ 2.5 mM TD at bare GC electrode in phosphate buffer solution (PBS) (pH 7) and at scan rate 0.1V/s.

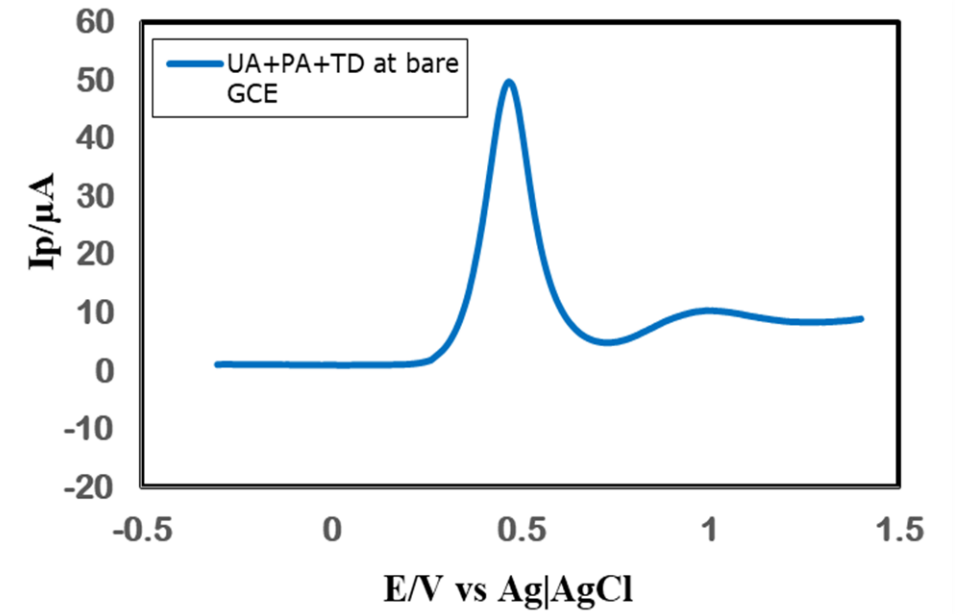

Figure 4.2: Differential pulse voltammogram (DPV) of 2.5 mM UA+ 2.5 mM PA+ 2.5 mM TD at bare GC electrode in phosphate buffer solution (PBS) (pH 7) and at scan rate 0.1V/s.

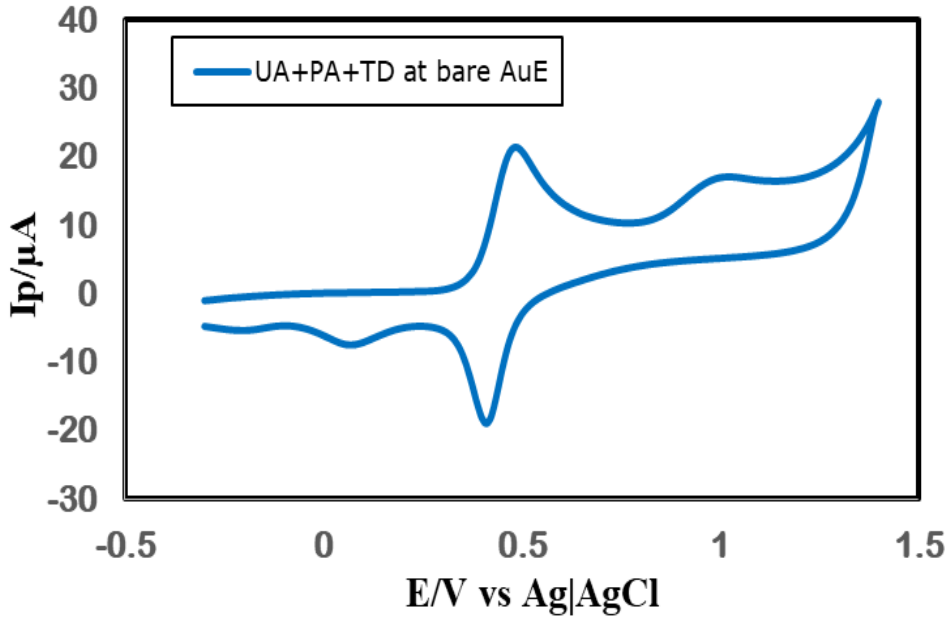

Figure 4.3: Cyclic voltammogram (CV) of 2.5 mM UA+ 2.5 mM PA+ 2.5 mM TD at bare Au electrode in phosphate buffer solution (PBS) (pH 7) and at scan rate 0.1V/s.

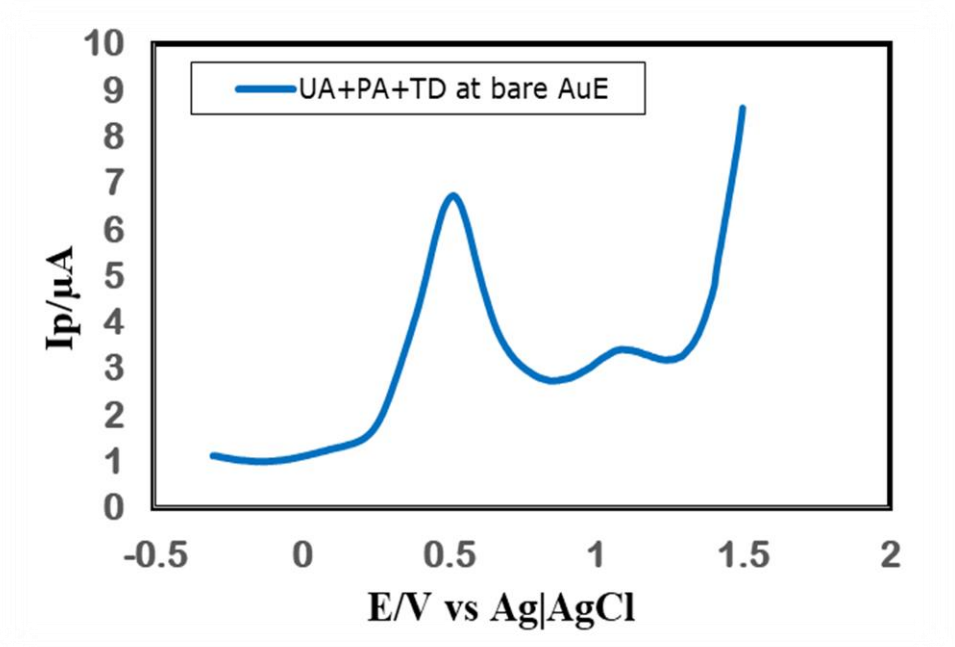

Figure 4.4: Differential pulse voltammogram (DPV) of 2.5 mM UA+ 2.5 mM PA+ 2.5 mM TD at bare Au electrode in phosphate buffer solution (PBS) (pH 7) and at scan rate 0.1V/s.

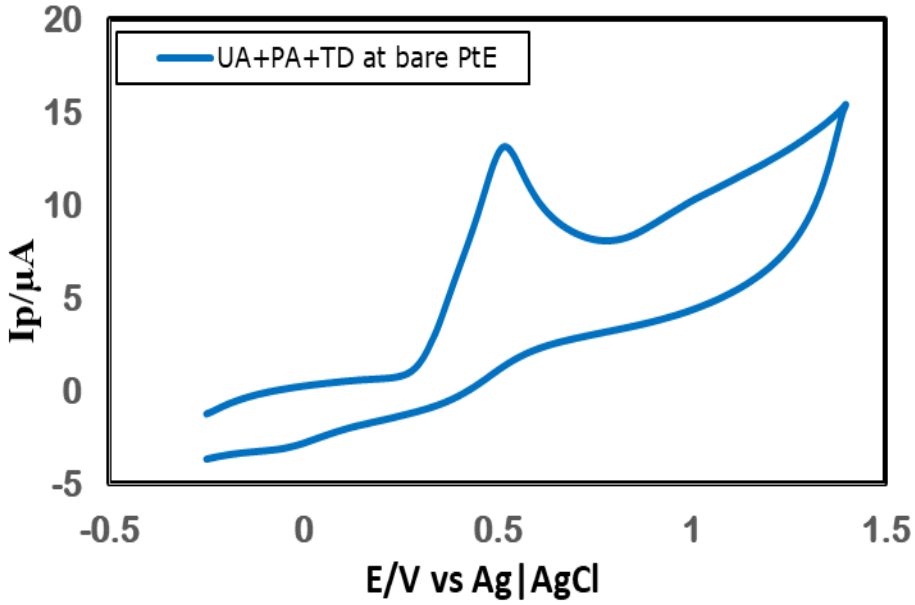

Figure 4.5: Cyclic voltammogram (CV) of 2.5 mM UA+ 2.5 mM PA+ 2.5 mM TD at bare Pt electrode in phosphate buffer solution (PBS) (pH 7) and at scan rate 0.1V/s.

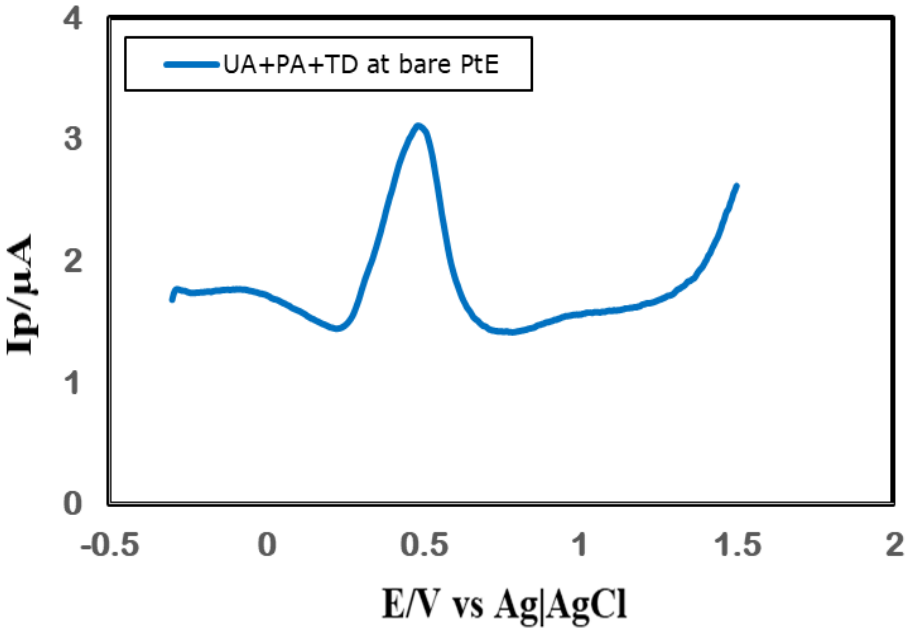

Figure 4.6: Differential pulse voltammogram (DPV) of 2.5 mM UA+ 2.5 mM PA+ 2.5 mM TD at bare Pt electrode in phosphate buffer solution (PBS) (pH 7) and at scan rate 0.1V/s.

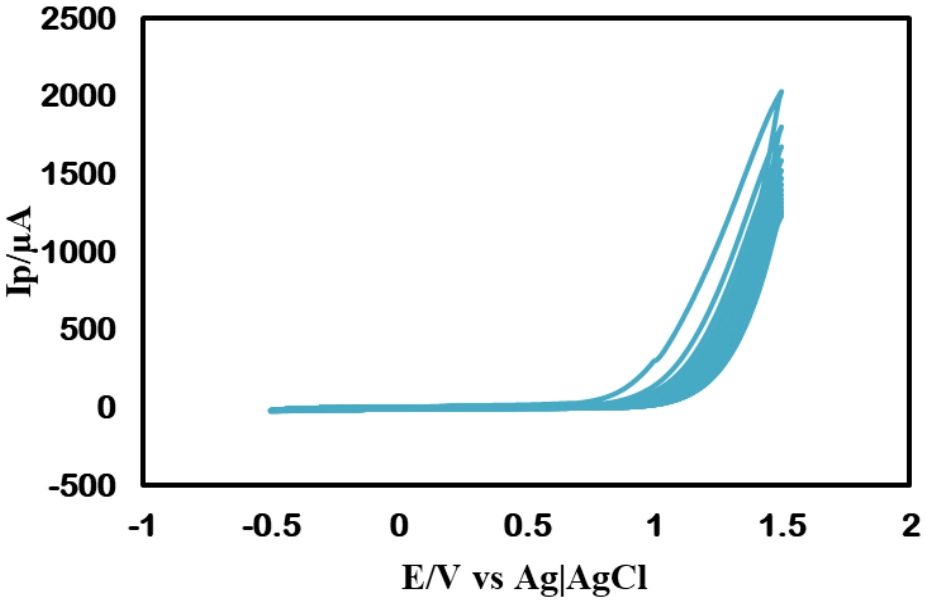

Figure 4.7: Cyclic voltammogram (CV) of Diethylamine (DEA) thin film growth on the surface of GC electrode at scan rate 0.2 V/s.

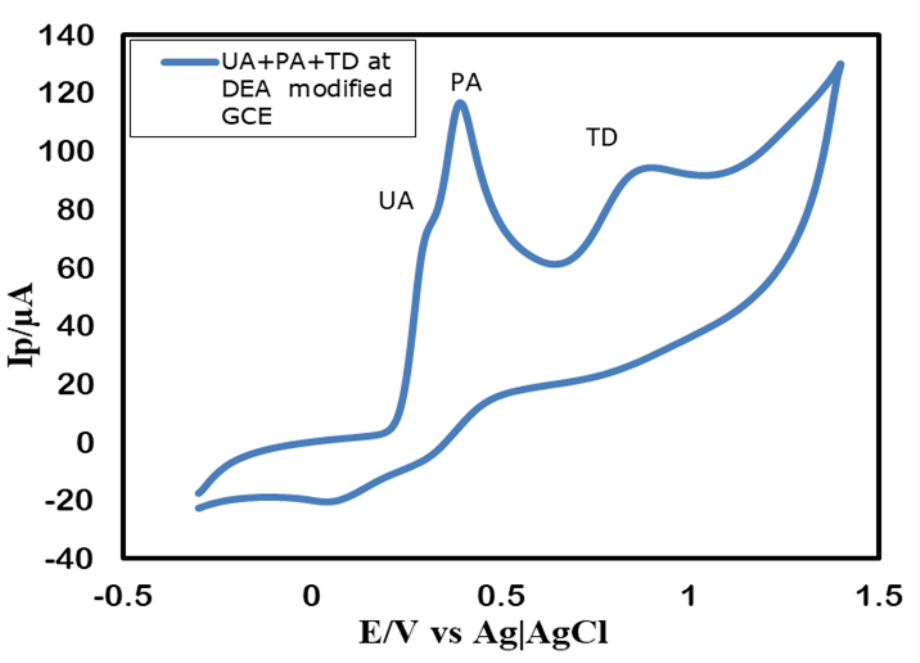

Figure 4.8: Cyclic voltammogram (CV) of 2.5 mM UA+ 2.5 mM PA+ 2.5 mM TD at DEA modified GC electrode in PBS (pH 7) and at scan rate 0.1V/s.

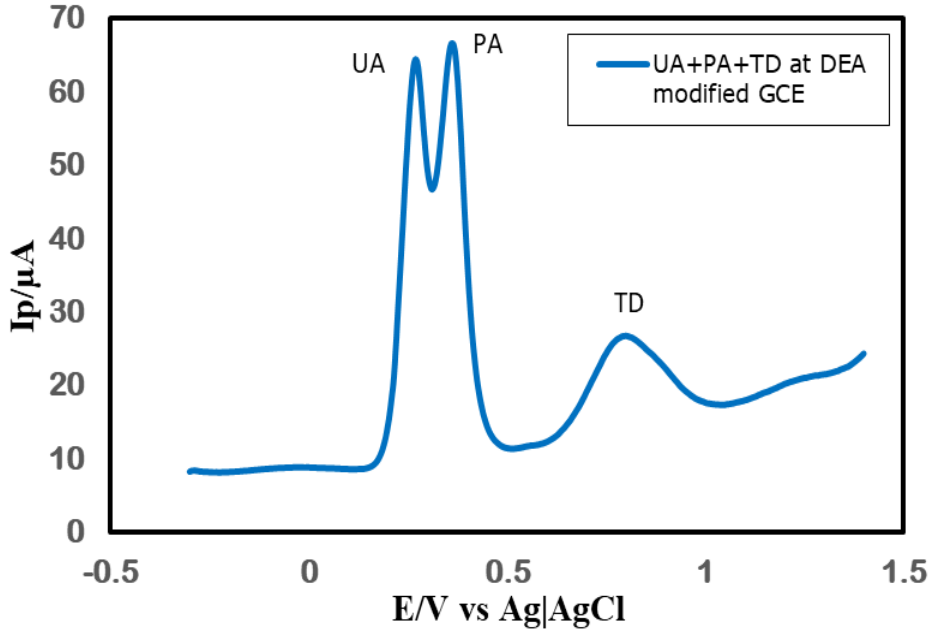

Figure 4.9: Differential pulse voltammogram (DPV) of 2.5 mM UA+ 2.5 mM PA+ 2.5 mM TD at DEA modified GC electrode in PBS (pH 7) and at scan rate 0.1V/s.

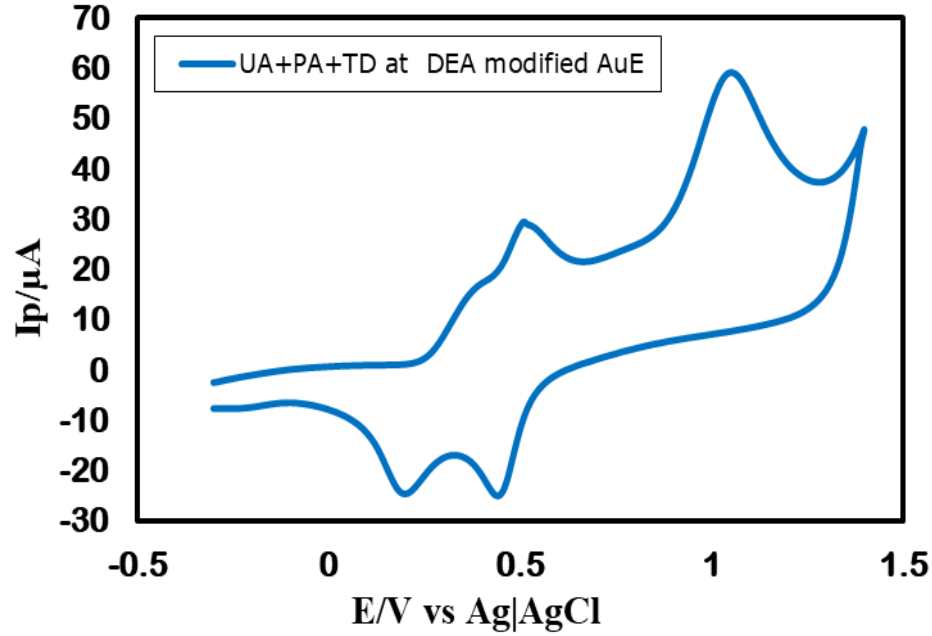

Figure 4.10: Cyclic voltammogram (CV) of 2.5 mM UA+ 2.5 mM PA+ 2.5 mM TD at DEA modified Au electrode in PBS (pH 7) and at scan rate 0.1V/s.

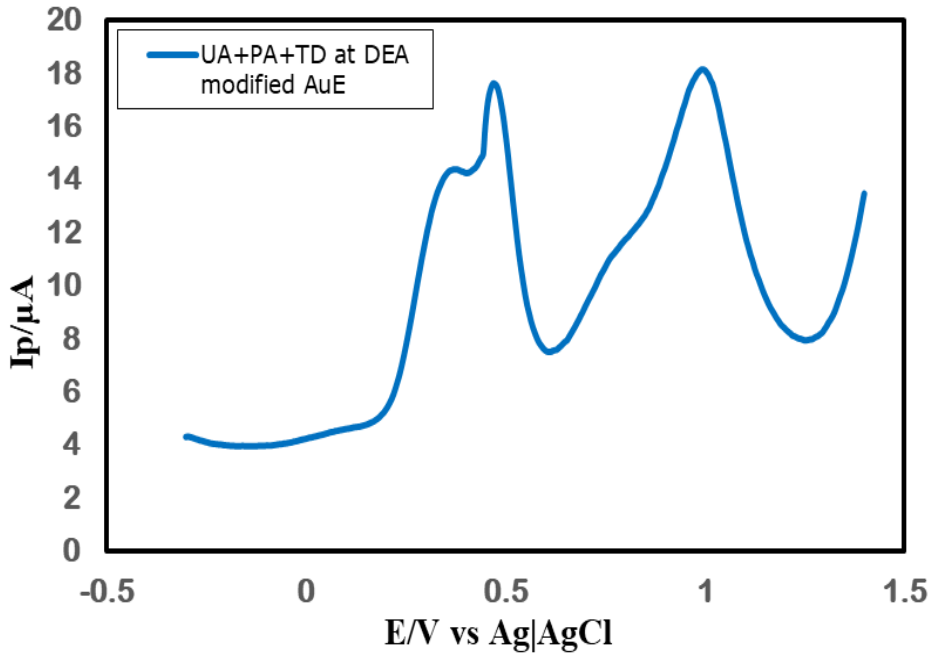

Figure 4.11: Differential pulse voltammogram (DPV) of 2.5 mM UA+ 2.5 mM PA+ 2.5 mM TD at DEA modified Au electrode in PBS (pH 7) and at scan rate 0.1V/s.

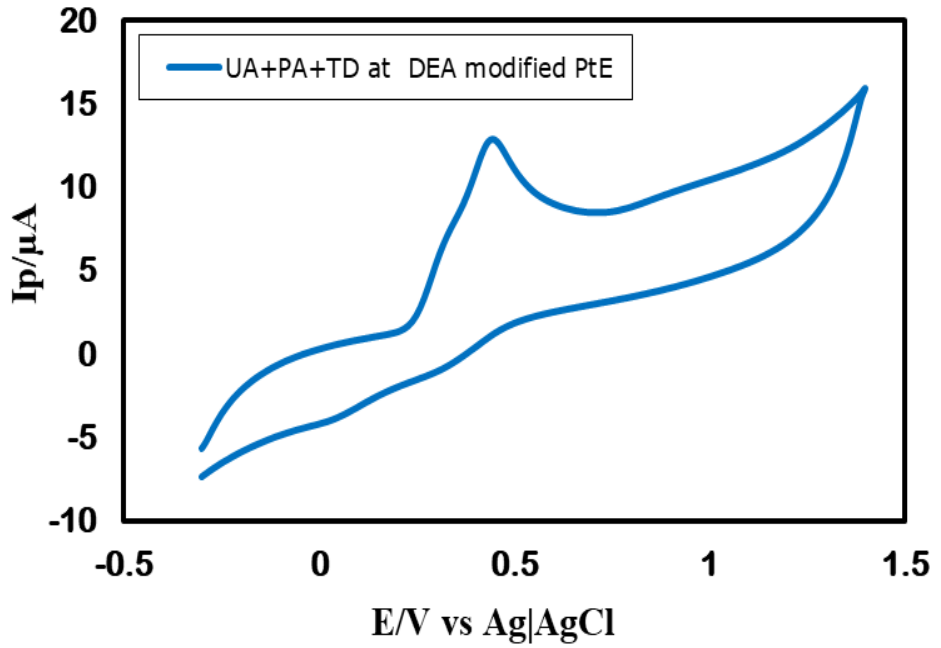

Figure 4.12: Cyclic voltammogram (CV) of 2.5 mM UA+ 2.5 mM PA+ 2.5 mM TD at DEA modified Pt electrode in PBS (pH 7) and at scan rate 0.1V/s.

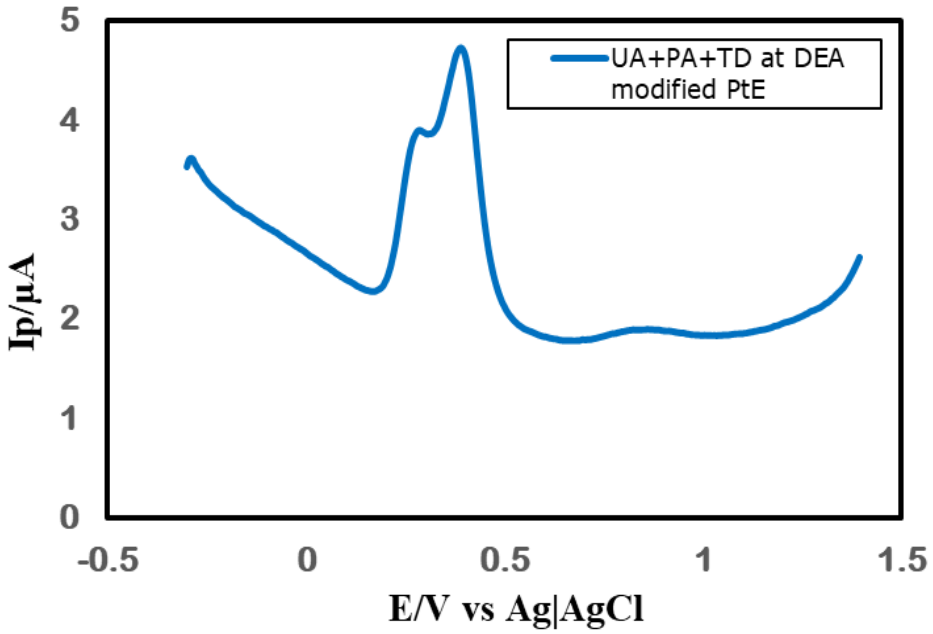

Figure 4.13: Differential pulse voltammogram (DPV) of 2.5 mM UA+ 2.5 mM PA+ 2.5 mM TD at DEA modified Pt electrode in PBS (pH 7) and at scan rate 0.1V/s.

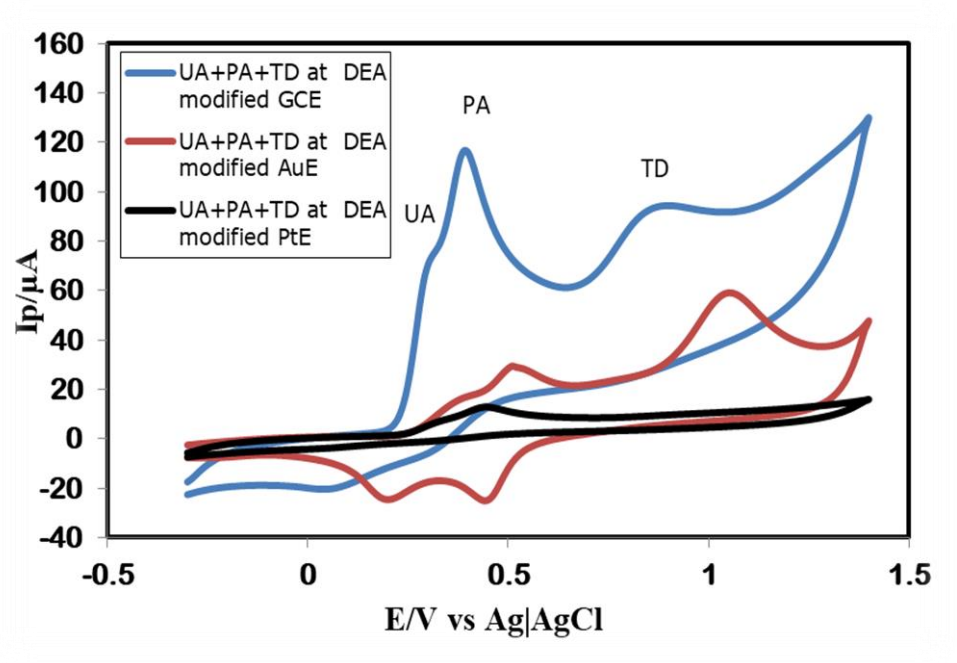

Figure 4.14: Cyclic voltammograms (CVs) of 2.5 mM UA+ 2.5 mM PA+ 2.5 mM TD in PBS (pH 7) at DEA modified GCE (blue line), DEA modified AuE (red line) and DEA modified PtE (black line) electrode at scan rate 0.1V/s.

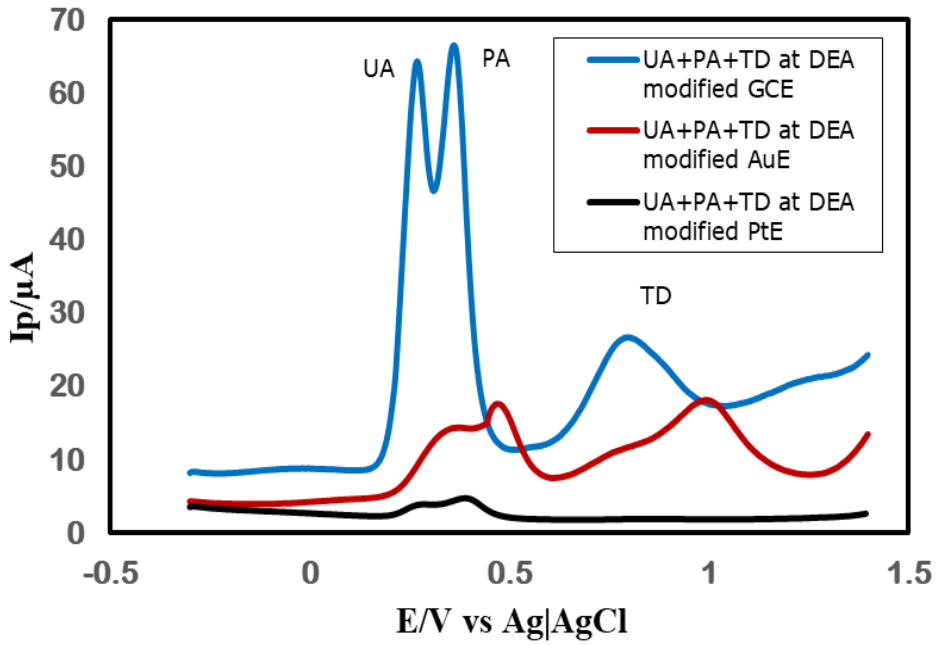

Figure 4.15: Differential pulse voltammograms (DPVs) of 2.5 mM UA+ 2.5 mM PA+ 2.5 mM TD in PBS (pH 7) at DEA modified GCE (blue line), DEA modified AuE (red line) and DEA modified PtE (black line) electrode at scan rate 0.1V/s.

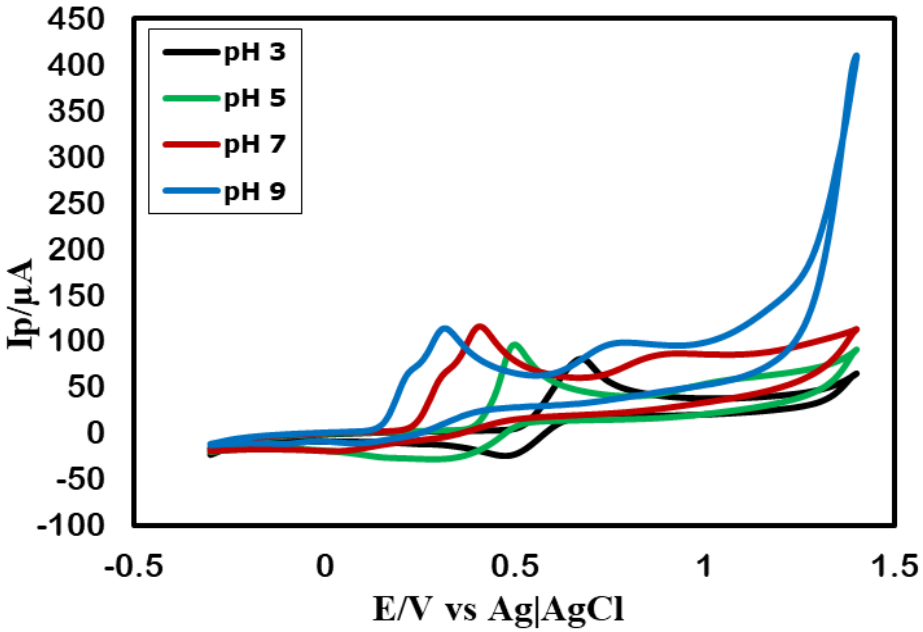

Figure 4.16: Cyclic voltammograms (CVs) of 2.5 mM UA+ 2.5 mM PA+ 2.5 mM TD in different buffer solution (pH 3, 5, 7 and 9) at DEA modified GC electrode.

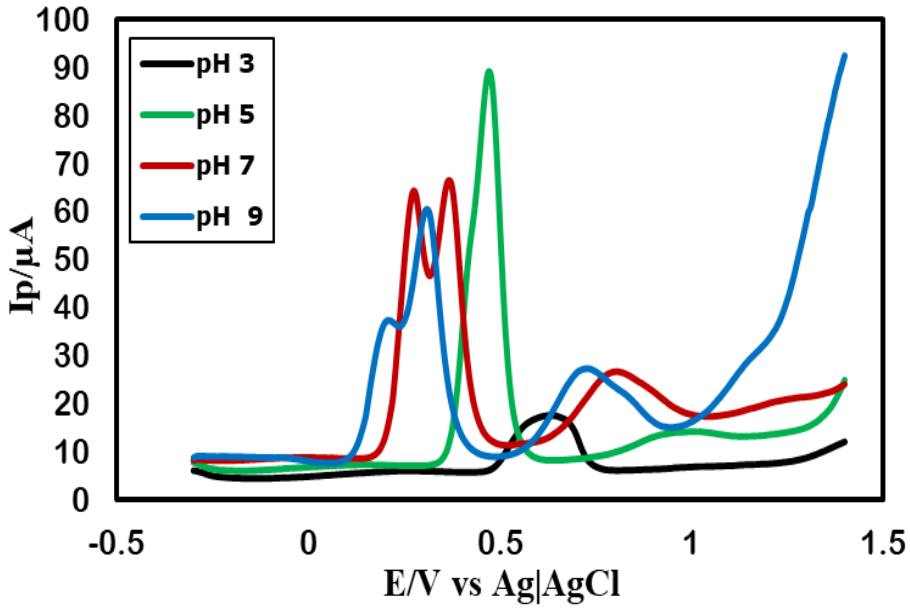

Figure 4.17: Differential pulse voltammograms (DPVs) of 2.5 mM UA+ 2.5 mM PA+ 2.5 mM TD in different buffer solution (pH 3, 5, 7 and 9) at DEA modified GC electrode.

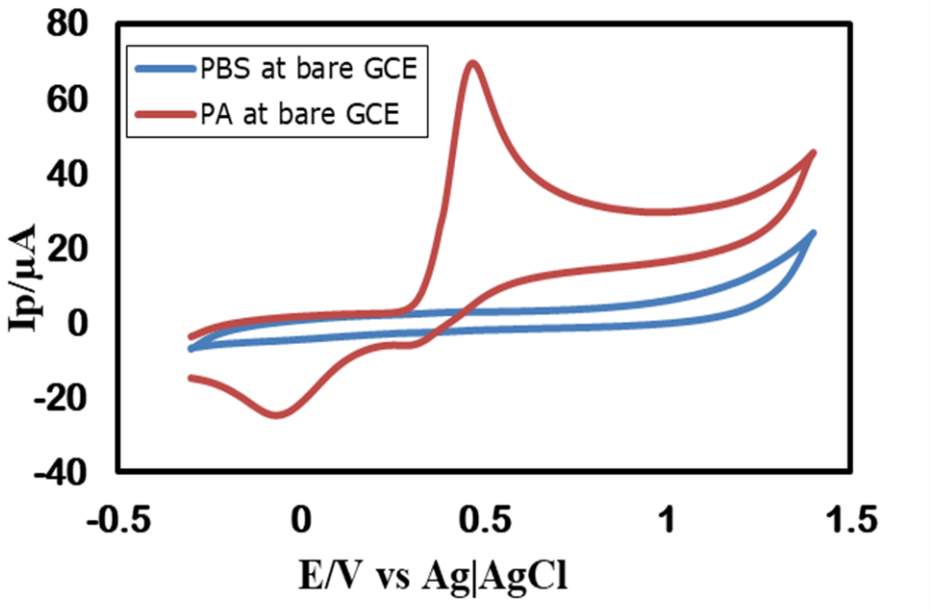

Figure 4.18: Cyclic voltammogrm (CV) of 2.5 mM PA in 0.5M PBS (pH 7) (red line) and only 0.5M PBS (pH 7) (blue line) at bare GC electrode at scan rate 0.1V/s.

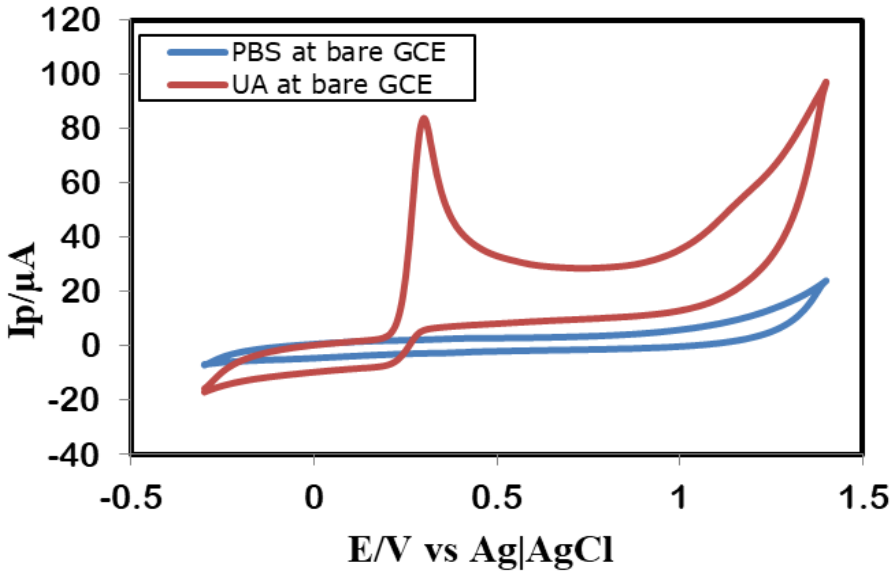

Figure 4.19: Cyclic voltammogrm (CV) of 2.5 mM UA in 0.5M PBS (pH 7) (red line) and only 0.5M PBS (pH 7) (blue line) of bare GC electrode at scan rate 0.1V/s.

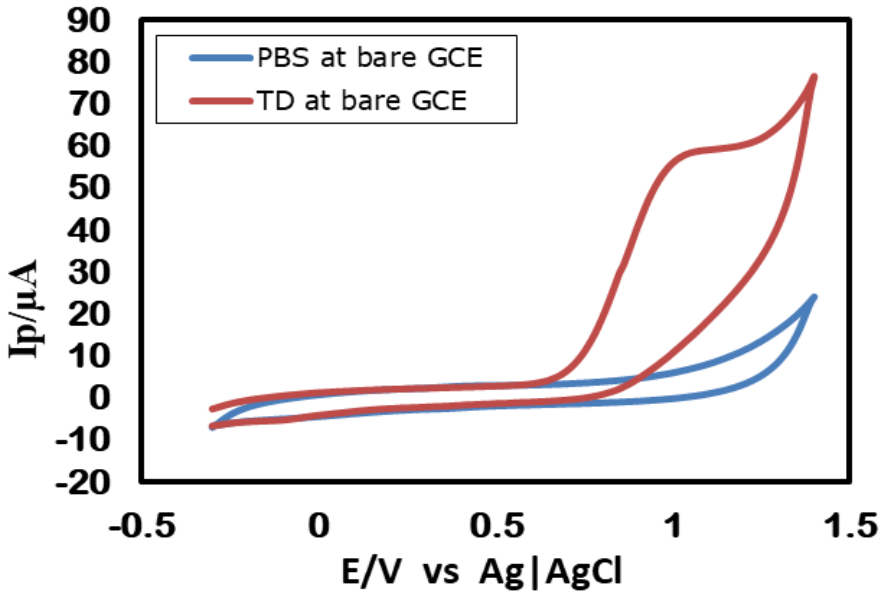

Figure 4.20: Cyclic voltammogrm (CV) of 2.5 mM Tramadol (TD) in 0.5M PBS (pH 7) (red line) and only 0.5M PBS (pH 7) (blue line) of bare GC electrode at scan rate 0.1V/s.

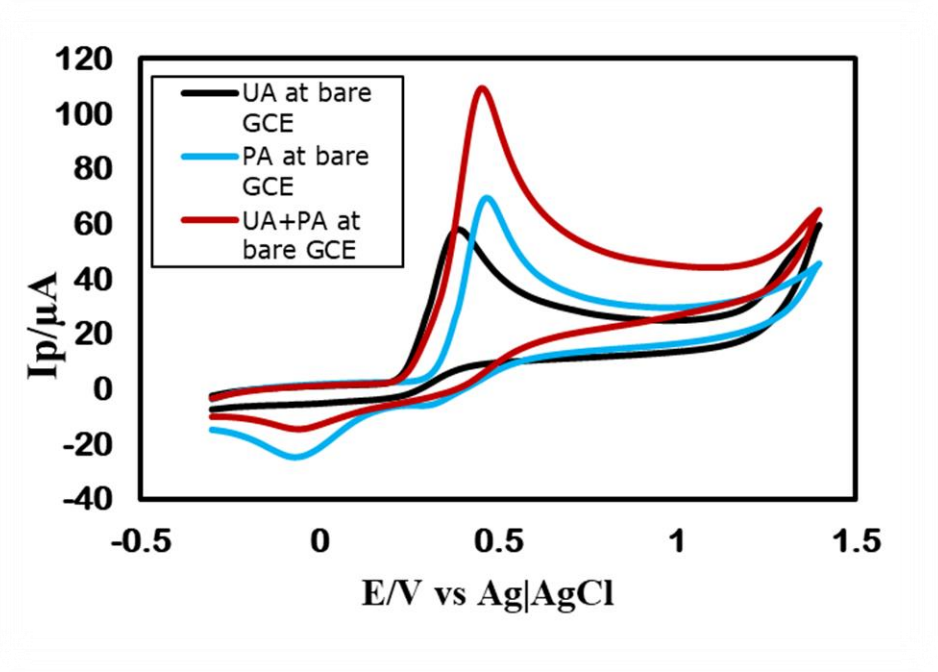

Figure 4.21: Cyclic voltammogram (CV) of 2.5 mM UA (black line), 2.5 mM PA (blue line) and 2.5 mM UA+ 2.5 mM PA (red line) of bare GC electrode in PBS (pH 7) at scan rate 0.1V/s.

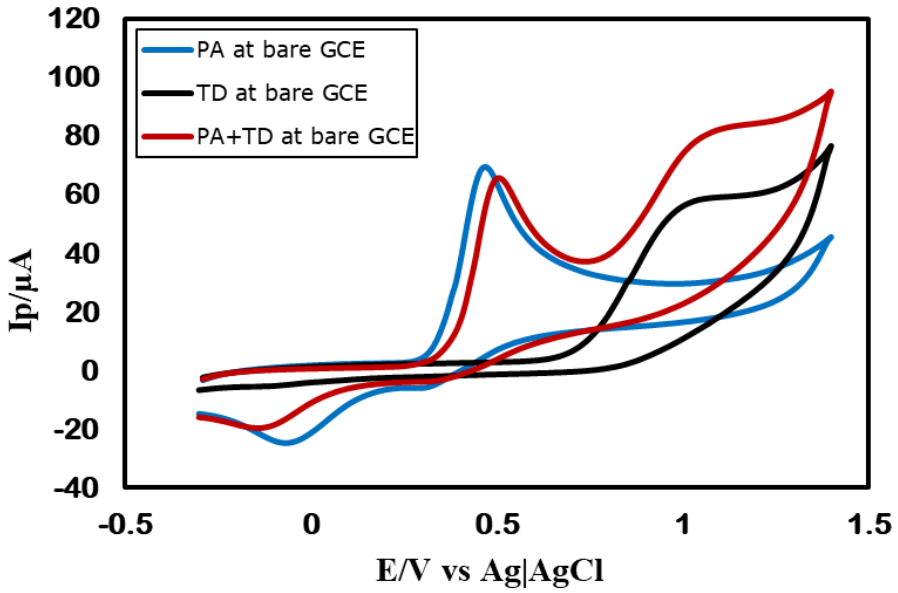

Figure 4.22: Cyclic voltammogram (CV) of 2.5 mM PA (blue line), 2.5 mM TD (black line) and 2.5 mM PA+ 2.5 mM TD (red line) of bare GC electrode in PBS (pH 7) at scan rate 0.1V/s.

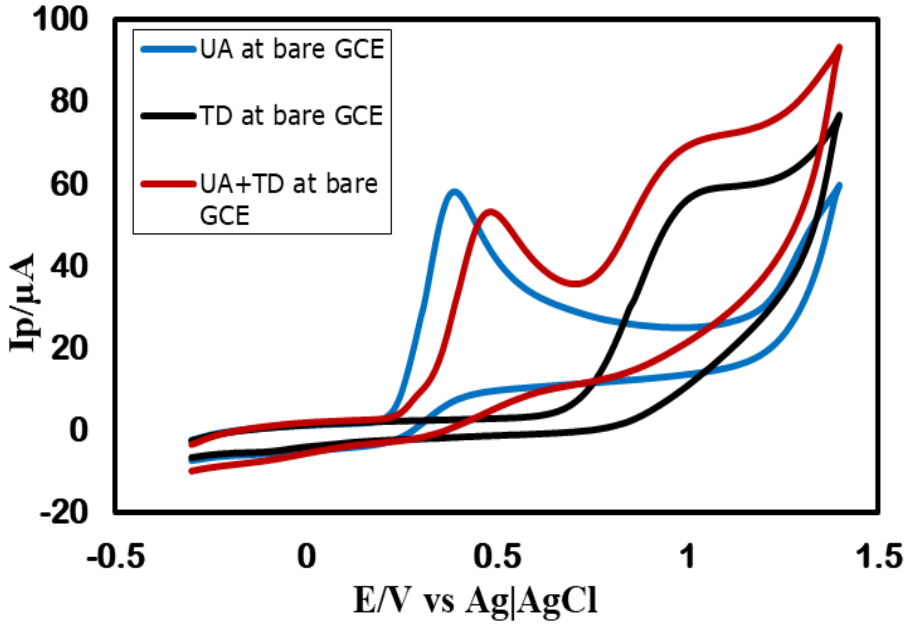

Figure 4.23: Cyclic voltammogram (CV) of 2.5 mM UA (blue line), 2.5 mM TD (black line) and 2.5 mM UA+ 2.5 mM TD (red line) of bare GC electrode in PBS (pH 7) at scan rate 0.1V/s.

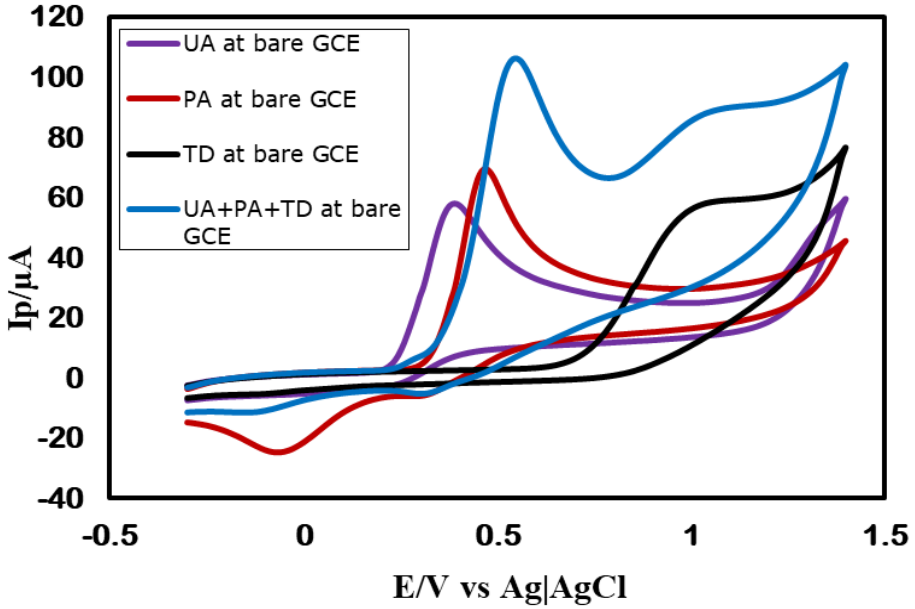

Figure 4.24: Cyclic voltammogram (CV) of 2.5 mM UA (black line), 2.5 mM PA (blue line) and 2.5 mM TD (purple line) and 2.5 mM UA+ 2.5 mM PA+ 2.5 mM TD (red line) of bare GC electrode in PBS (pH 7) at scan rate 0.1V/s.

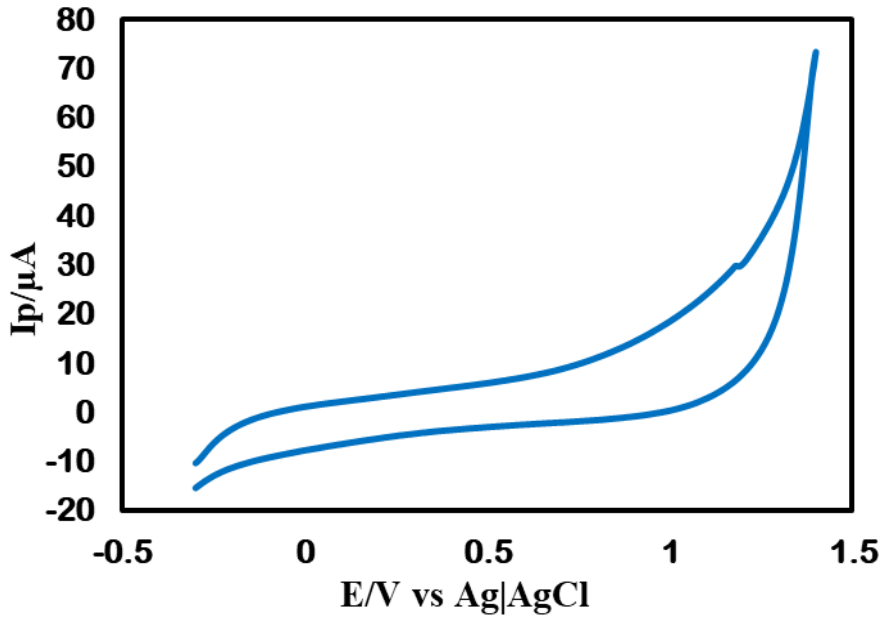

Figure 4.25: Cyclic voltammogram (CV) of DEA in PBS (pH 7) at modified GC electrode at scan rate 0.1 V/s.

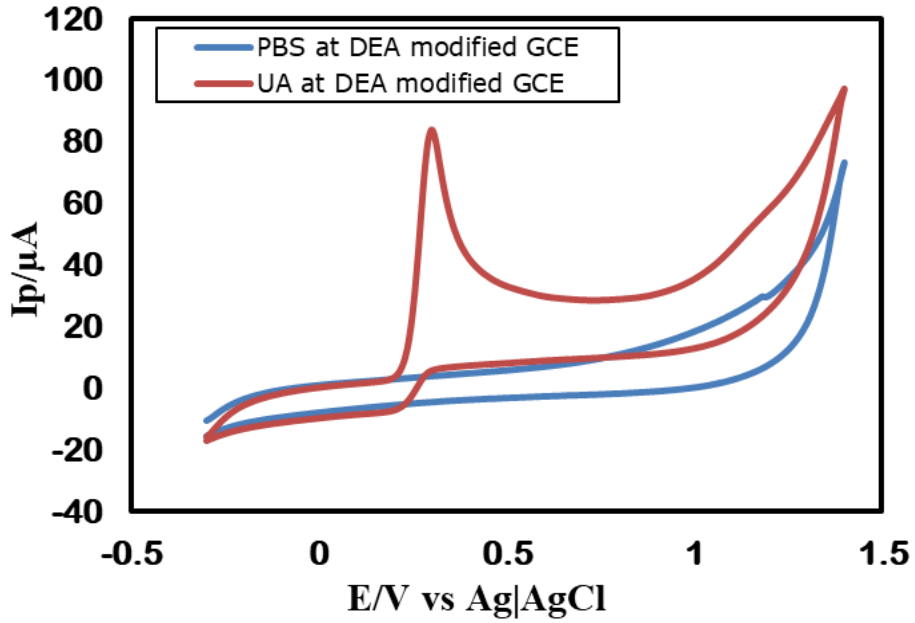

Figure 4.26: Cyclic voltammogram (CV) of 2.5 mM UA in 0.5M PBS (pH 7) (red line) and only 0.5M PBS (pH 7) (blue line) at DEA modified GC electrode at scan rate 0.1V/s.

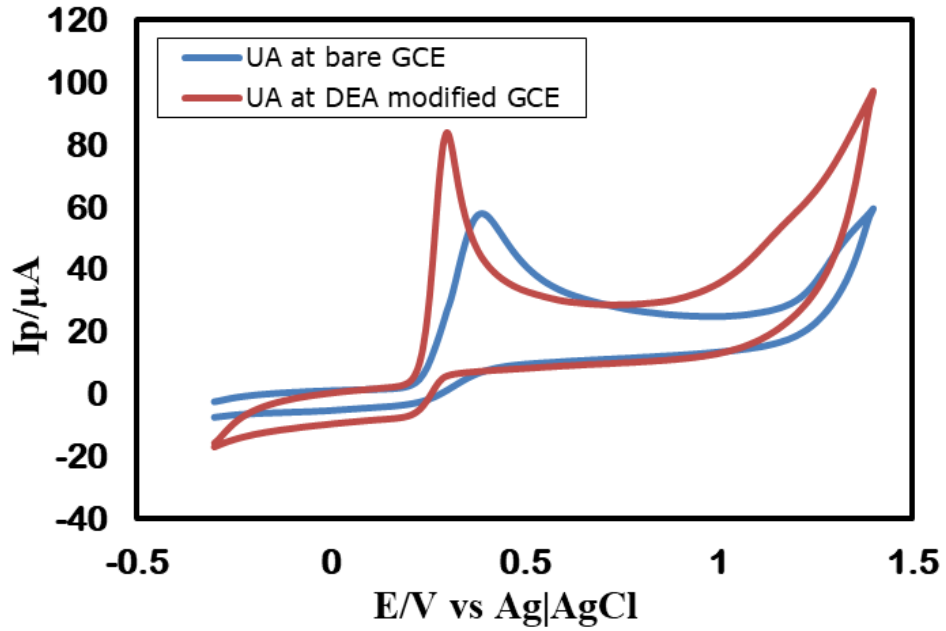

Figure 4.27: Cyclic voltammogram (CV) of 2.5 mM UA in 0.5M PBS (pH 7) at bare (blue line) and DEA modified (red line) GC electrode at scan rate 0.1V/s.

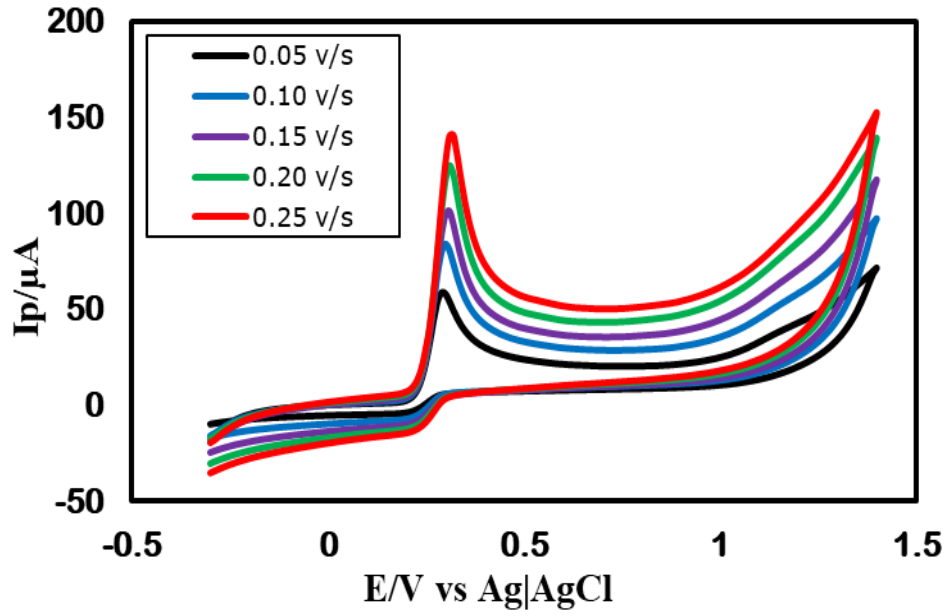

Figure 4.28: Cyclic Voltammogram (CV) of 2.5 mM UA at DEA modified GC electrode in PBS (pH 7) at different scan rate 0.05 v/s, 0.10 v/s, 0.15 v/s, 0.20 v/s and 0.25v/s.

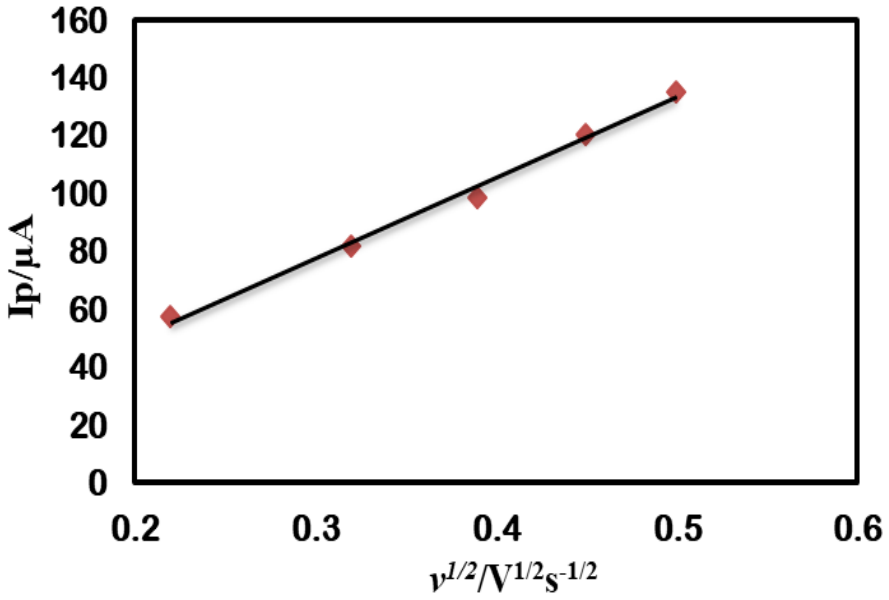

Figure 4.29: Plots of peak current (I_p) vs square root of scan rate ($v^{1/2}$) of 2.5 mM UA at DEA modified GC electrode in PBS (pH 7).

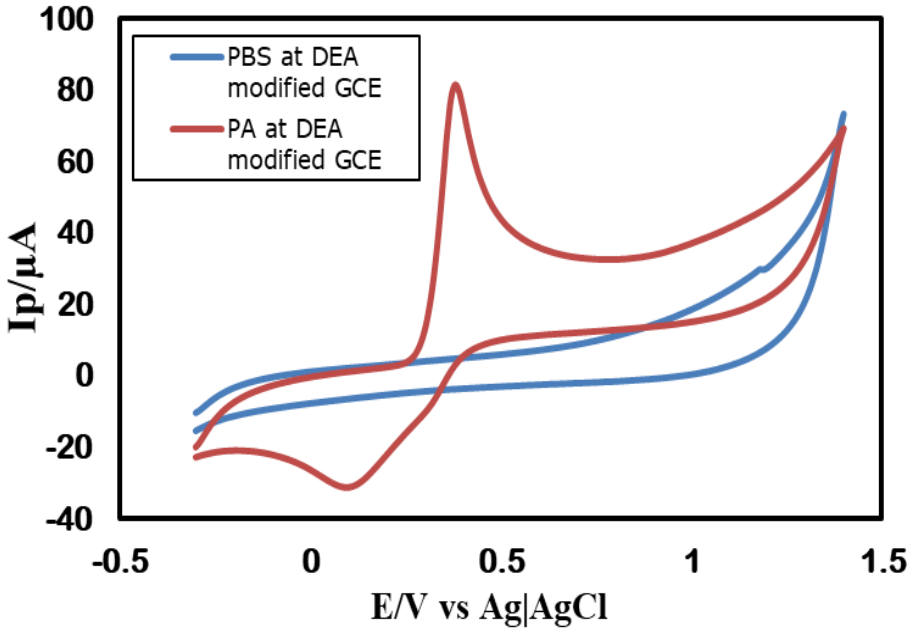

Figure 4.30: Cyclic Voltammogram (CV) of 2.5 mM PA in 0.5M PBS (pH 7) (red line) and only 0.5M PBS (pH 7) (blue line) at DEA modified GC electrode at scan rate 0.1V/s.

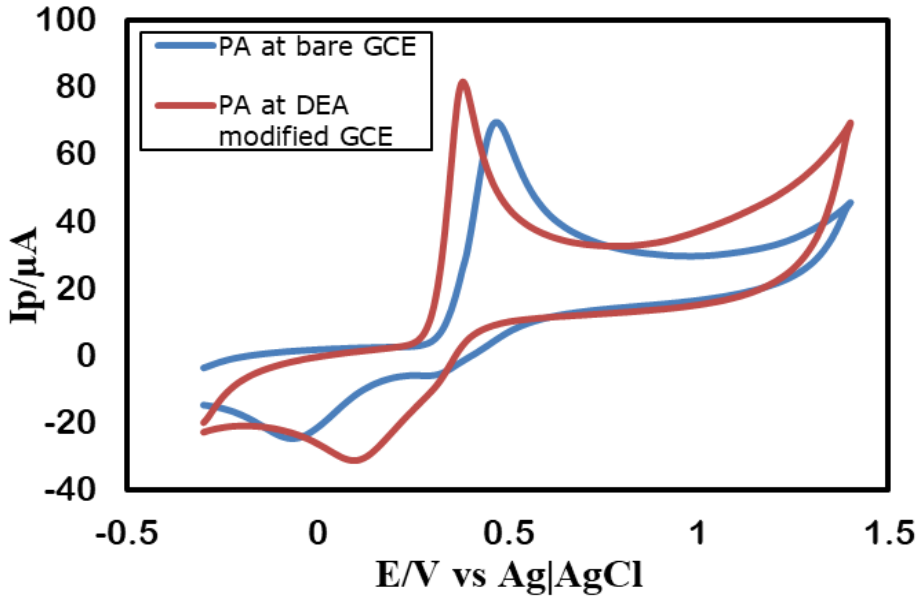

Figure 4.31: Cyclic voltammogram (CV) of 2.5 mM PA in 0.5M PBS (pH 7) at bare (blue line) and DEA modified (red line) GC electrode at scan rate 0.1V/s.

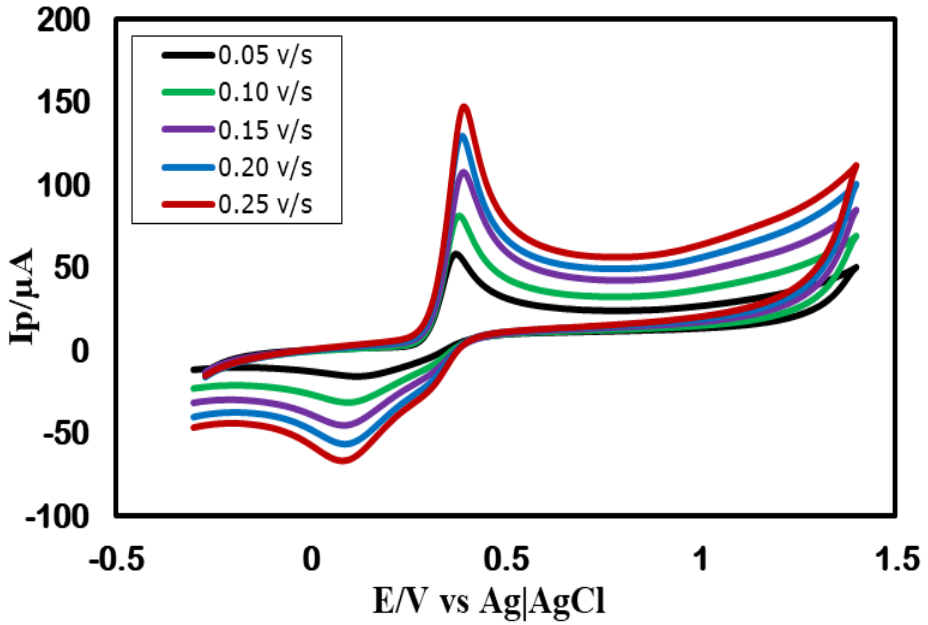

Figure 4.32: Cyclic Voltammogram (CV) of 2.5 mM PA at DEA modified GC electrode in PBS (pH 7) at different scan rate 0.05 v/s, 0.10 v/s, 0.15 v/s, 0.20 v/s and 0.25 v/s.

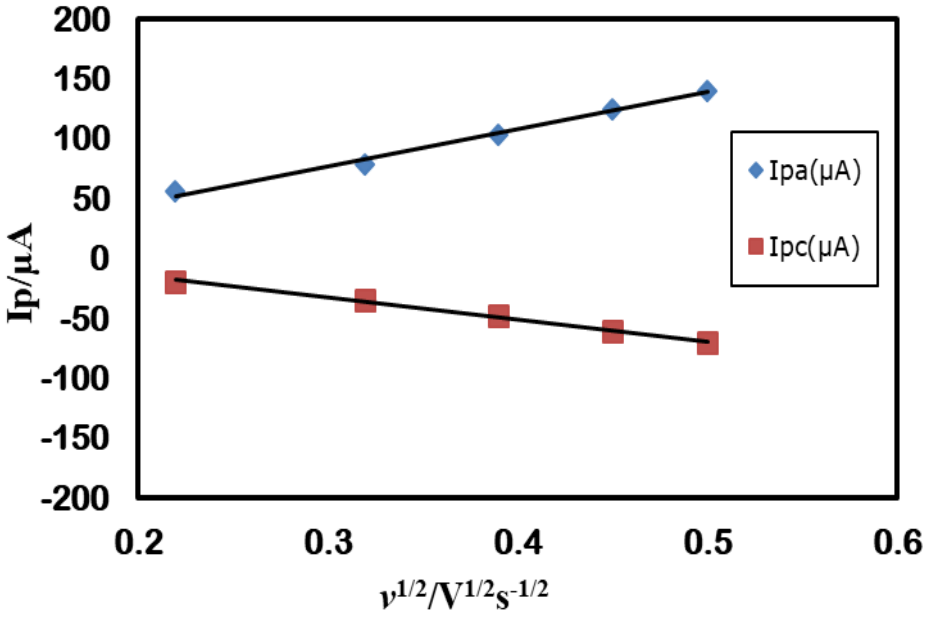

Figure 4.33: Plots of peak currents (Ipa and Ipc) vs square root of scan rate ($v^{1/2}$) of 2.5 mM PA at DEA modified GC electrode in PBS (pH 7).

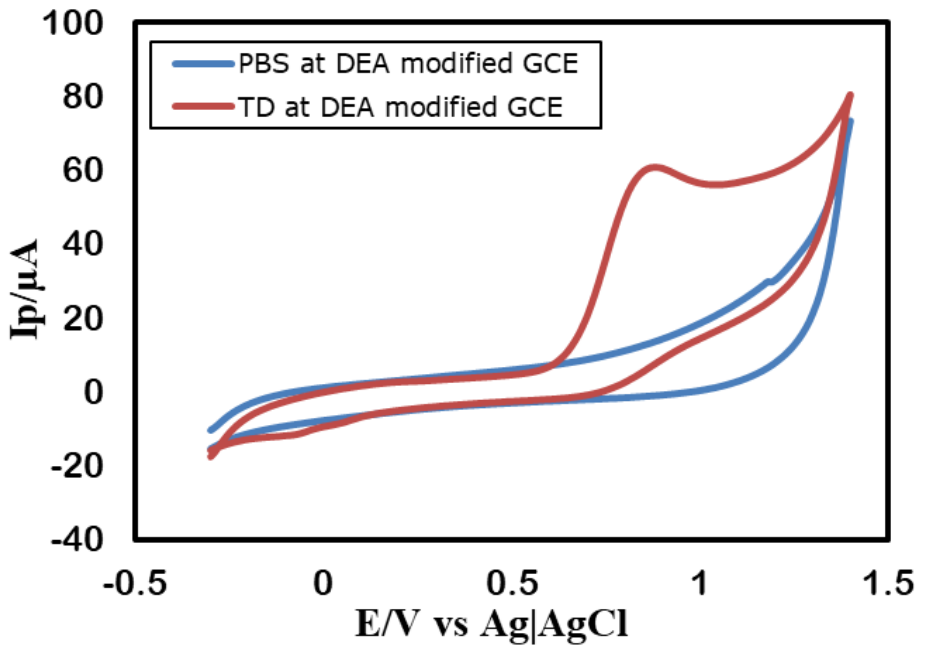

Figure 4.34: Cyclic Voltammogram (CV) of 2.5 mM TD in 0.5M PBS (pH 7) (red line) and only 0.5M PBS (pH 7) (blue line) at DEA modified GC electrode at scan rate 0.1V/s.

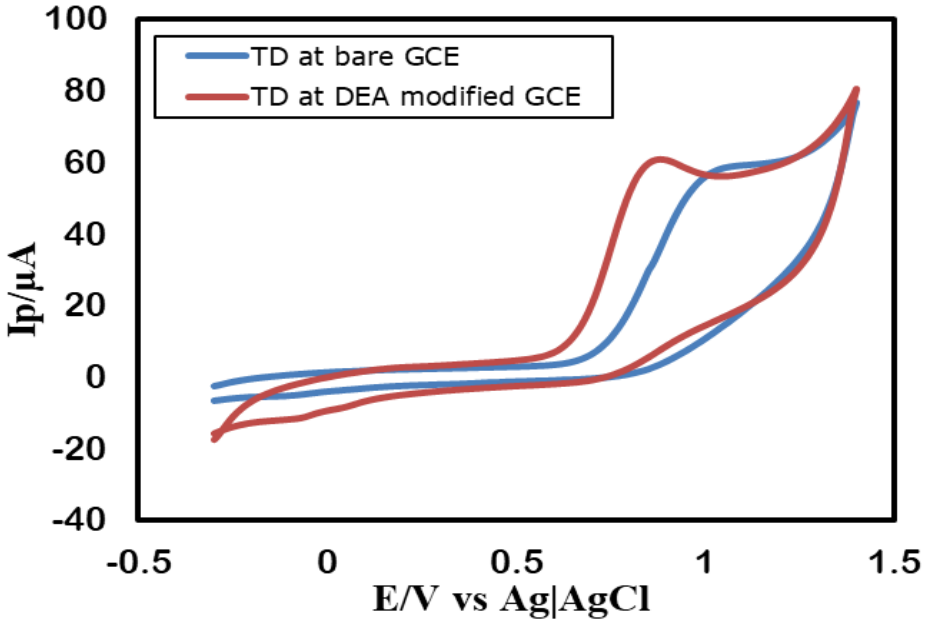

Figure 4.35: Cyclic voltammogram (CV) of 2.5 mM TD in 0.5M PBS (pH 7) at bare (blue line) and DEA modified (red line) GC electrode at scan rate 0.1V/s.

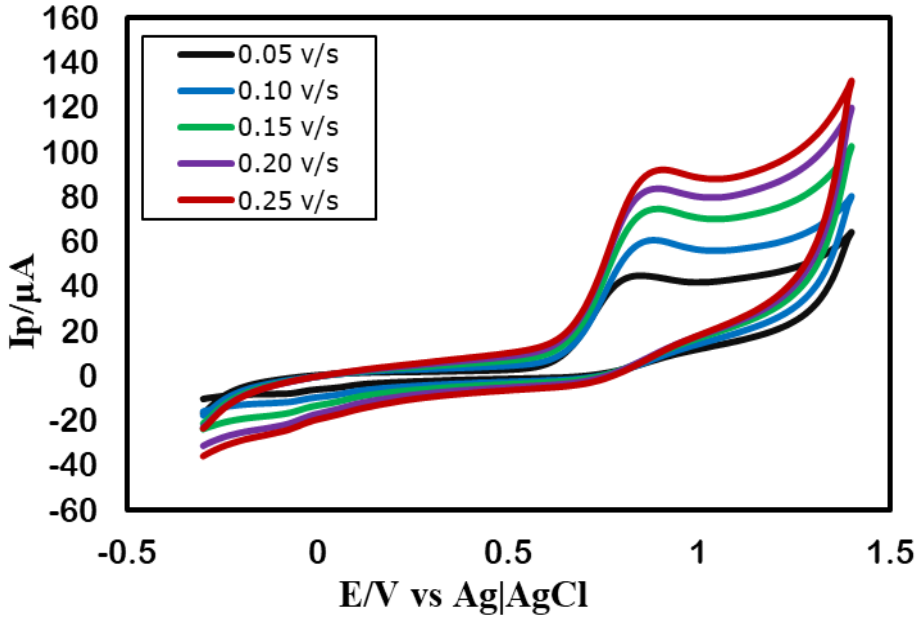

Figure 4.36: Cyclic Voltammogram (CV) of 2.5 mM TD at DEA modified GC electrode in PBS (pH 7) at different scan rate 0.05 v/s, 0.10 v/s, 0.15 v/s, 0.20 v/s and 0.25 v/s.

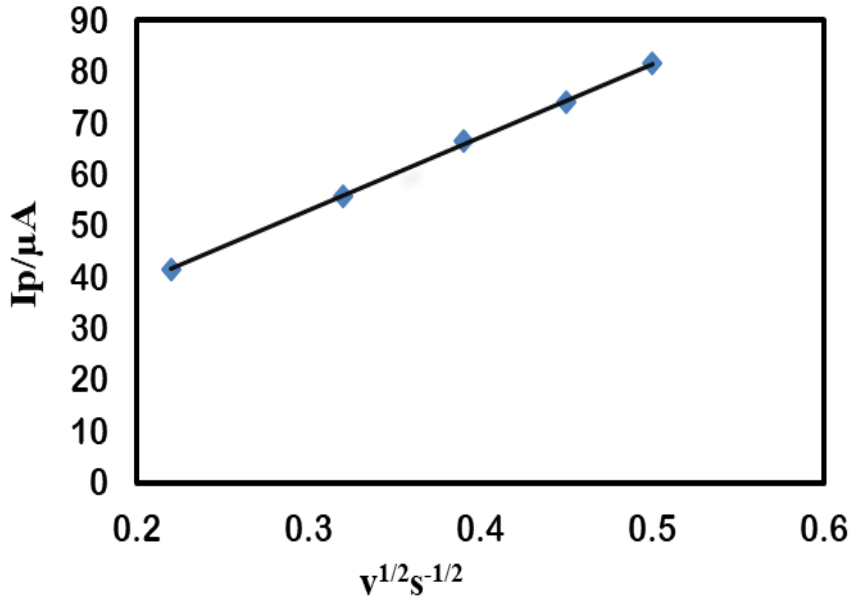

Figure 4.37: Plots of peak current (I_p) vs square root of scan rate ($v^{1/2}$) of 2.5 mM TD at DEA modified GC electrode in PBS (pH 7).

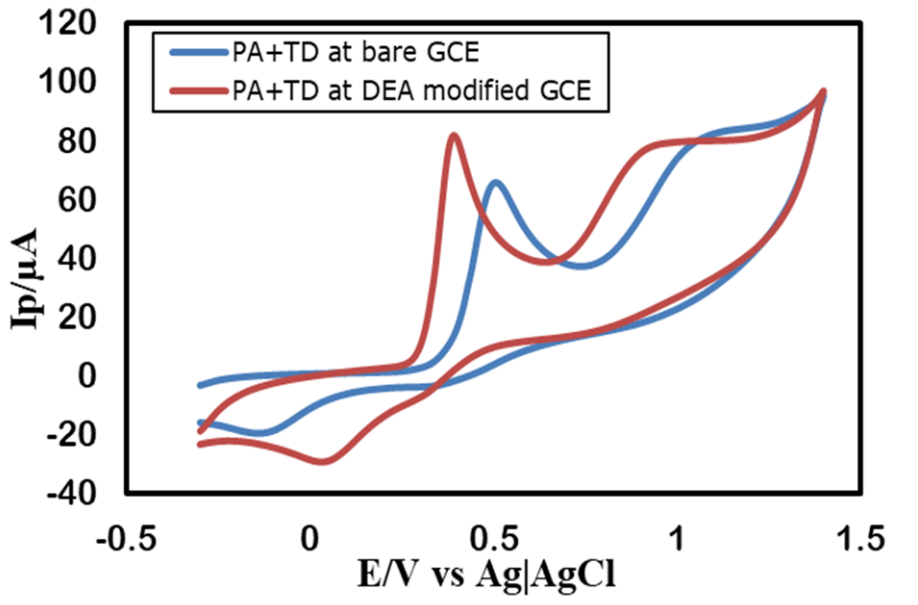

Figure 4.38: CV comparison of 2.5 mM PA+ 2.5 mM TD at bare (blue line) and DEA modified GC electrode (red line) at scan rate 0.1 V/s.

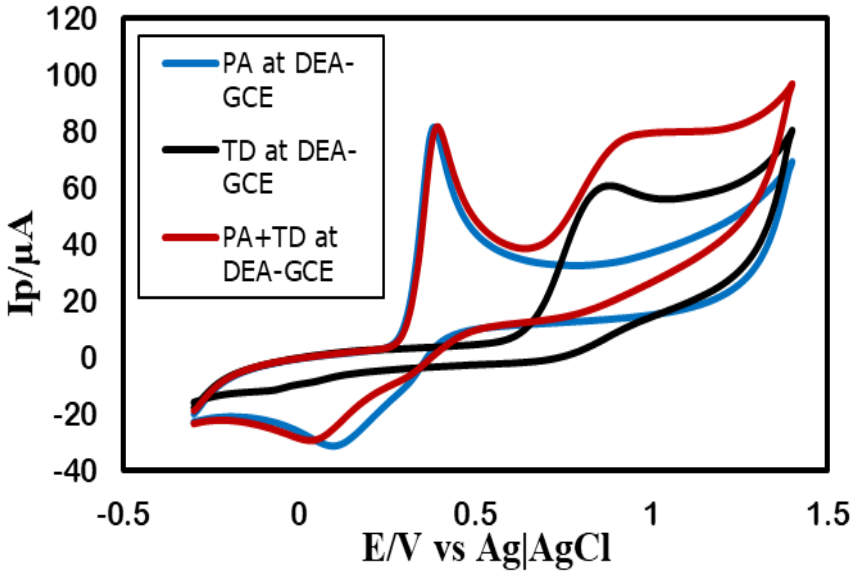

Figure 4.39: Cyclic voltammogram (CV) of 2.5 mM PA (blue line), 2.5 mM TD (black line) and simultaneous 2.5 mM PA+ 2.5 mM TD (red line) at DEA modified GC electrode at scan rate 0.1V/s.

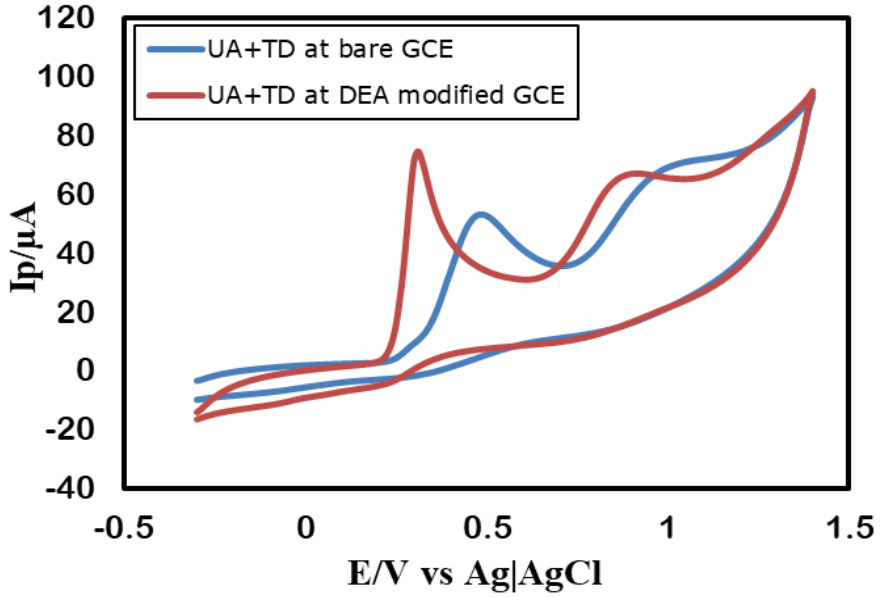

Figure 4.40: CV comparison of 2.5 mM UA+ 2.5 mM TD at bare (blue line) and DEA modified GC electrode (red line) in PBS (pH 7) at scan rate 0.1 V/s.

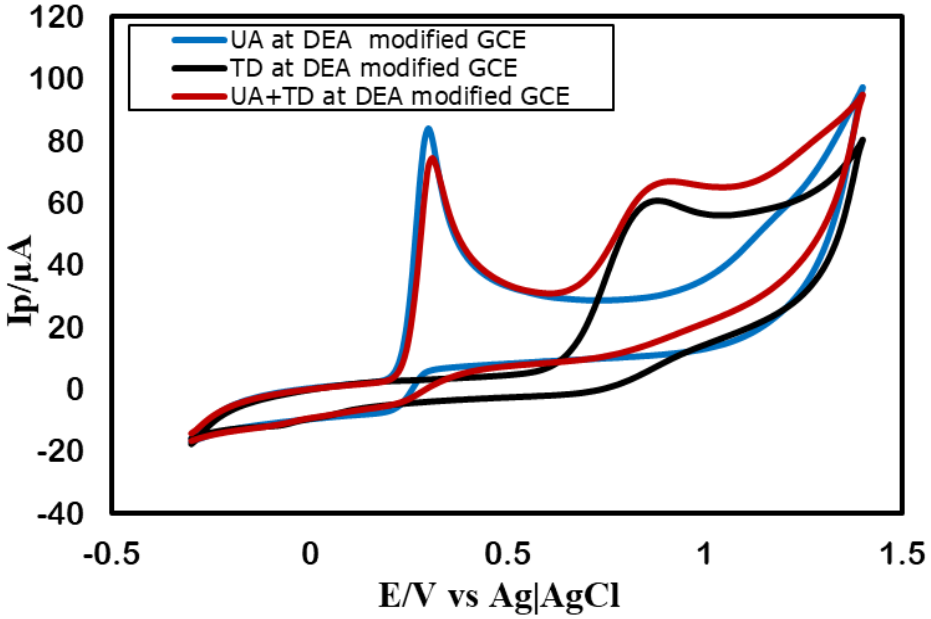

Figure 4.41: Cyclic voltammogram (CV) of 2.5 mM UA (blue line), 2.5 mM TD (black line) and 2.5 mM UA+ 2.5 mM TD (red line) at DEA modified GC electrode in PBS (pH 7) at scan rate 0.1V/s.

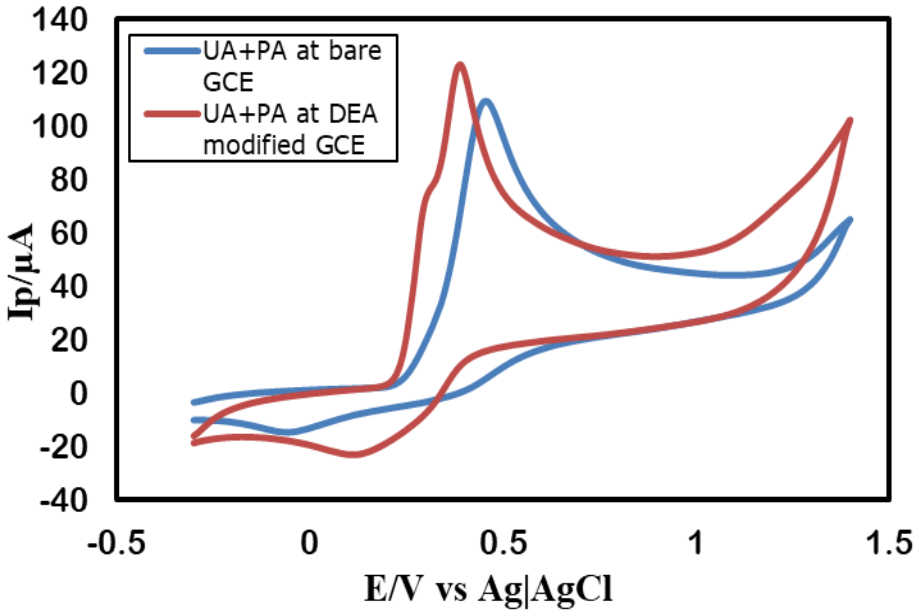

Figure 4.42: CV comparison of 2.5 mM UA+ 2.5 mM PA at bare (blue line) and DEA modified GC electrode (red line) in PBS (pH 7) at scan rate 0.1 V/s.

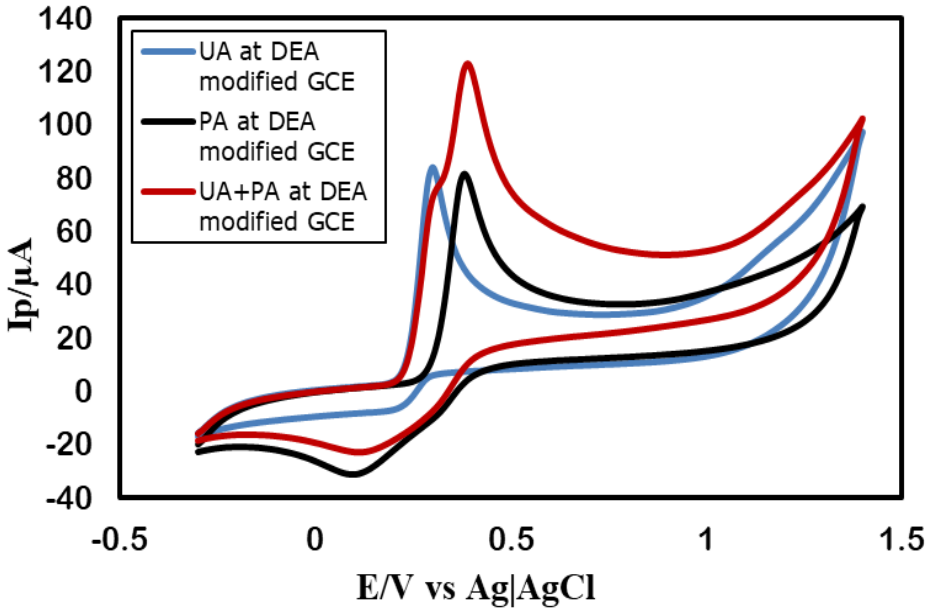

Figure 4.43: Cyclic voltammogram (CV) of 2.5 mM UA (blue line), 2.5 mM PA (black line) and 2.5 mM UA+ 2.5 mM PA (red line) at DEA modified GC electrode in PBS (pH 7) at scan rate 0.1V/s.

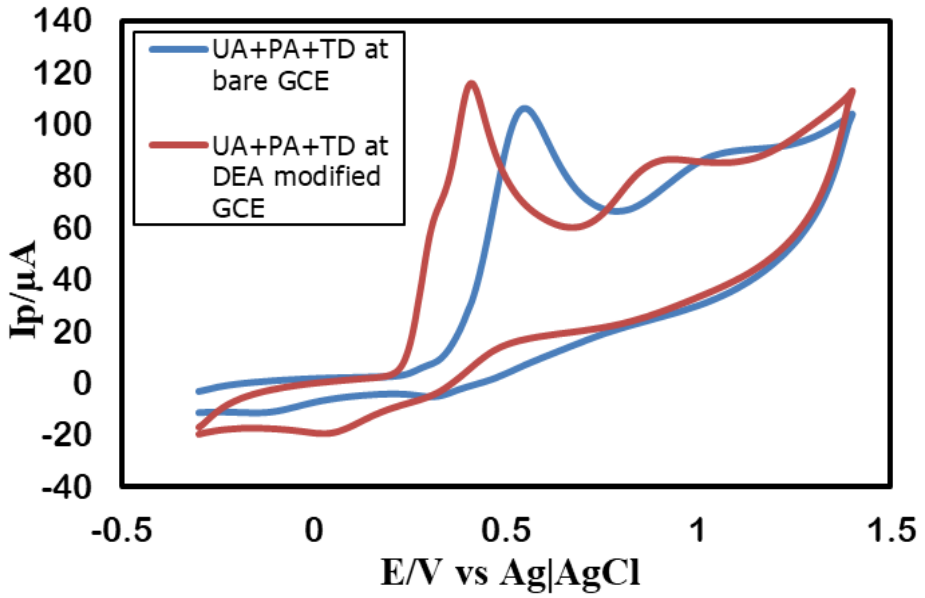

Figure 4.44: CV comparison of 2.5 mM UA+ 2.5 mM PA+ 2.5 mM TD at bare (blue line) and DEA modified GC electrode (red line) in PBS (pH 7) at scan rate 0.1 V/s.

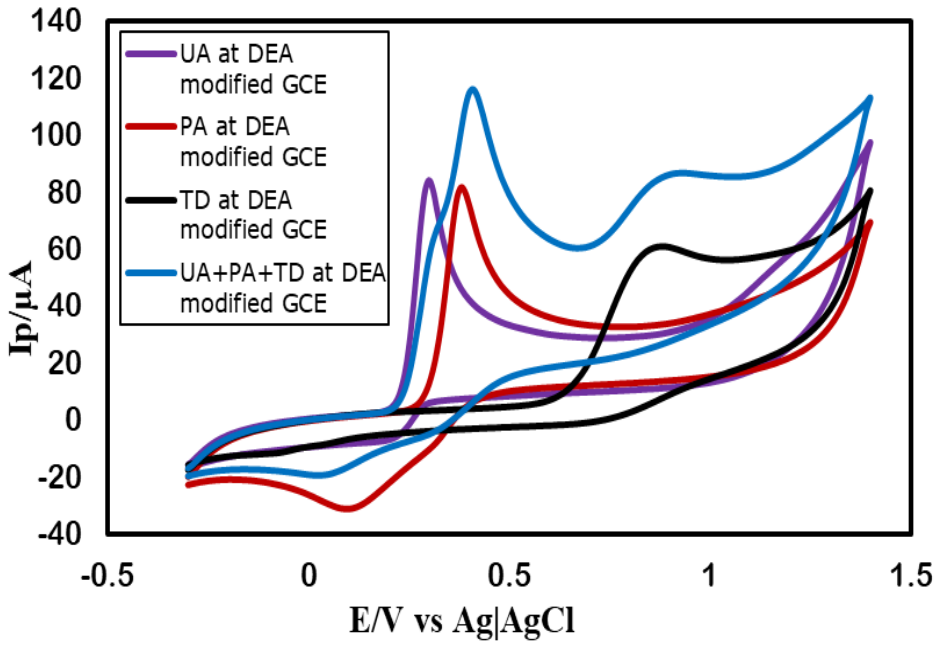

Figure 4.45: Cyclic voltammogram (CV) of 2.5 mM UA (purple line), 2.5 mM PA (red line), 2.5 mM TD (black line) and 2.5 mM UA+ 2.5 mM PA+ 2.5 mM TD (blue line) at DEA modified GC electrode in PBS (pH 7) at scan rate 0.1V/s.

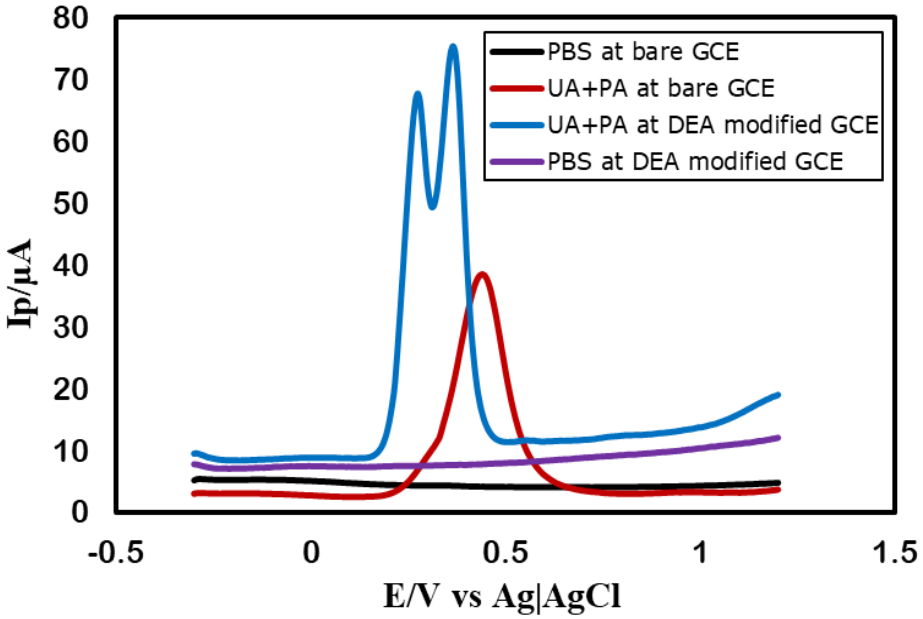

Figure 4.46: Differential pulse voltammogram (DPV) comparison of only PBS (pH 7) at bare (black line) and DEA modified GC electrode (purple line) and 2.5 mM UA+ 2.5 mM PA at bare (red line) and DEA modified GC electrode (blue line) at scan rate 0.1 V/s.

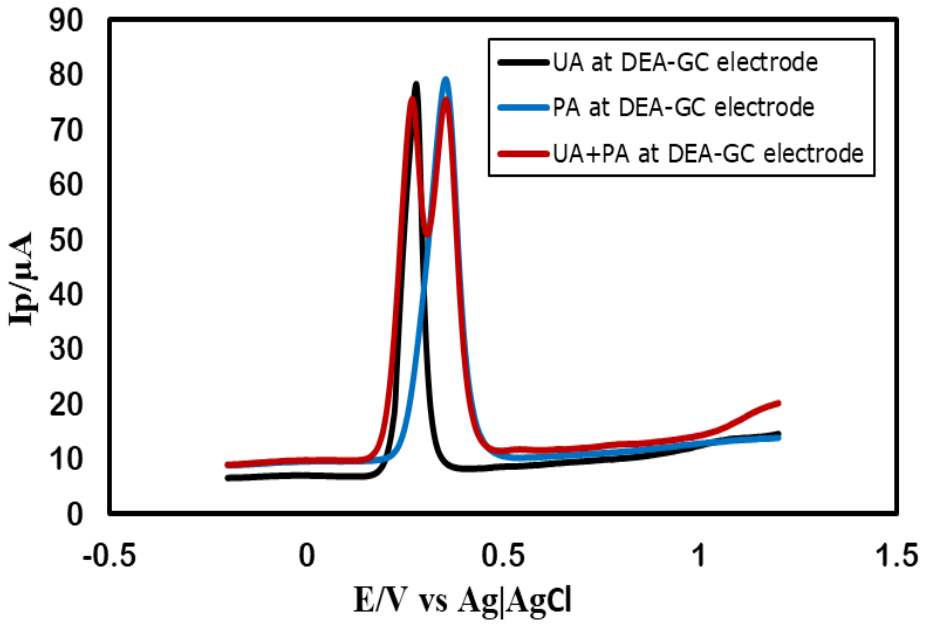

Figure 4.47: DPVs of 2.5 mM UA (black line), 2.5 mM PA (blue line) and 2.5 mM UA+ 2.5 mM PA (red line) in PBS (pH 7) at DEA modified GC electrode at scan rate 0.1 V/s.

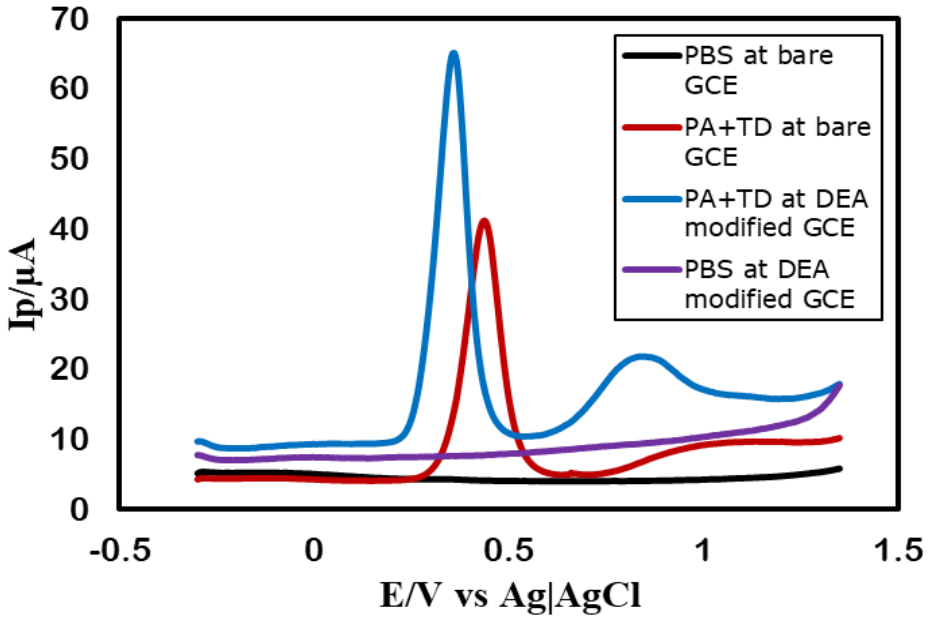

Figure 4.48: DPVs comparison of only PBS (pH 7) at bare (blue line) and DEA modified GC electrode (purple line) and 2.5 mM PA+ 2.5 mM TD at bare (red line) and DEA modified GC electrode (green line) at scan rate 0.1 V/s.

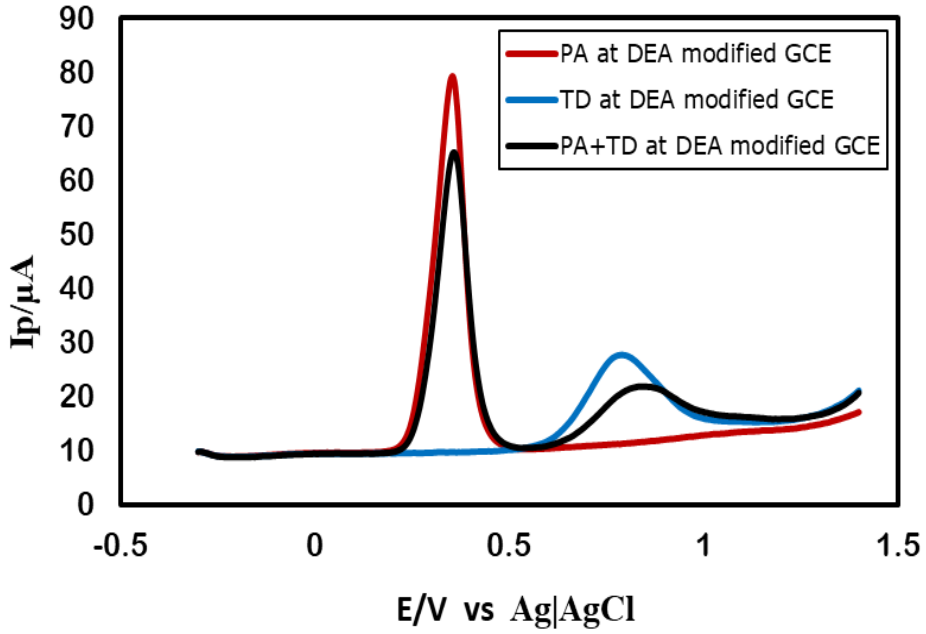

Figure 4.49: DPVs of 2.5 mM PA (blue line), 2.5 mM TD (red line) and 2.5 mM PA+2. 5 mM TD (green line) in PBS (pH 7) at DEA modified GC electrode at scan rate 0.1 V/s.

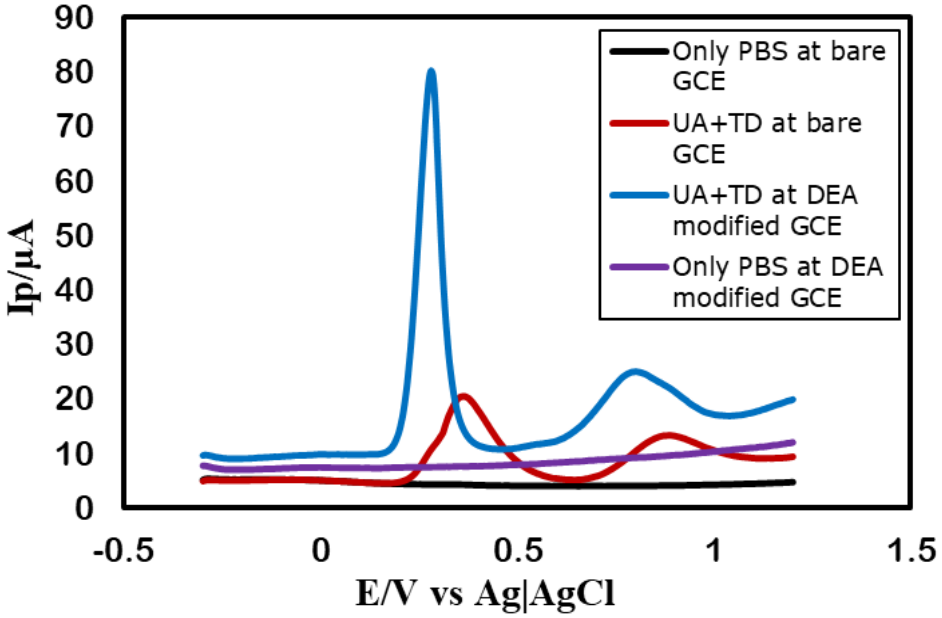

Figure 4.50: DPVs comparison of only PBS (pH 7) at bare (black line) and DEA modified GC electrode (purple line) and 2.5 mM UA+ 2.5 mM TD at bare (red line) and DEA modified GC electrode (blue line) at scan rate 0.1 V/s.

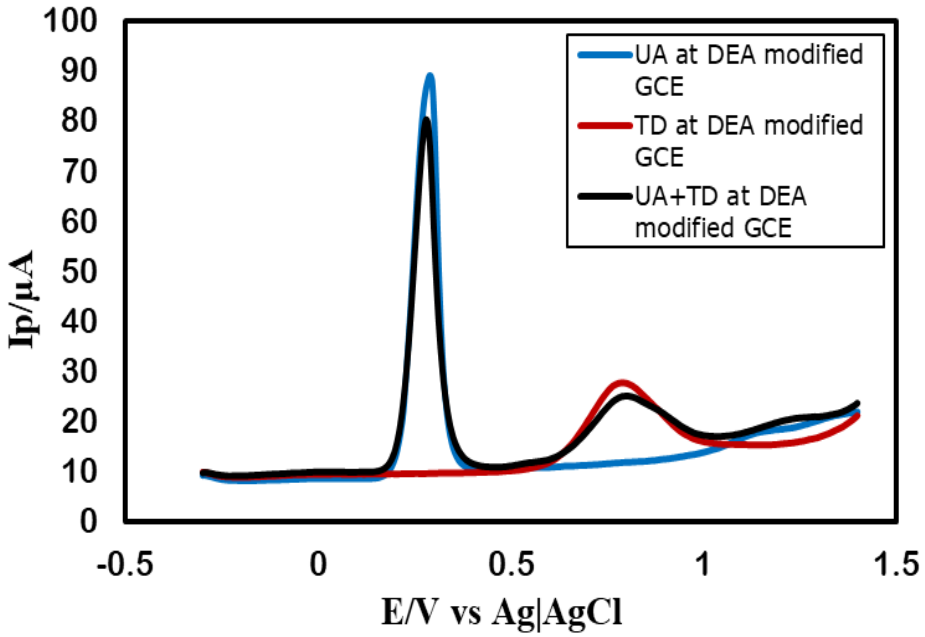

Figure 4.51: DPVs of 2.5 mM UA (blue line), 2.5 mM TD (red line) and 2.5 mM UA+ 2.5 mM TD (black line) in PBS (pH 7) at DEA modified GC electrode at scan rate 0.1 V/s.

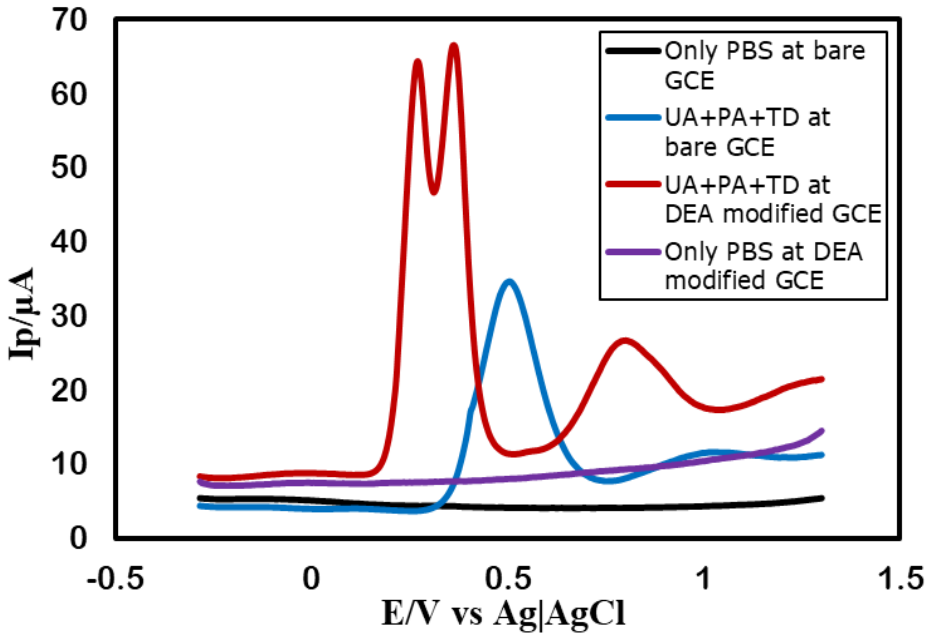

Figure 4.52: DPVs comparison of only PBS (pH 7) at bare (black line) and DEA modified GC electrode (purple line) and 2.5 mM UA+ 2.5 mM PA+ 2.5 mM TD at bare (blue line) and DEA modified GC electrode (red line) at scan rate 0.1 V/s.

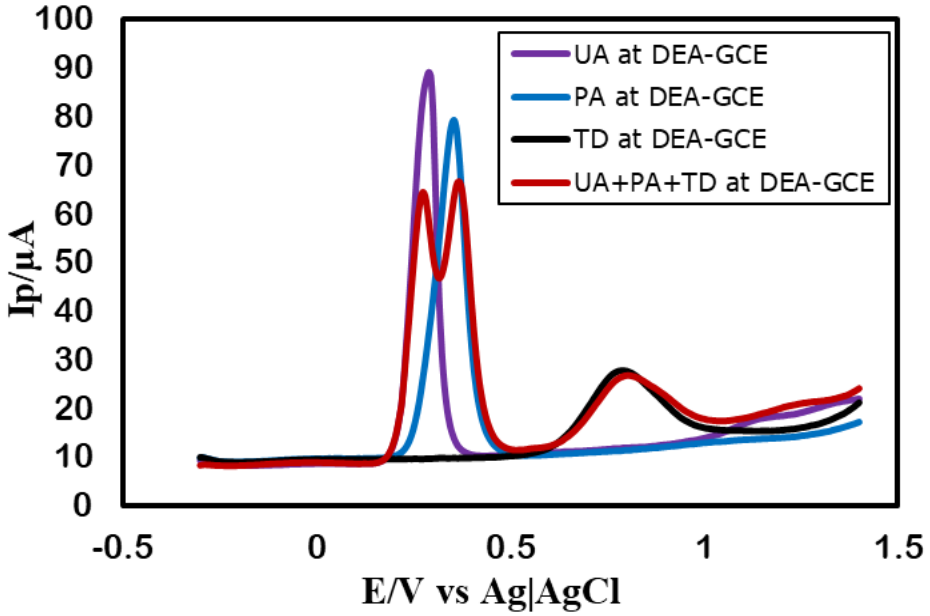

Figure 4.53: DPVs of 2.5 mM UA (purple line), 2.5 mM PA (blue line) and 2.5 mM TD (black line) and 2.5 mM UA+ 2.5 mM PA+2.5 mM TD (red line) in PBS (pH 7) at DEA modified GC electrode at scan rate 0.1 V/s.

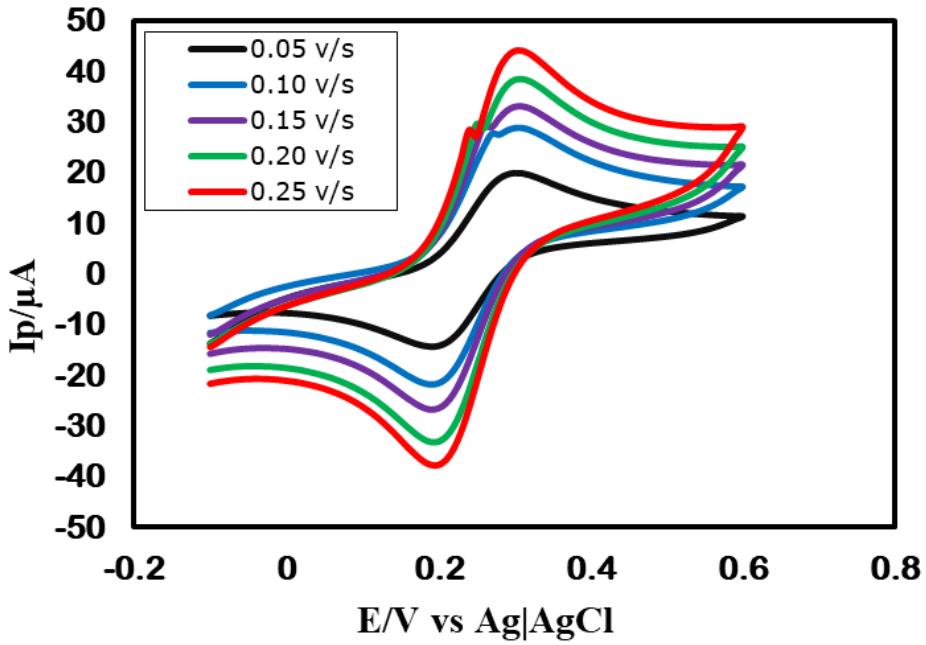

Figure 4.54: Cyclic voltammograms (CVs) of 2 mM potassium ferrocyanide on DEA modified GCE at different scan rate of 0.05 V/s, 0.10 V/s, 0.15 V/s, 0.20 V/s and 0.25 V/s in 1 M KCl as supporting electrolyte.

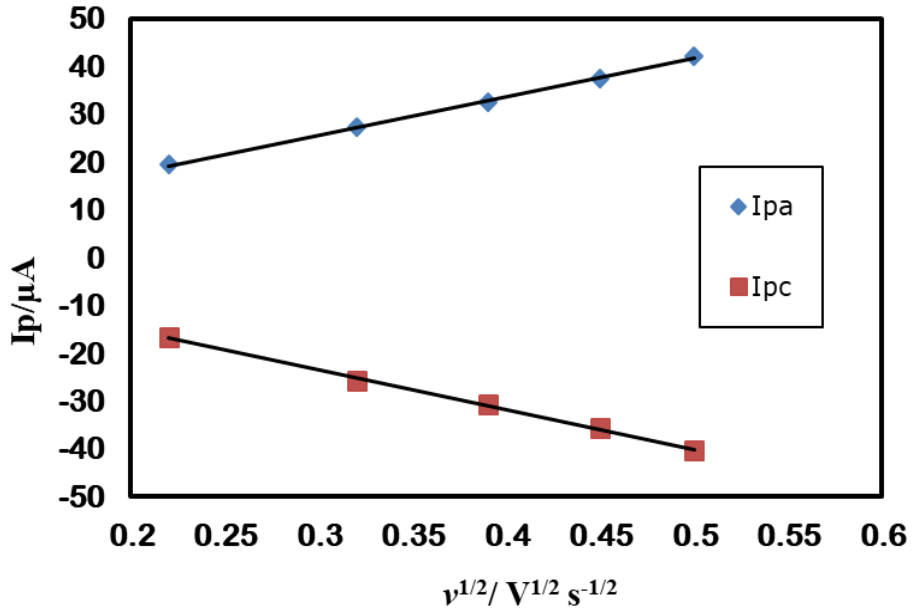

Figure 4.55: The anodic and the cathodic peak current of ferrocyanide vs square root of the scan rates.

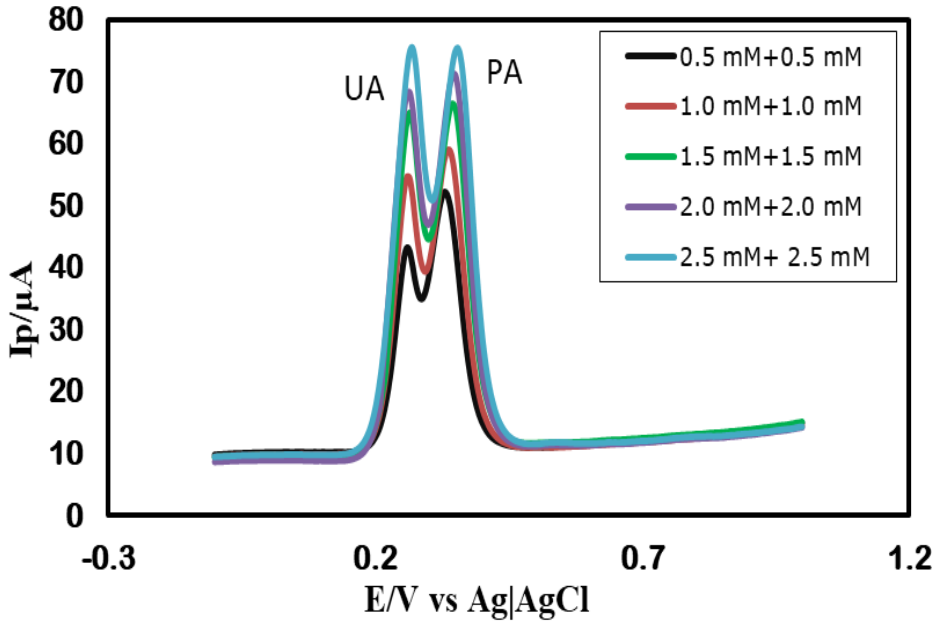

Figure 4.56: DPVs of simultaneous concentration change of UA+PA (0.5-2.5 mM) at DEA modified GC electrode in PBS (pH 7) at scan rate 0.1 V/s.

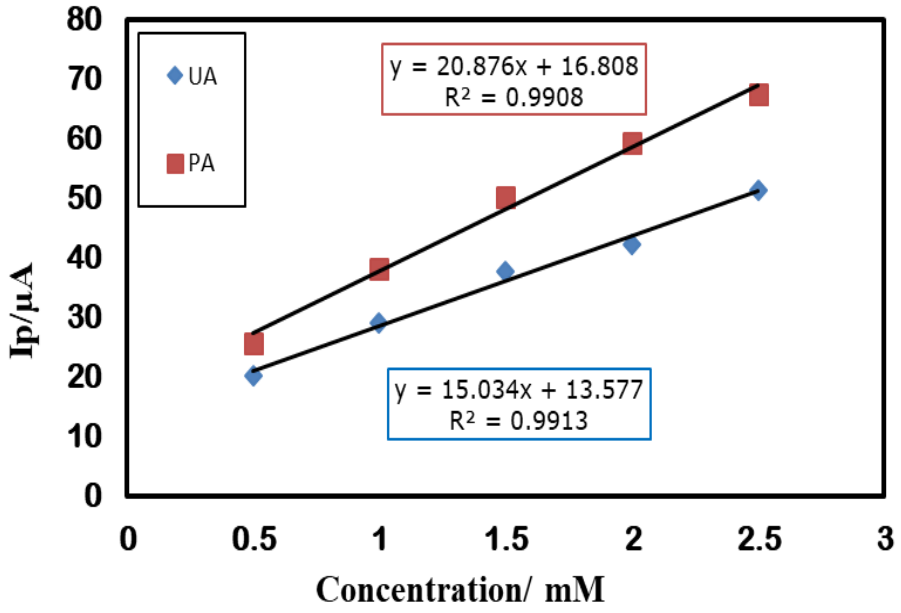

Figure 4.57: Calibration curve for simultaneous estimation of UA (blue markers) and PA (red markers) in a binary mixture at DEA modified GC electrode.

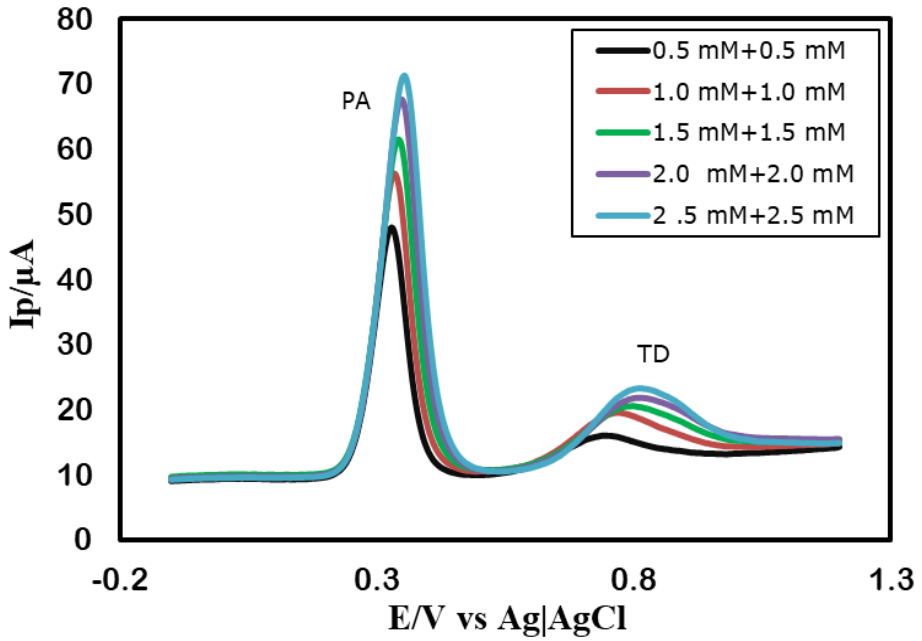

Figure 4.58: DPVs of simultaneous concentration change of PA+TD (0.5-2.5 mM) at DEA modified GC electrode in PBS (pH 7) at scan rate 0.1 V/s.

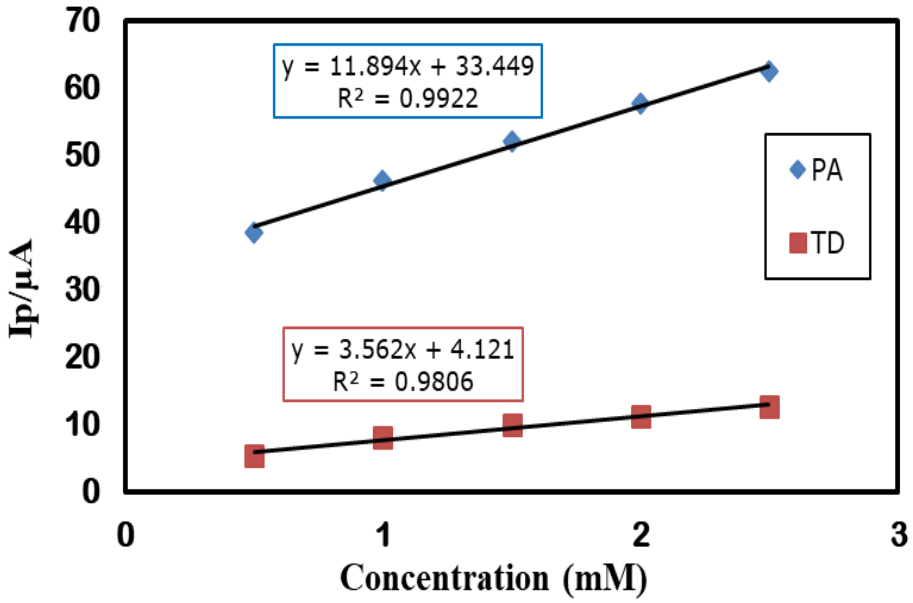

Figure 4.59: Calibration curve for simultaneous estimation of PA (blue markers) and TD (red markers) in a binary mixture at DEA modified GC electrode.

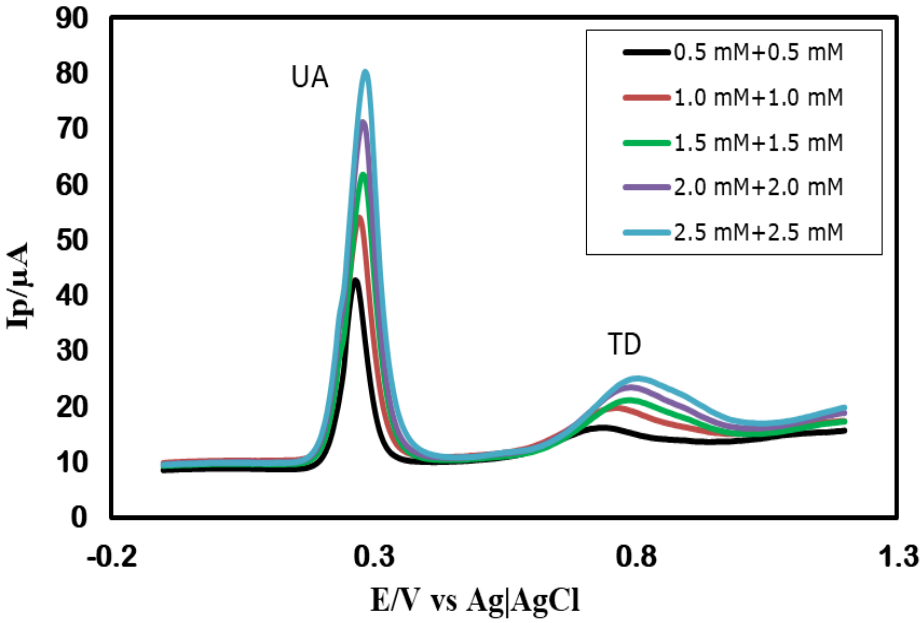

Figure 4.60: DPVs of simultaneous concentration change of UA+TD (0.5-2.5 mM) of DEA modified GC electrode in PBS (pH 7) at scan rate 0.1 V/s.

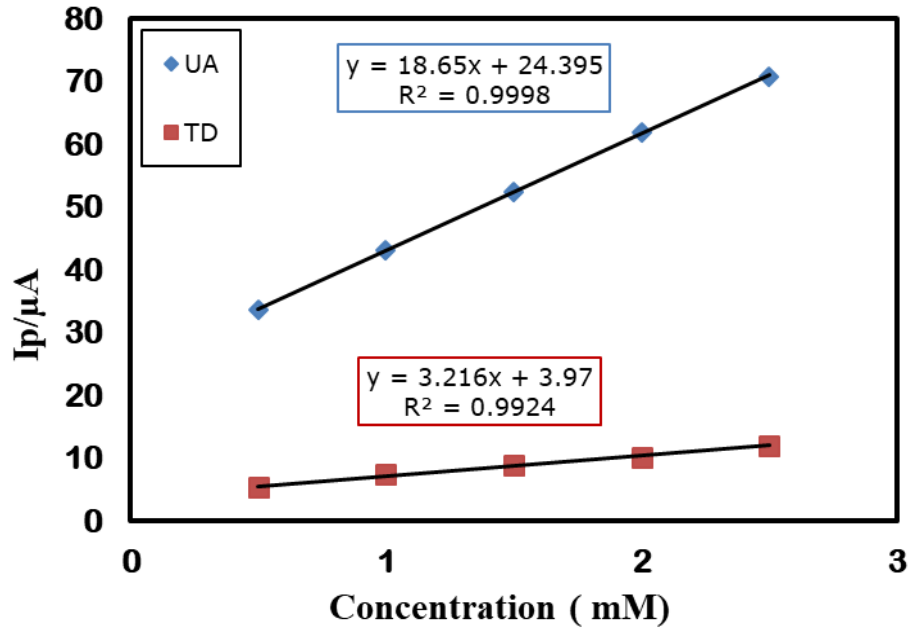

Figure 4.61: Calibration curve for simultaneous estimation of UA (blue markers) and TD (red markers) in a binary mixture at DEA modified GC electrode.

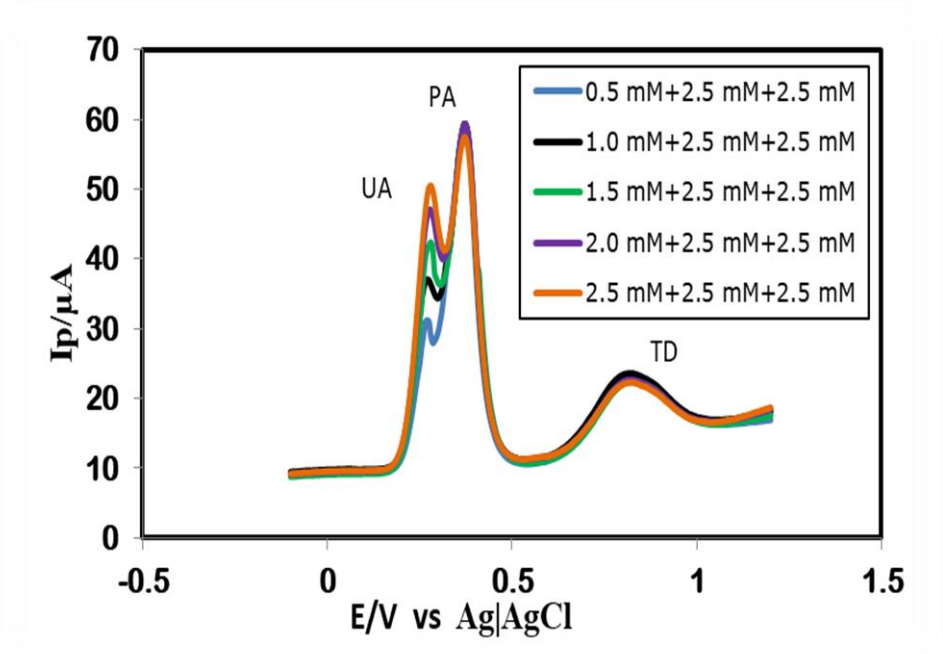

Figure 4.62: DPVs of different concentration of UA (0.5-2.5 mM) in constant PA+TD concentration (2.5 mM) ternary mixture of UA+PA+TD in PBS (pH 7) at DEA modified GC electrode at scan rate 0.1V/s.

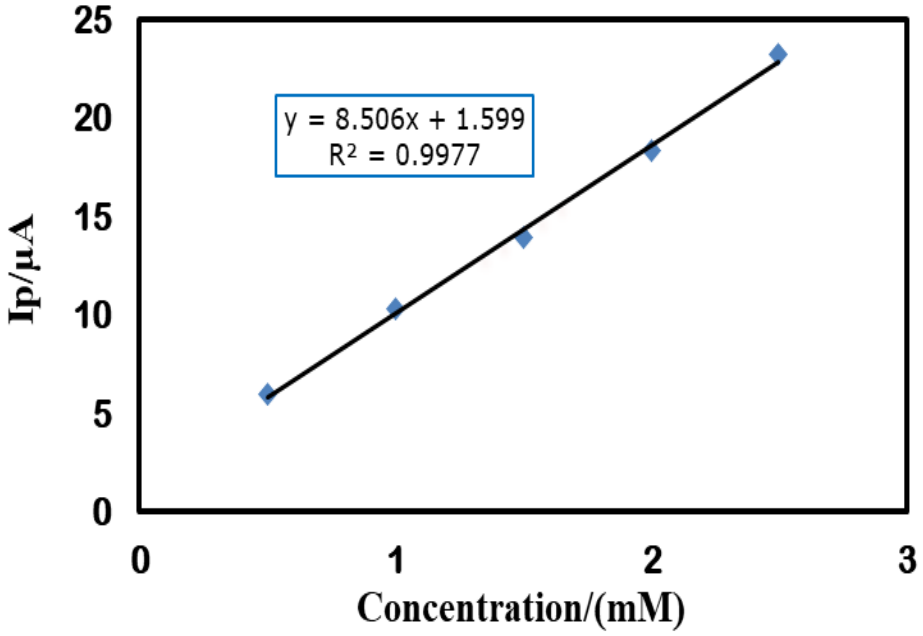

Figure 4.63: Plots of peak currents (Ip) of UA vs concentrations (0.5-2.5 mM) at constant concentration of PA+TD (2.5 mM) in a ternary mixture of UA+PA+TD at DEA modified GC electrode.

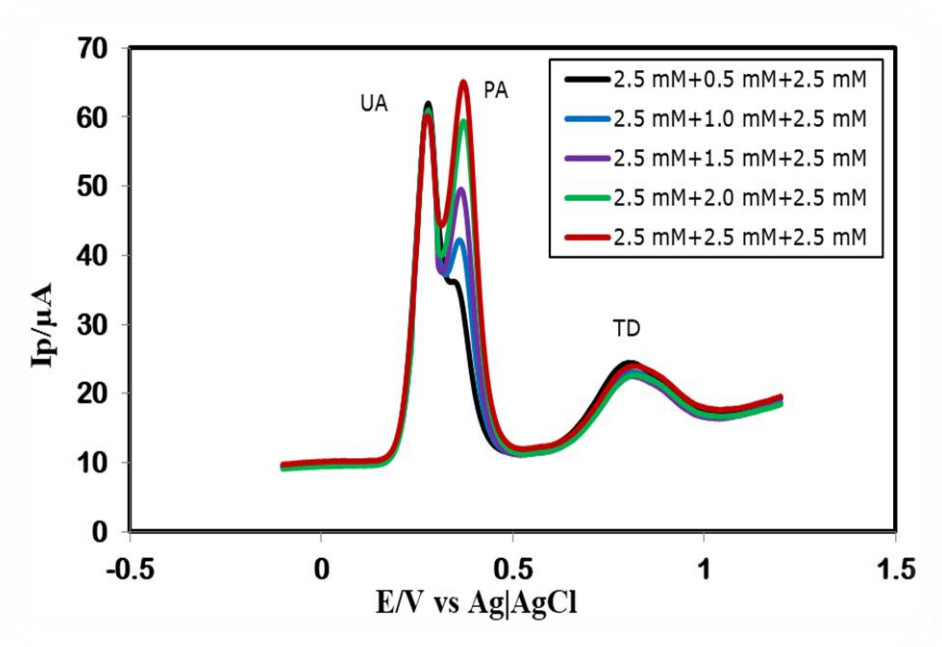

Figure 4.64: DPVs of different concentration of PA (0.5-2.5 mM) in constant UA+TD concentration (2.5 mM) ternary mixture in PBS (pH 7) at DEA modified GC electrode at scan rate 0.1V/s.

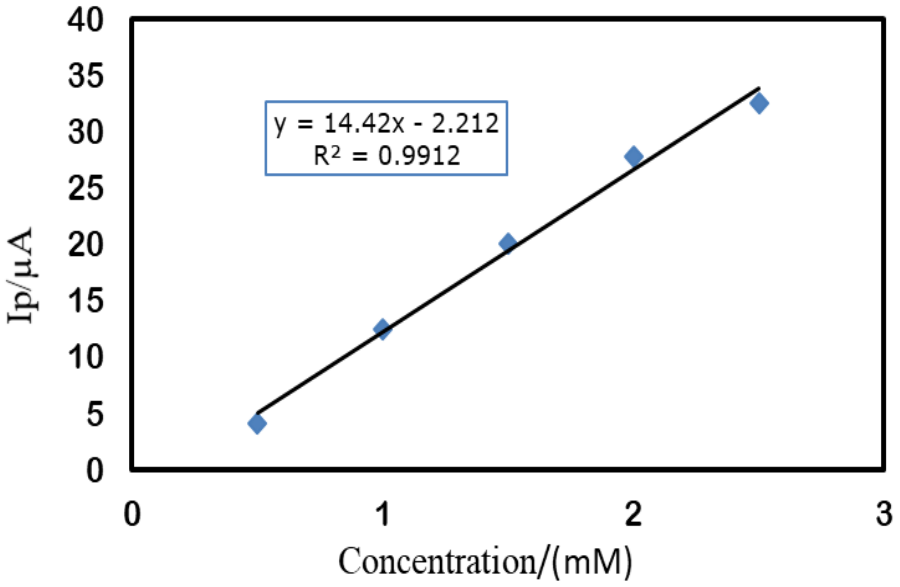

Figure 4.65: Plots of peak currents (Ip) of PA vs concentrations (0.5-2.5 mM) at constant concentration of UA+TD (2.5 mM) in a ternary mixture of UA+PA+TD at DEA modified GC electrode.

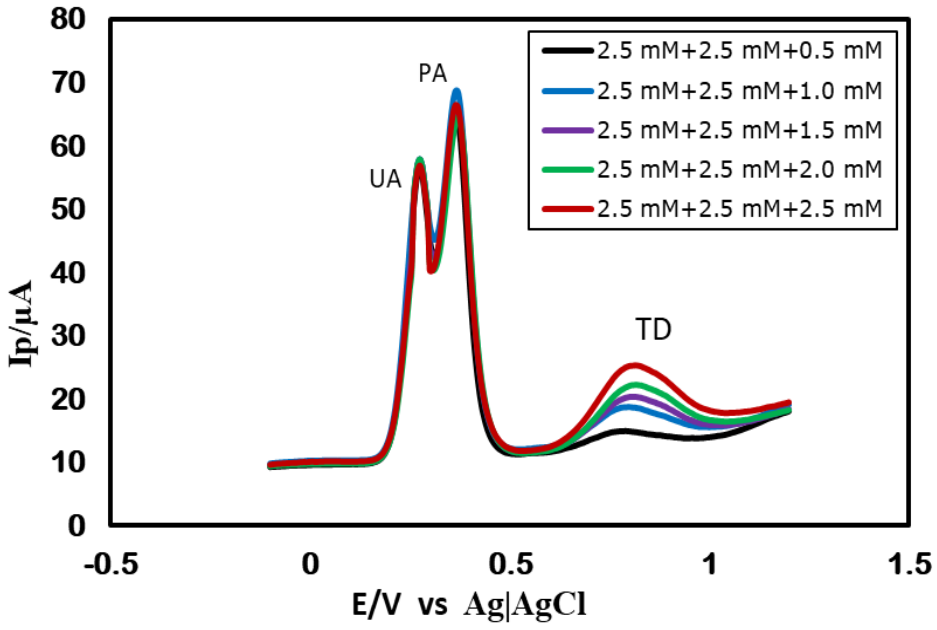

Figure 4.66: DPVs of different concentration of TD (0.5-2.5 mM) in constant UA+PA concentration (2.5 mM) ternary mixture in PBS (pH 7) at DEA modified GC electrode at scan rate 0.1V/s.

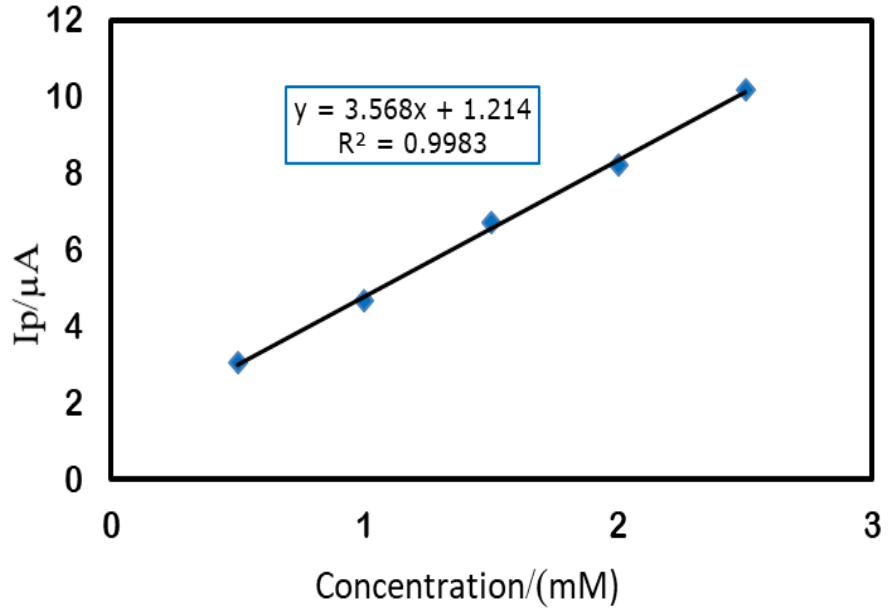

Figure 4.67: Plots of peak currents (Ip) of TD vs concentrations (0.5-2.5 mM) at constant concentration of UA+PA (2.5 mM) in a ternary mixture of UA+PA+TD at DEA modified GC electrode.

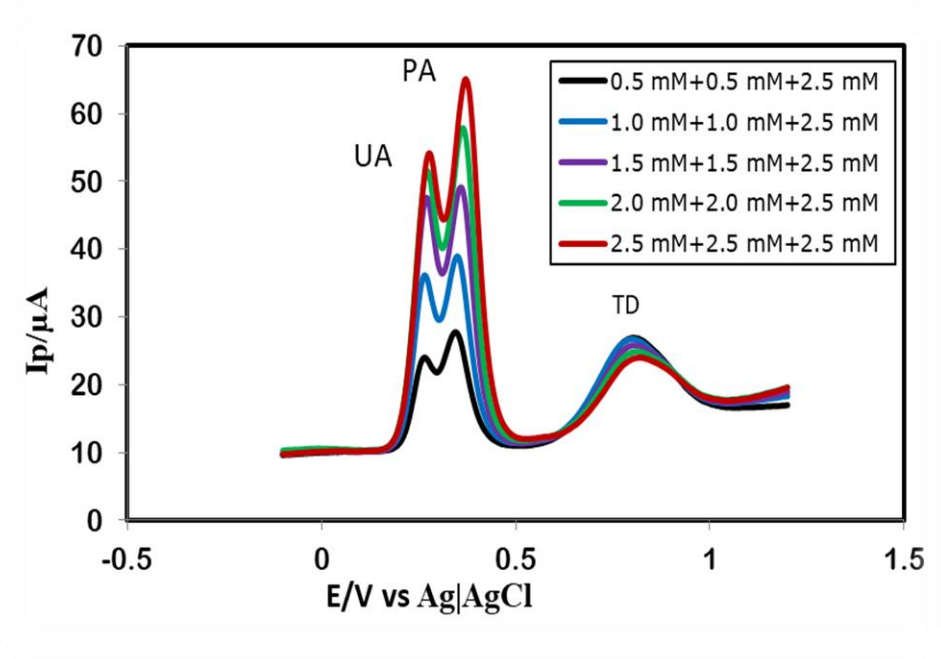

Figure 4.68: DPVs of different concentration of UA+PA (0.5-2.5 mM) in constant TD concentration (2.5 mM) ternary mixture in PBS (pH 7) at DEA modified GC electrode at scan rate 0.1V/s.

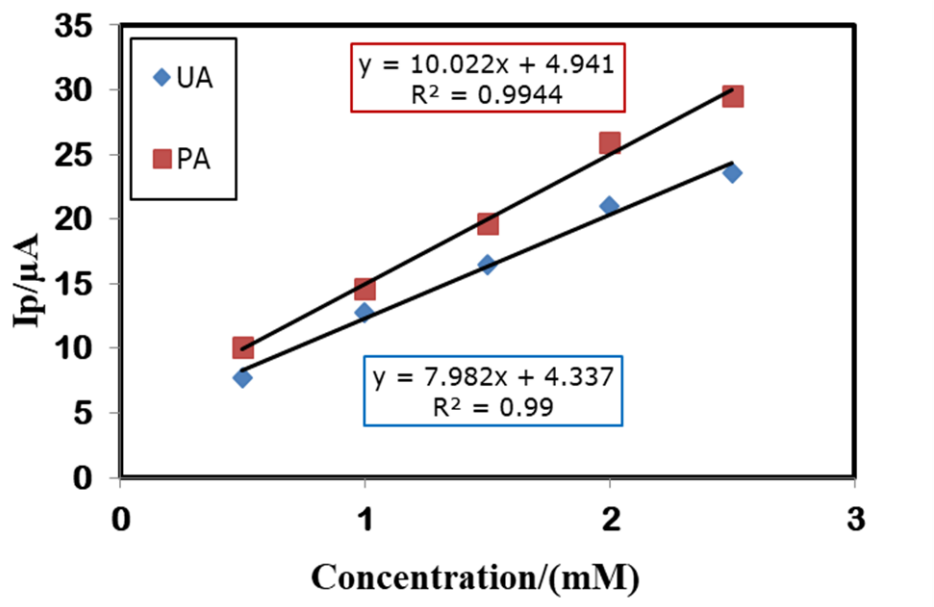

Figure 4.69: Plots of peak currents (Ip) of UA and PA vs concentrations (0.5-2.5 mM) at constant concentration of TD (2.5 mM) in a ternary mixture of UA+PA+TD at DEA modified GC electrode.

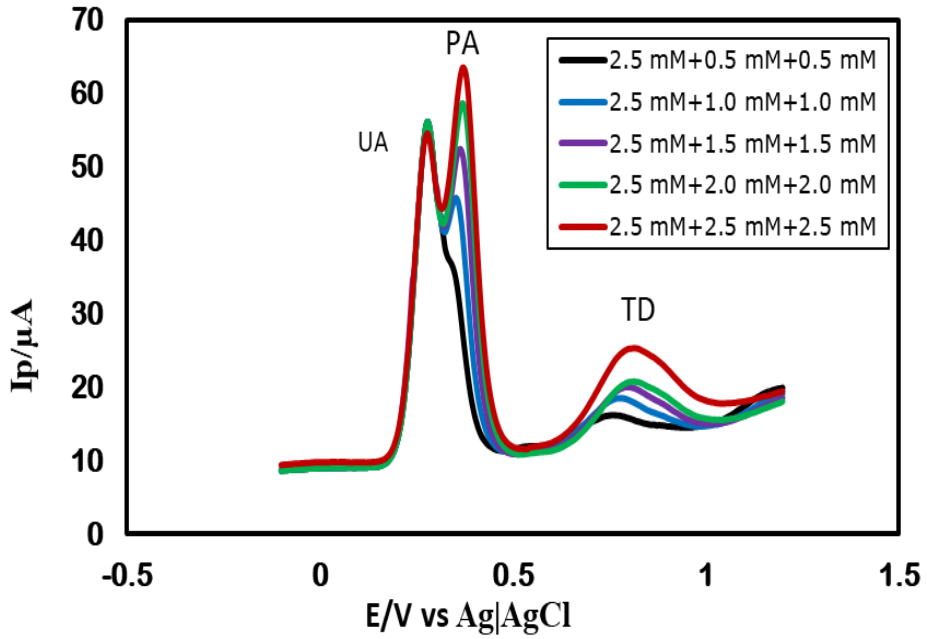

Figure 4.70: DPVs of different concentration of PA+TD (0.5-2.5 mM) in constant UA concentration (2.5 mM) ternary mixture in PBS (pH 7) at DEA modified GC electrode at scan rate 0.1V/s.

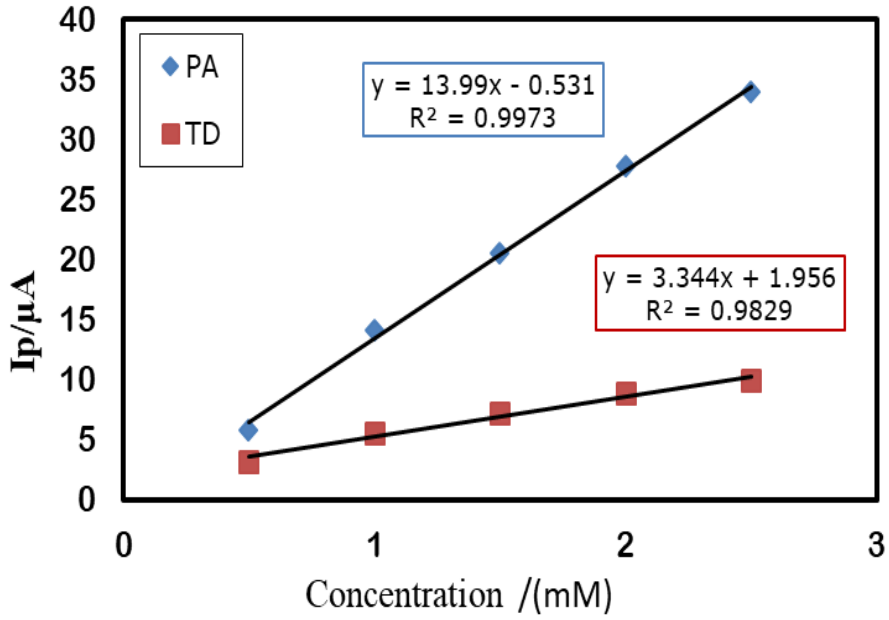

Figure 4.71: Plots of peak currents (Ip) of PA and TD vs concentrations (0.5-2.5 mM) at constant concentration of UA (2.5 mM) in a ternary mixture of UA+PA+TD at DEA modified GC electrode.

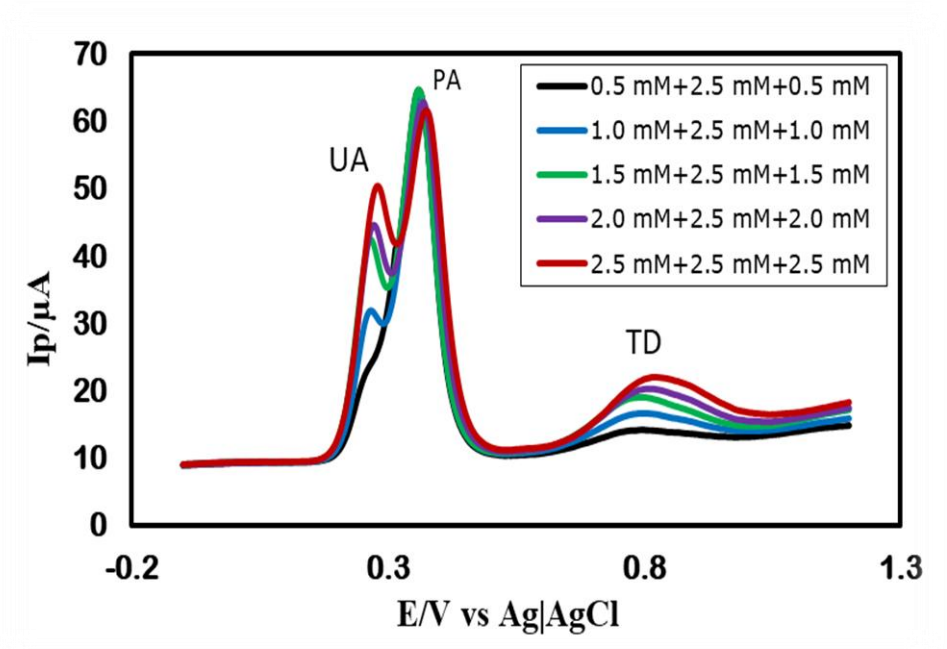

Figure 4.72: DPVs of different concentration of UA+TD (0.5-2.5 mM) in constant PA concentration (2.5 mM) ternary mixture in PBS (pH 7) at DEA modified GC electrode at scan rate 0.1V/s.

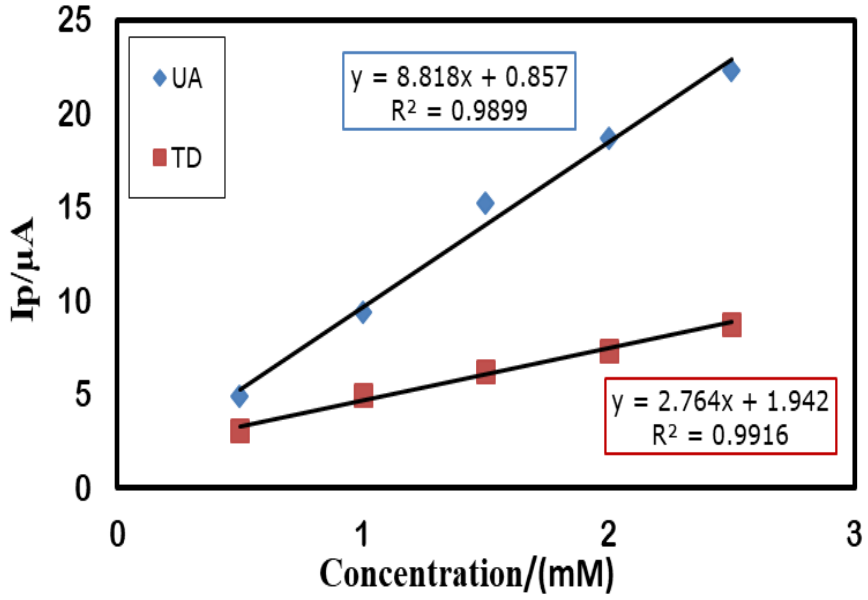

Figure 4.73: Plots of peak currents (Ip) of UA and TD vs concentrations (0.5-2.5 mM) at constant concentration of PA (2.5 mM) in a ternary mixture of UA+PA+TD at DEA modified GC electrode.

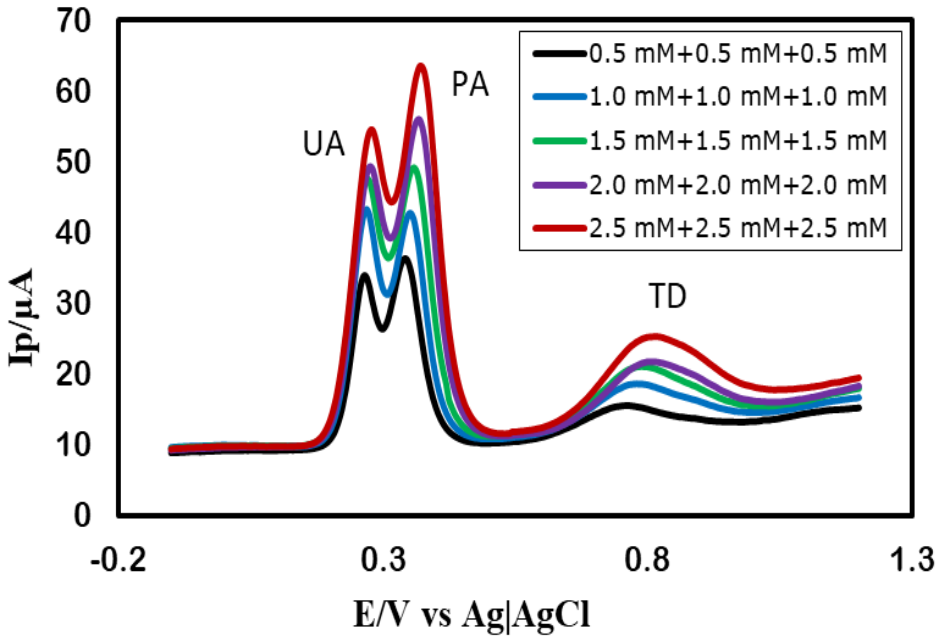

Figure 4.74: DPVs of different concentrations of the ternary mixture of UA+PA+TD (0.5-2.5 mM) in PBS (pH 7) at DEA modified GC electrode at scan rate 0.1V/s.

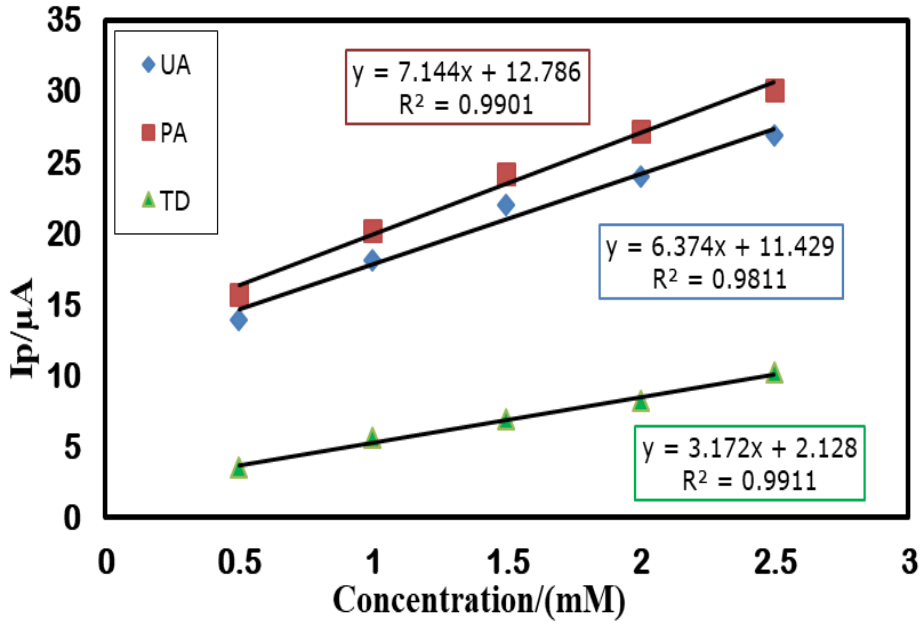

Figure 4.75: Plots of peak currents (Ip) of UA, PA and TD vs concentrations (0.5-2.5 mM) in a ternary mixture of UA+PA+TD at DEA modified GC electrode.

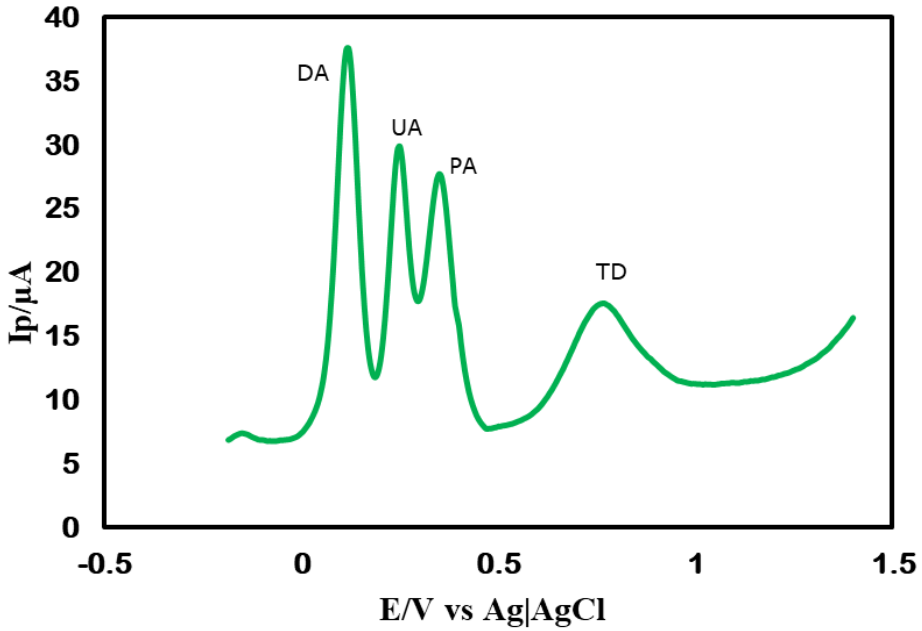

Figure 4.76: DPV of the ternary solution of UA, PA and TD in presence of aspirin, lysine, arginine, glycine, thiamine (vitamin B1), nicotinamide (vitamion B3) and dopamine (DA) in PBS (pH 7) at DEA modified GC electrode.

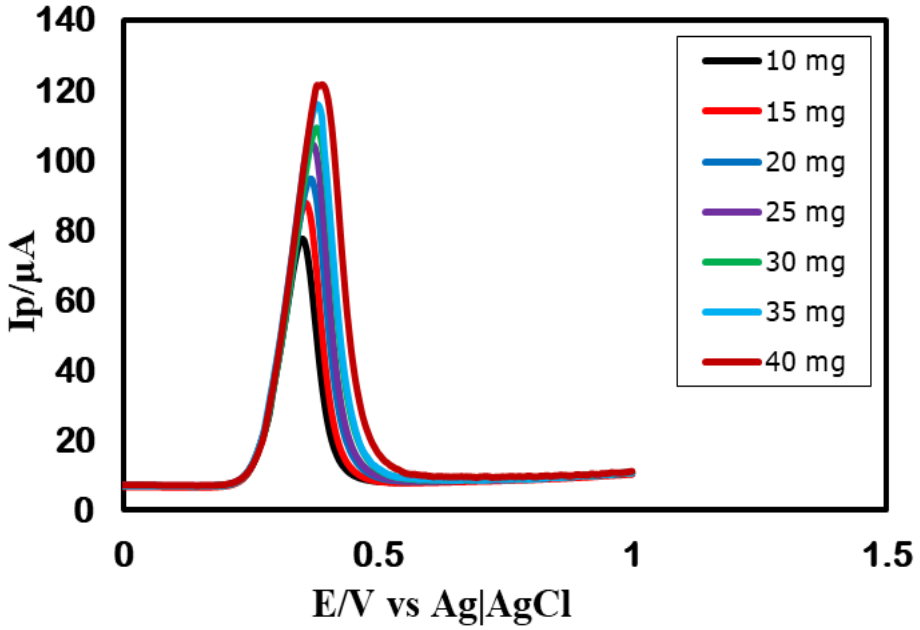

Figure 4.77: DPVs of different amount (10-40 mg) of standard PA in 50 mL PBS (pH 7) solution at DEA modified GC electrode.

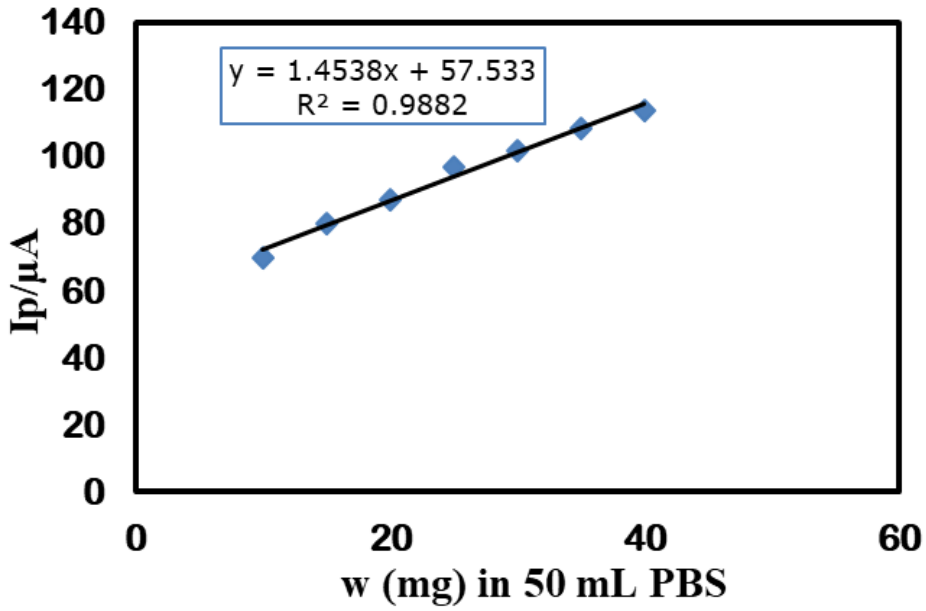

Figure 4.78: Calibration curve of PA with response to different amount (10-40 mg) in 50 mL PBS (pH 7).

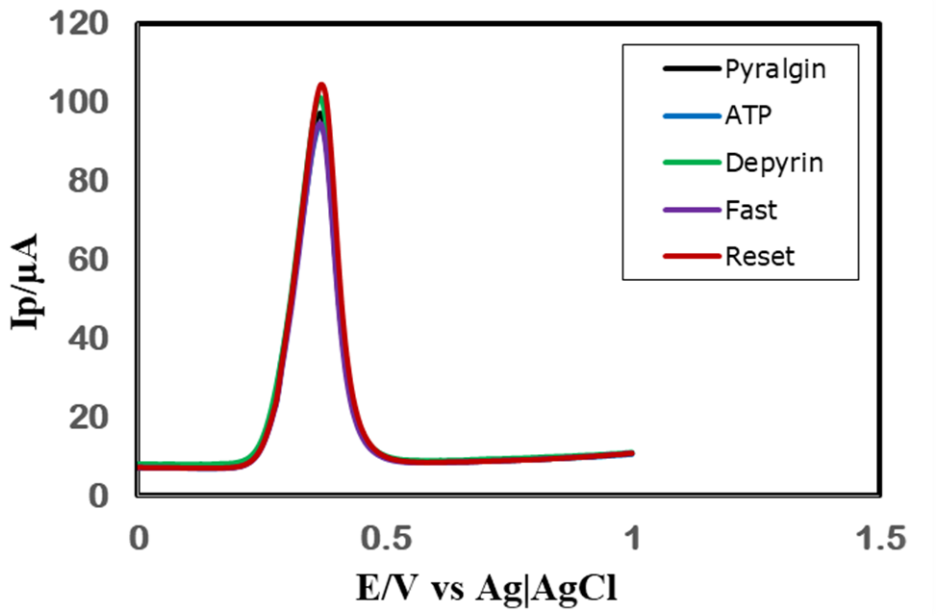

Figure 4.79: DPVs of PA in Reset (red line), Fast (purple line), Depyrin (green line), ATP (blue line) and Pyralgin (black line) tablets in PBS (pH 7) at DEA modified GC electrode.

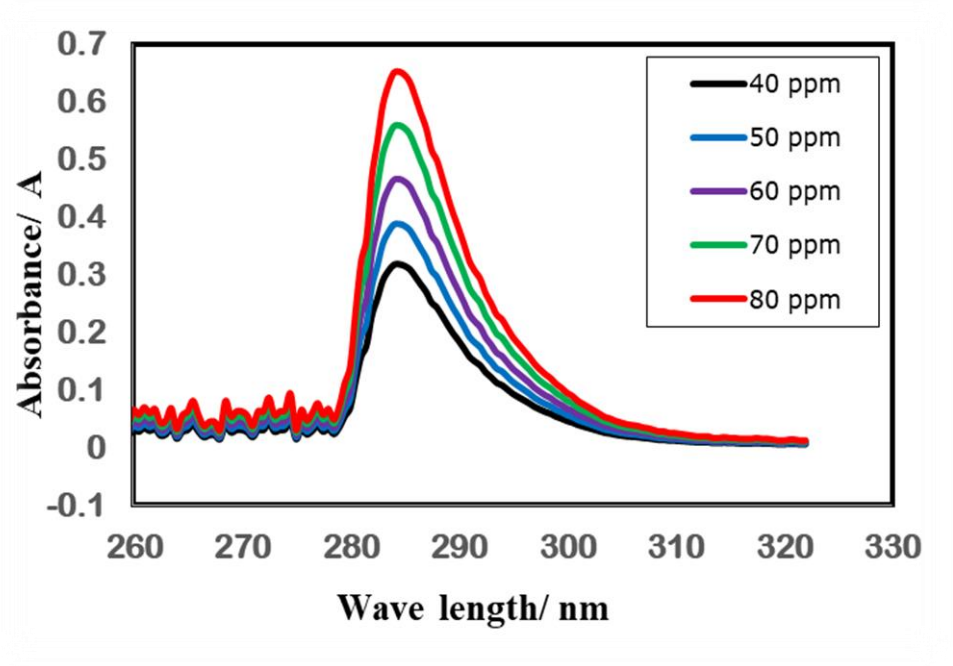

Figure 4.80: UV-Visible spectra of the different concentration (40-80 ppm) of standard PA in PBS (pH 7).

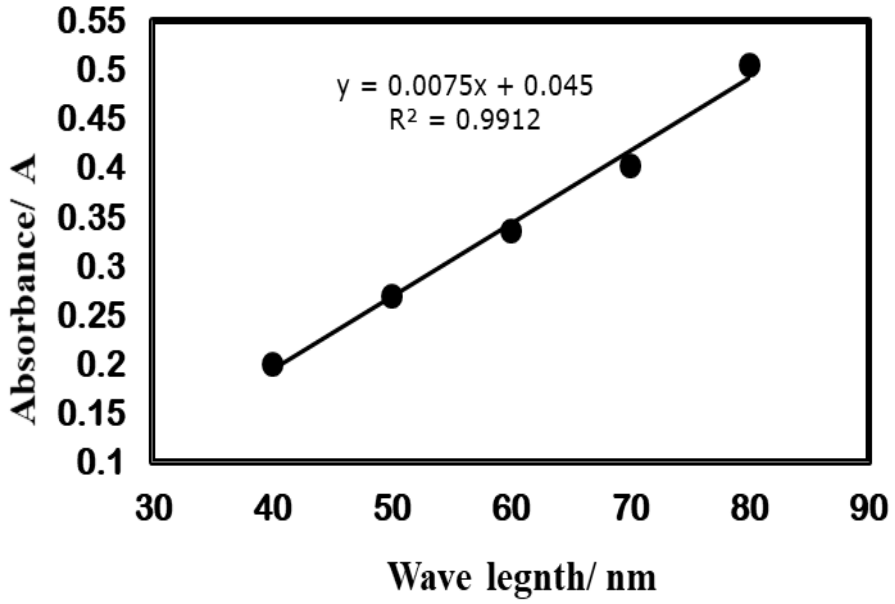

Figure 4.81: Calibration curve of standard PA with response different concentrations (40-80 ppm) in PBS (pH 7).

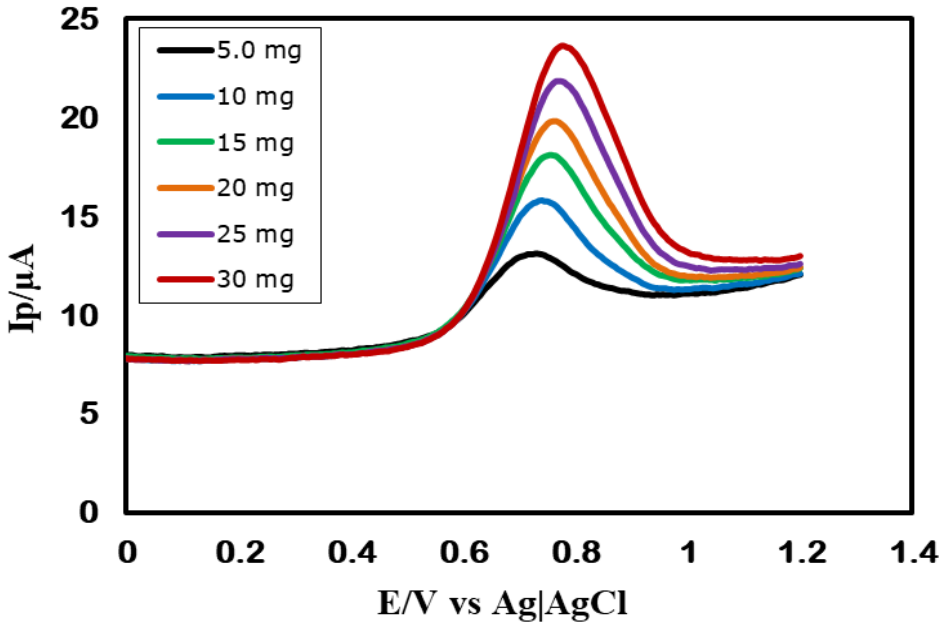

Figure 4.82: DPVs of different amount (5-30 mg) of standard TD in 50 mL PBS (pH 7) solution at DEA modified GC electrode.

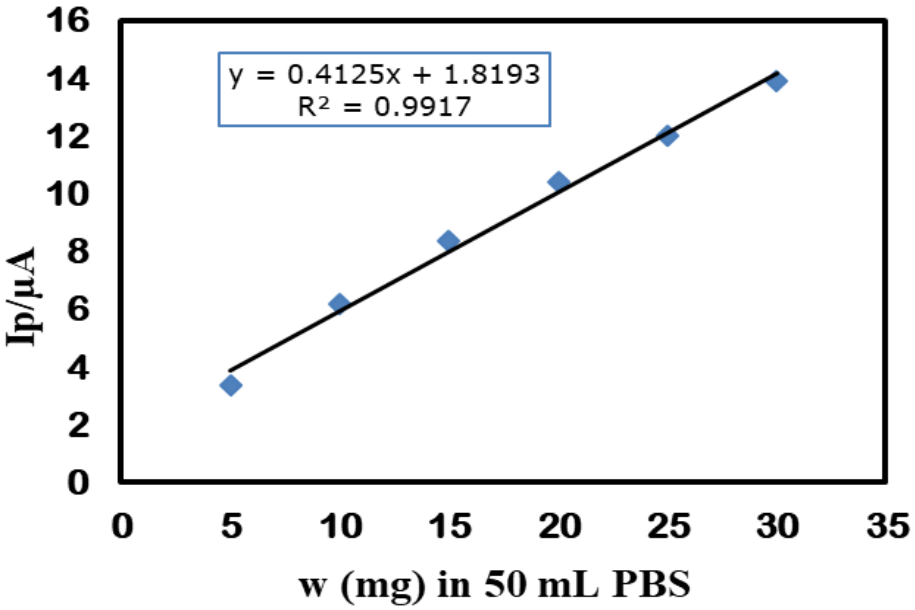

Figure 4.83: Calibration curve of TD with response to different amount (5-30 mg) in 50 mL PBS (pH 7).

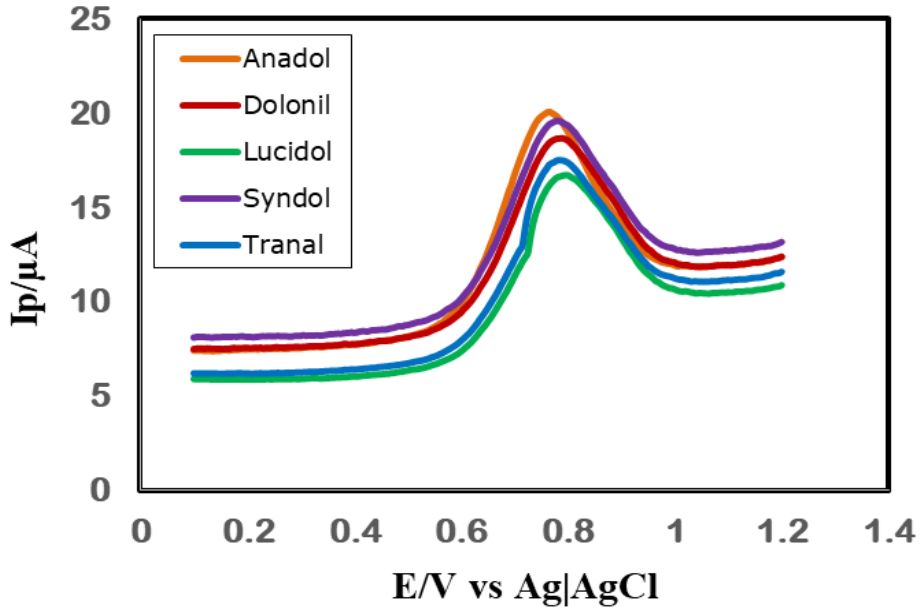

Figure 4.84: DPVs of TD in Anadol (orange line), Dolonil (red line), Lucidol (green line), Syndol (purple line),) and Tranal (light blue line) tablets in PBS (pH 7) at DEA modified GC electrode.

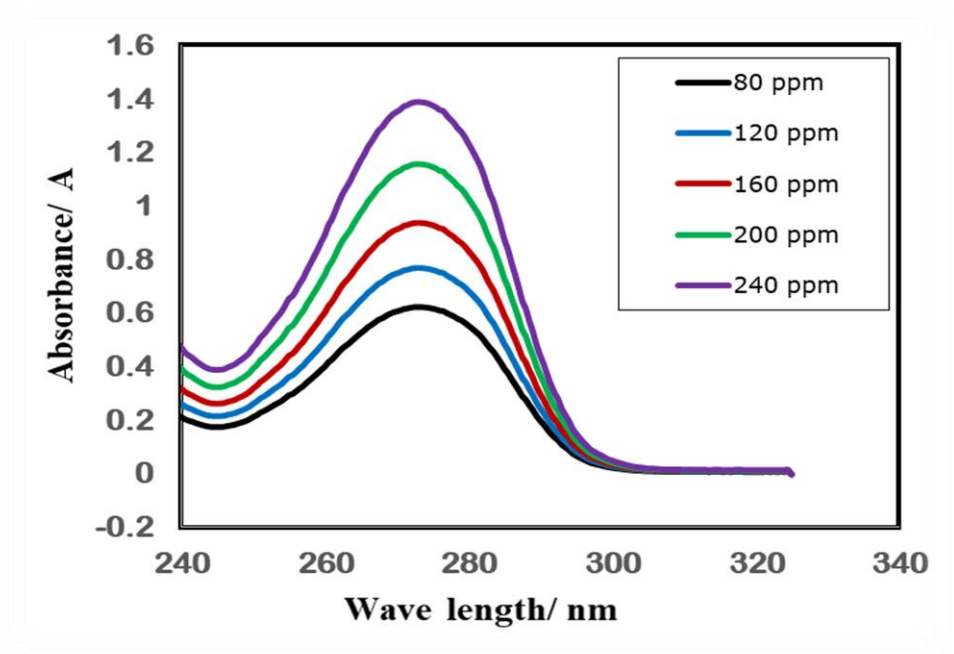

Figure 4.85: UV-Visible spectra of the different concentration (80-240 ppm) of standard TD in PBS (pH 7).

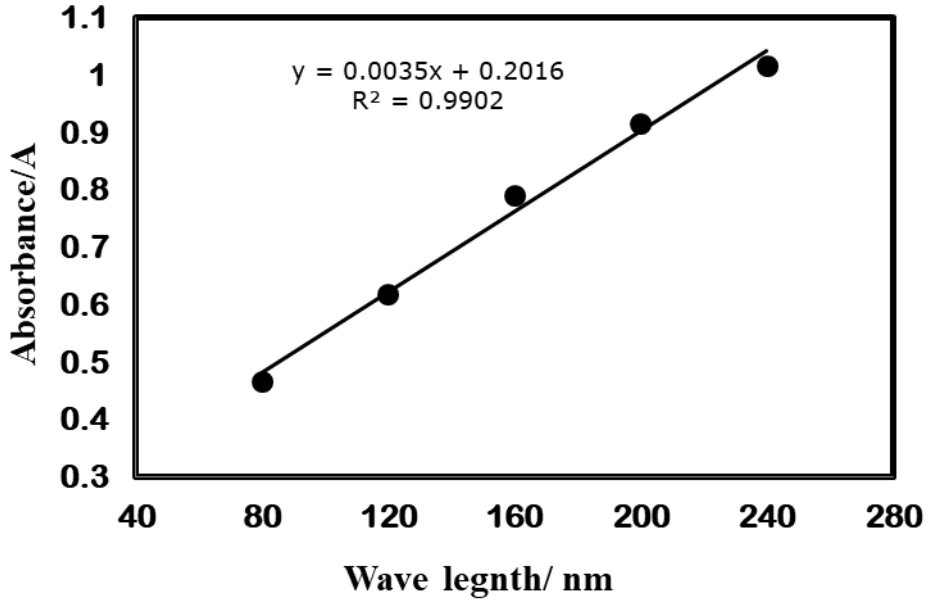

Figure 4.86: Calibration curve of standard TD with response to different concentrations (80-240 ppm) in PBS (pH 7).

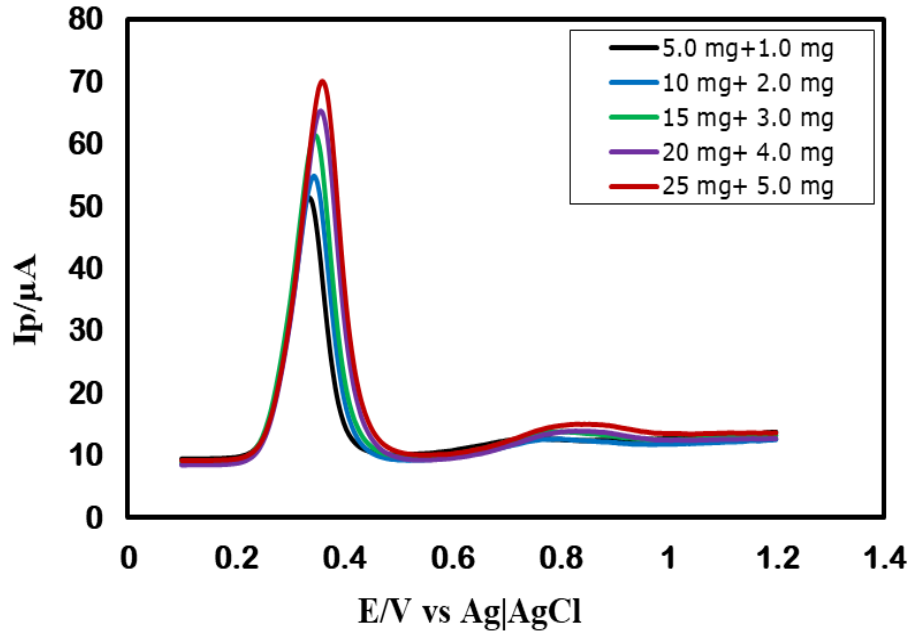

Figure 4.87: DPVs of different amount of standard PA+TD in 50 mL PBS (pH 7) solution at DEA modified GC electrode.

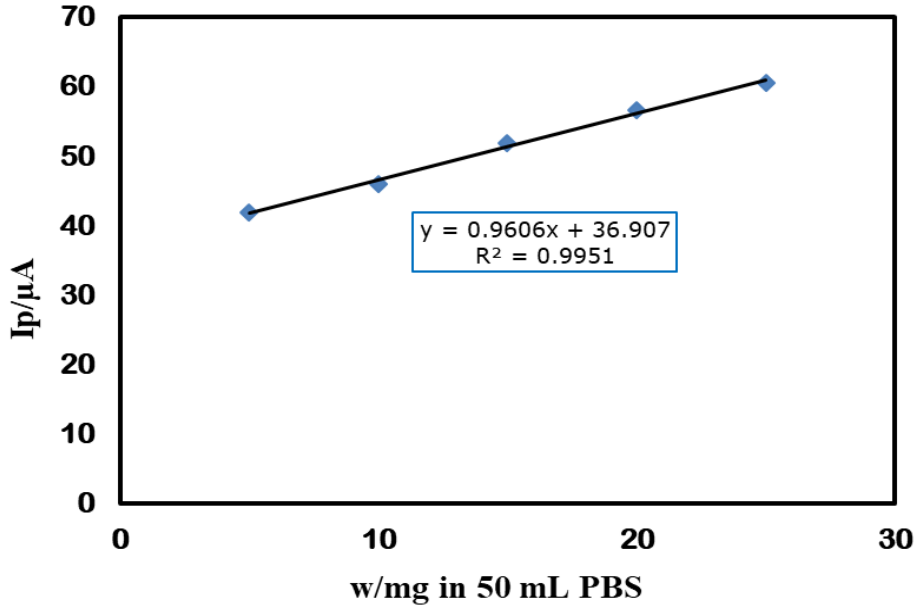

Figure 4.88: Calibration curve of PA with response to different amount (mg) of binary mixture of PA+TD in 50 mL PBS (pH 7).

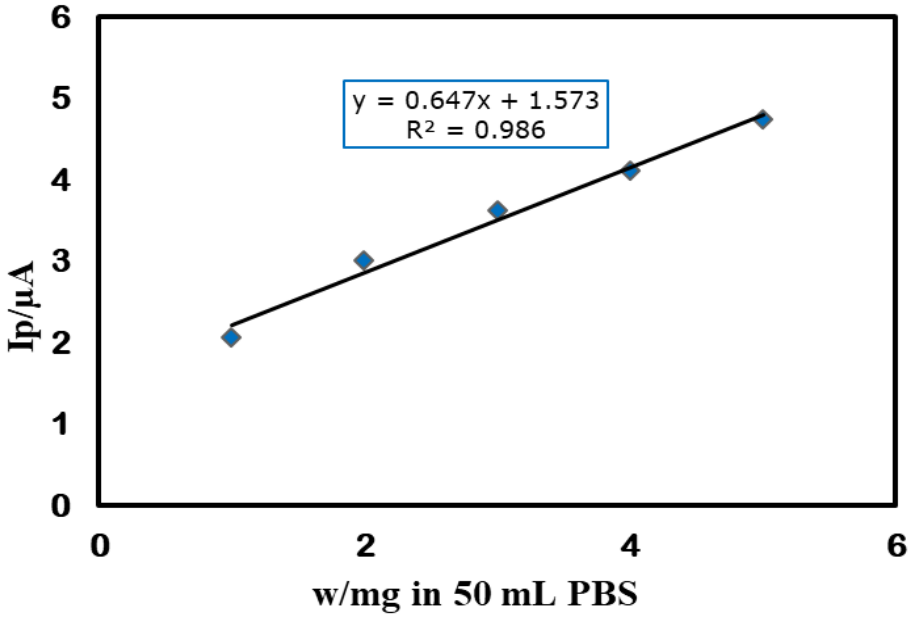

Figure 4.89: Calibration curve of TD with response to different amount (mg) of binary mixture of PA+TD in 50 mL PBS (pH 7).

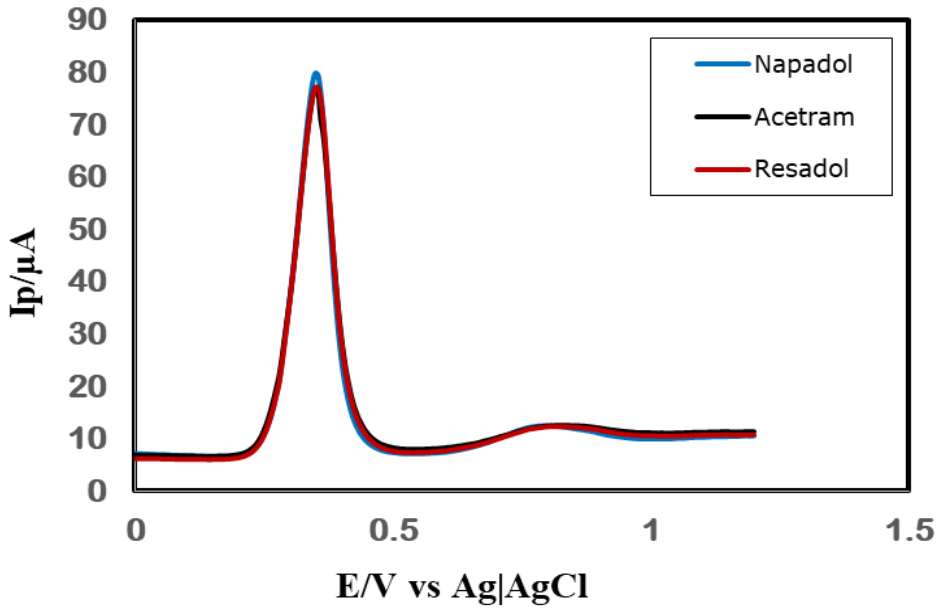

Figure 4.90: DPVs of PA+TD in Napadol (blue line), Resadol (red line) and Acetram (black line) tablets in PBS (pH 7) at DEA modified GC electrode.

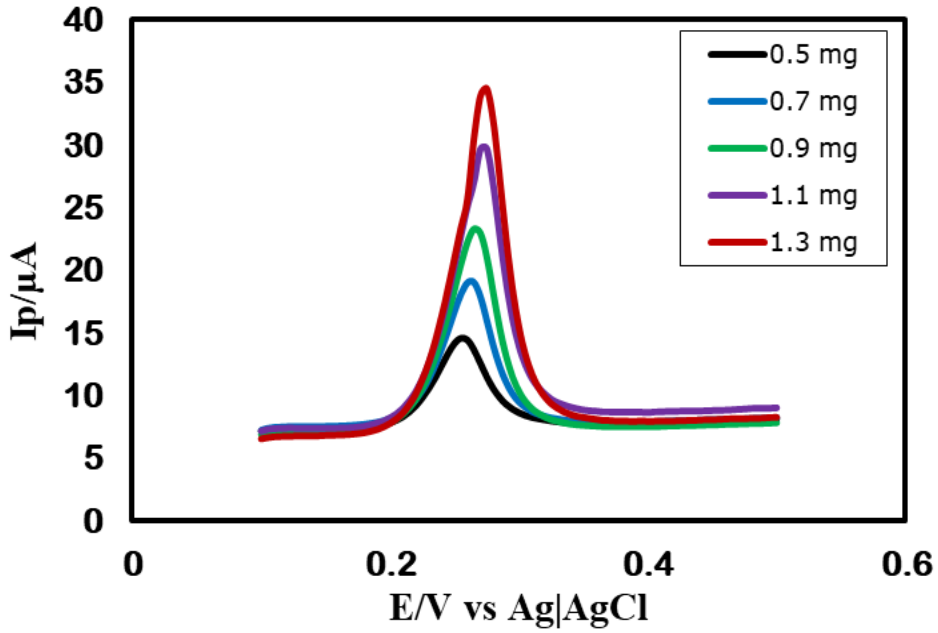

Figure 4.91: DPVs of different amount of standard UA in 50 mL PBS (pH 7) solution at DEA modified GC electrode.

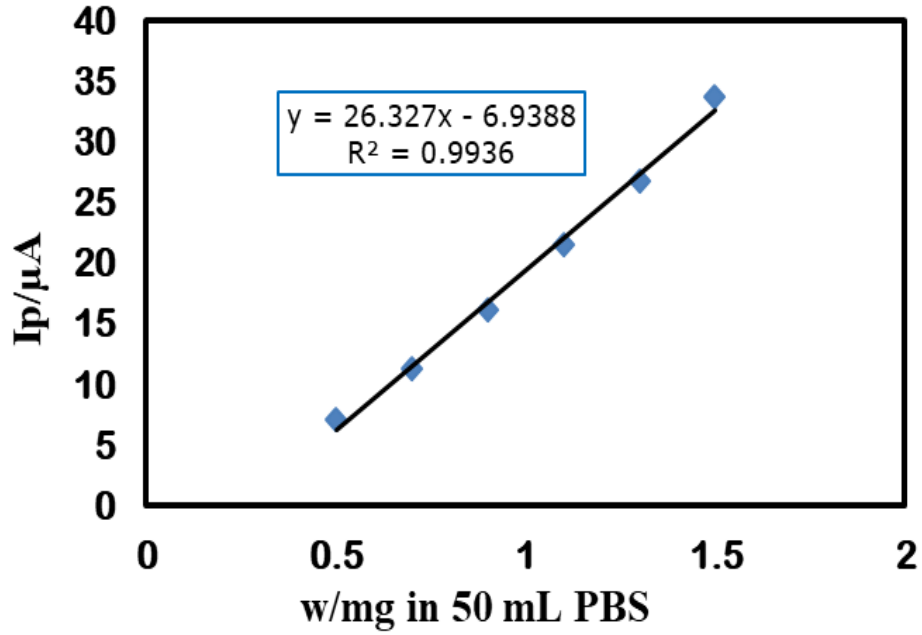

Figure 4.92: Calibration curve of UA with response to different amount (mg) in 50 mL PBS (pH 7).

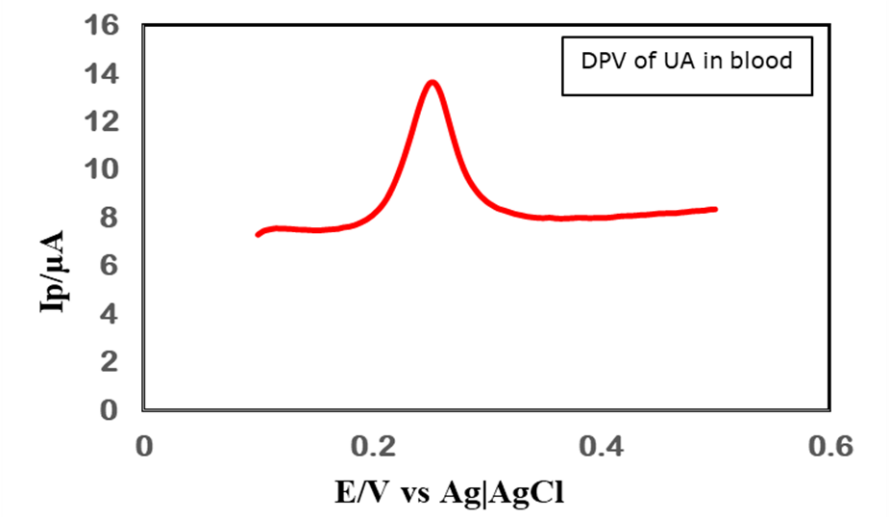

Figure 4.93: DPV of UA in blood sample (7.5 mL blood + 22.5 mL PBS) at DEA modified GC electrode.

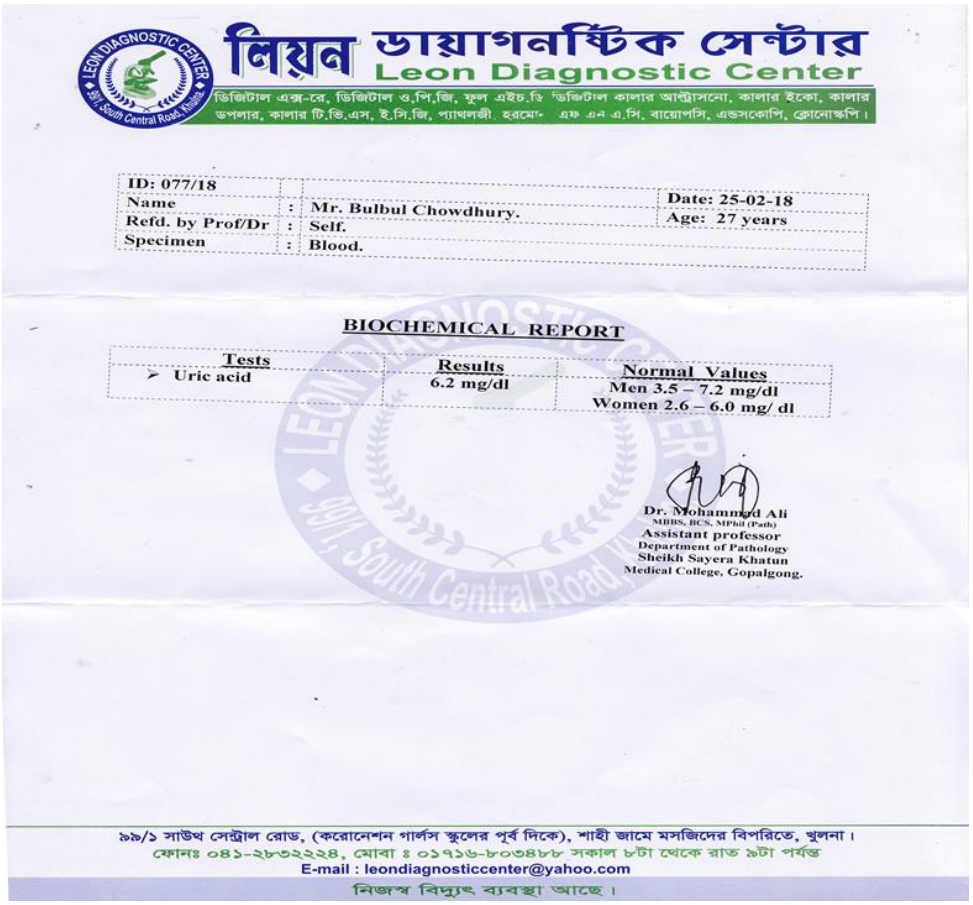

লিয়ন ডায়াগনষ্টিক সেন্টার
Leon Diagnostic Center
ডিজিটাল এক্স-রে, ডিজিটাল ও.পি.জি, ফুল এইচ.ডি ডিজিটাল কালার আল্ট্রাসনো, কালার ইকো, কালার ডপলার, কালার টি.ভি.এস, ই.সি.জি, প্যাথলজী, হরমো- এফ এন এ.সি, বায়োপসি, এন্ডসকোপি, ক্রোনোস্কপি।

ID: 077/18			
Name	:	Mr. Bulbul Chowdhury.	Date: 25-02-18
Refd. by Prof/Dr	:	Self.	Age: 27 years
Specimen	:	Blood.	

BIOCHEMICAL REPORT

Tests	Results	Normal Values
➢ Uric acid	6.2 mg/dl	Men 3.5 – 7.2 mg/dl Women 2.6 – 6.0 mg/ dl

Dr. Mohammad Ali
MBBS, BCS, MPhil (Path)
Assistant professor
Department of Pathology
Sheikh Sayera Khatun
Medical College, Gopalgong.

৯৯/১ সাউথ সেন্ট্রাল রোড, (করোনেশন গার্লস স্কুলের পূর্ব দিকে), শাহী জামে মসজিদের বিপরিতে, খুলনা।
ফোনঃ ০৪১-২৮৩২২২৪, মোবা ঃ ০১৭১৬-৮০৩৪৮৮ সকাল ৮টা থেকে রাত ৯টা পর্যন্ত
E-mail : leondiagnosticcenter@yahoo.com
নিজস্ব বিদ্যুৎ ব্যবস্থা আছে।

Figure 4.94: Pathological report for the determination of UA in human blood sample.

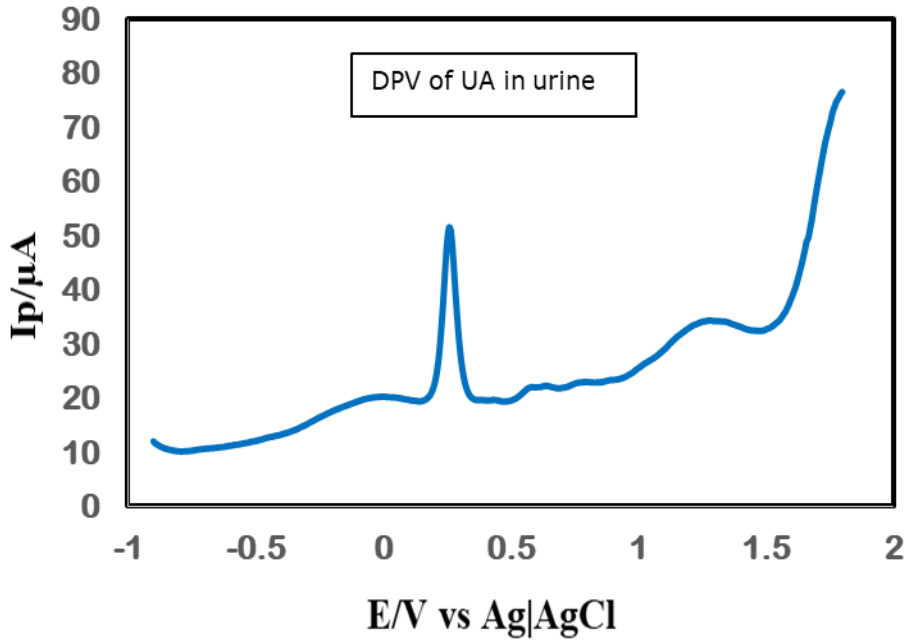

Figure 4.95: DPV of UA in urine sample (20 mL urine + 30 mL PBS) at DEA modified GC electrode.

CHAPTER V

Conclusions

A simple and sensitive modified electrode sensor based on Diethylamine (DEA) modified Glassy carbon (GC) electrode has been developed for the determination of Paracetamol (PA), Tramadol (TD) and Uric acid (UA). The DEA modified GC electrode has been found to have sensing capability for the simultaneous detection and quantitative determination of PA, TD and UA.

The detection is mostly favorable at pH 7. The performance of modified GC electrode is better than modified Au and Pt electrodes. DEA modified GC electrode shows very good sensitivity than bare GC electrode with considerable detection limit. In simultaneous detection, the limit of detection (LoD) for PA, TD and UA are 1.45 μmol L^{-1}, 1.26 μmol L^{-1} and 1.95 μmol L^{-1} respectively at DEA modified GC electrode. The sensitivity for PA, TD and UA are 62.25 μA/mM/cm^2, 33.67 μA/mM/cm^2 and 52.08 μA/mM/cm^2 respectively.

DEA modified GC electrode shows very good recovery value with minimum standard deviations. It has been successfully used to determine the amount of PA and TD in their relevant tablets of some different pharmaceutical companies of Bangladesh and UA in blood and urine sample. The modified electrode sensor values are consistent with spectroscopic measurement value. DEA modified electrode is simple and rapid to fabricate. The modified electrode shows a stable output response and good selectivity in the presence of interfering species.

DEA modified GC electrode sensor is recommended to the pharmaceutical industries for the determination of PA and TD. This sensor can also be recommended for the determination of UA in blood sample. It may save testing time and testing reagents to reduce the testing cost of the tablets, blood and urine sample.

REFERENCES

1. Lubert K. H. and Kalcher K., 2010, "History of Electroanalytical Methods" Electroanalysis, Vol. 22, pp. 1937-1946.
2. J. A. Plambeck., 1982, Electroanalytical Chemistry, Basic Principles and Application, Wiley Interscience Pub., USA.
3. M. R. Smyth and J. G. Vos, 1992, "Analytical Voltammetry. XXVII", Elsevier Science Pub., Amsterdam.
4. J. Wang, 2006, "Electroanalytical Chemistry", Wiley-VCH Pub., New Jersey, 3rd Ed.
5. P. T. Kissenger and W. R. Heineman, 1996, "Laboratory Techniques in Electroanalytical Chemistry", Marcel Dekker, New York, 2nd Ed.
6. Holford, T. R. J., Davis, F. and Higson, S.P.J., 2012, "Recent trends in antibody based sensors", Biosensors & Bioelectronics, Vol. 34, pp. 12-24.
7. Palchetti, I. and Mascini, M., 2012, "Electrochemical Nanomaterial Based Nucleic Acid Apta sensors", Analytical and Bioanalytical Chemistry, Vol 402, pp. 3103-3114.
8. Perfezou, M., Turner, A. and Merkoci, A., 2012, "Cancer Detection Using Nanoparticle - Based Sensors", Chemical Society Reviews, Vol. 41, pp. 2606-2622.
9. A. J. Bard and L. R. Faulkner, 2000, "Electrochemical Methods, Fundamentals and Applications", John wiley & sons, inc., USA, 2nd Ed.
10. Skoog, D. A., West, D. M., Holler, F. J. and Crouch, S. R., 2007, "Principles of Instrumental Analysis", Belmont, CA: Brooks/Cole, Thomson. p. 1. ISBN 0-495-01201-7.
11. Skoog, D. A., West, D. M. and Holler, F. J., 2014, Fundamentals of Analytical Chemistry, 7th Ed.). Harcourt Brace College Publishers, ISBN 0-03-005938-0.
12. Murray, R. W., 1984, "Chemically Modified Electrodes", Electroanalytical Chemistry, Vol. 13 pp. 379-382.
13. Janata, J. and Huber, R. J., 1985, "Solid State Chemical Sensors," Academic Press, Orlando, FL.

14. Palchetti, I. and Mascini, M., 2012, “Electrochemical Nanomaterial Based Nucleic Acid Apta sensors”, Analytical and Bioanalytical Chemistry, Vol. 402, pp. 3103-3114.

15. X. Zhang, H. Ju and J. Wang, 2008, Electrochemical sensors, biosensors and their biomedical applications, Elsevier, Academic press.

16. Buck, R. P., Freiser, H. and Plenum, N.Y., 1978, “Theory and Principles of Membrane Electrodes”, Chapt. 1, Ion-Selective Electrodes in Analytical Chemistry, Vol. 1.

17. Ross, J. W., Riseman, J. H. and J. A. Krueger., 1973, “Theory and applications of ion-selective electrodes” Pure Appl. Chem., Vol. 36(4), pp. 473-476.

18. Clark, L. C. Trans. Am. SOC. Artif, 1956, “Monitor and control of blood and tissue oxygen tensions” Int. Organs., Vol. 2, pp. 41-46.

19. Eggins, B. R., 2008, “Chemical Sensors and Biosensors (Google eBook)”, John Wiley & Sons.

20. Ren, W., Luo, H. Q. and Li, N. B., 2006, “Simultaneous voltammetric measurement of ascorbic acid, epinephrine and uric acid at a glassy carbon electrode modified with caffeic acid” Biosens. Bioelectron., Vol. 21, pp. 1086-1088.

21. Duvall, S. H. and McCreery, R. L., 1999, “Control of Catechol and Hydroquinone Electron. Transfer Kinetics on Native and Modified Glassy Carbon Electrodes” Anal. Chem., Vol. 71, pp. 4594.

22. Murray, R. W., 1980, “Chemically modified electrodes” Acc. Chem. Res., Vol. 13, pp. 135-141.

23. Qi, H. L. and Zhang, C. X., 2005, “Simultaneous determination of hydroquinone and catechol at a glassy carbon electrode modified with multiwall carbon nanotubes” Electroanal., Vol. 17, pp. 832-838.

24. Diab, N., Oni, J. and Schuhmann, W., 2005, “Electrochemical nitric oxide sensor preparation” Bioelectrochem., Vol. 66, pp. 105-110.

25. Deng, C., Li, M., Xie, Q. Liu, M. Tan, Y. Xu, X. and Yao, S., 2006, “Electrochemical quartz crystal impedance study on immobilization of glucose oxidase in a polymer grown from dopamine oxidation at an Au electrode for glucose sensing” Anal. Chem. Act., Vol. 557, pp. 85-88.

26. Chen, Z., and Zhou, Y., 2006, “Surface modification of resistance welding electrodes by electro-spark deposited composite coatings Surface and Coatings Technology: Part II. Metallurgical behavior during welding,” Electroanalytical Chemistry, Vol. 201, pp. 2419-2430.

27. Shahin Ara Mitu, 2017, “Development of Sulfolane Modified Electrode Sensor for the Determination of Vitamin-B6, Vitamin-C and Uric Acid,” M.Sc Thesis, Dept. of Chemistry, KUET.

28. Sivakumar, C., Nian, J. N. and Teng, H., 2005, “Poly (o-toluidine) for carbon fabric electrode modification to enhance the electrochemical capacitance and conductivity” Journal of Power Sources, Vol. 144, pp. 295-301.

29. Urray, R. W., 1980, “Chemically modified electrodes” Acc. Chem. Res., Vol. 13, pp. 135-141.

30. Qi, H. L. and Zhanh, C. X., 2005 “Simultaneous determination of hydroquinone and catechol at a glassy carbon electrode modified with multiwall carbon nanotubes” Electroanal., Vol. 17, pp. 832-838.

31. Juan, L. and Xiaoli, Z., 2012, “Fabrication of Poly (Aspartic Acid)-Nanogold Modified Electrode and Its Application for Simultaneous Determination of Dopamine, Ascorbic Acid and Uric Acid,” American Journal of Analytical Chemistry, Vol. 3, pp. 195-203.

32. Bensalah, N., Gadri, A., Canizares, P., Saez, C., Lobato, J. and Rodrigo, M. A., 2005, “Electrochemical Oxidation Characteristics of p-Substituted Phenols Using a Boron-Doped Diamond Electrode” Environ. Sci. Technol., Vol. 39, pp. 7234-7239.

33. Lau, O.W., Luk, S. F. and Cheung, Y. M., 1989, “Simultaneous determination of ascorbic acid, caffeine and paracetamol in drug formulations by differential-pulse voltammetry using a glassy carbon electrode” Analyst, Vol. 114, pp. 1047-1051.

34. Keng H., and Kuwana T., 1986, “Oxidative mechanism of ascorbic acid at glassy carbon electrodes” Anal. Chem. Vol. 58 (14), pp. 3235–3239.

35. Wee T., and Halim A., 2011, “Fabrication of Nanostructured Copper Thin Films at Disposable Pencil Graphite Electrode and its Application to Elecrocatalytic Reduction of Nitrate” Int. J. Electrochem. Sci., Vol. 6, pp. 279 – 288.

36. Zhao F., Wang F., and Zhou J., 2011, “Voltammetric sensor for caffeine based on a glassy carbon electrode modified with Nafion and graphene oxide” Microchimica Acta,Vol. 174, pp. 383-390.

37. Kutluay, A., and Aslanoglu, M., 2013, “Modification of electrodes using conductive porous layers to confer selectivity for the voltammetric detection of paracetamol in the presence of ascorbic acid, dopamine and uric acid” Sensor. Actuat. B Chem. Vol.185, pp. 398–404.

38. Zhao, H., Zhang, Y. Z. and Yuan, Z. B., 2002, “Determination of Dopamine in the Presence of Ascorbic Acid using Poly (Hippuric Acid) Modified Glassy Carbon Electrode” Electroanal., Vol. 14, pp. 1031-1034.

39. Roy, P. R., saha, M. S., Okajima, T., Park, S. G., Fujishima, A. and Ohsaka, T., 2004, “Selective determination of 3,4-dihydroxyphenylacetic acid in the presence of ascorbic and uric acids using polymer film modified electrode” Electroanal. Vol. 16, pp. 1777-1781.

40. Roy, P. R., Saha, M. S., Okajima, T., and Ohsaka, T., 2004, “An electroanalytical study for the amperometric determination of ascorbic acid (AA) in a human urine sample” Electroanal., Vol. 16, pp. 289.

41. Roy, R. R., Okajima, T. and Ohsaka, T., 2004, “Comparison of the electrochemical and electroanalytical behavior of ascorbic acid, dopamine and uric acid at bare, activated and multi-wall carbon nanotubes modified glassy carbon electrodes” J. Electroanal. Chem., Vol. 75, pp. 561.

42. Afkhami, A., Khoshsafar, H., Bagheri, H. and Madrakian, T., 2014, “Preparation of NiFe2O4/graphene nanocomposite and its application as a modifier for the fabrication of an electrochemical sensor for the simultaneous determination of tramadol and acetaminophen Anal. Chim. Acta, Vol. 831, pp. 50-59.

43. Bertolini, A., Ferrari, A., Ottani, A., Guerzoni, S., Tacchi, R. and Leone, S., 2006, "Paracetamol: new vistas of an old drug". CNS Drug Reviews. Vol. 12, pp.250–75.

44. Viswanathan, A. N., Feskanich, D., Schernhammer, E. S., Hankinson, S. E., 2008, "Aspirin, NSAID, and Acetaminophen Use and the Risk of Endometrial Cancer". Cancer Research. Vol.68, pp.2507–2513.

45. Altinoz, M. A., Korkmaz, R., 2004, "NF-kappaB, macrophage migration inhibitory factor and cyclooxygenase-inhibitions as likely mechanisms behind the acetaminophen- and NSAID-prevention of the ovarian cancer," Neoplasma. Vol.51, pp.239–247.

46. Babaei, A., Garrett, D. J., Downard, A. J., 2011, “Selective Simultaneous Determination of Paracetamol and Uric Acid Using a Glassy Carbon Electrode Modified with Multiwalled Carbon Nanotube/Chitosan Composite,” Electroanalysis, Vol. 23 pp.417-423.

47. Perrott, D. A., Piira, T., Goodenough, B., Champion, G. D., 2004, "Efficacy and safety of acetaminophen vs ibuprofen for treating children's pain or fever: a meta-analysis". Arch Pediatr Adolesc Med. Vol.158 (6) pp. 521–526.

48. Larson, A. M., Polson, J., Fontana, R. J., 2005, "Acetaminophen-induced acute liver failure: results of a United States multicenter, prospective study," Hepatology. Vol. 42 (6) pp.1364–1372.

49. Jeevagan A. J., and John, S.A., 2012, “Electrochemical determination of caffeine in the presence of paracetamol using a self-assembled monolayer of non-peripheral amine substituted copper (II) phthalocyanine” Electrochim. Acta, Vol.77, pp-137-142.

50. Hayden, M. R. and Tyagi, S. C., 2004, “Uric acid: A new look at an old risk marker for cardiovascular disease, metabolic syndrome, and type 2 diabetes mellitus: The urate redox shuttle”, Nutrition & Metabolism, Vol. 1(1), pp. 10-13.

51. Hillis O. Folkins, 2005, “Benzene” Ullmann’s Encyclopedia of Industrial Chemistry, Wiley-VCH, Weinheim.

52. T. A. Nieman, D. A. Skoog and F. J. Holler, 1988, Principles of instrumental analysis, Pacific Grove, California.

53. J. A. Plambeck, 1982, Electroanalytical Chemistry, Basic Principles and Application, Wiley Inter science Pub., USA.

54. P. Dyer, J. Desmeules, L. Collart, 1997, “Pharmacology of tramadol” Drugs, Vol.53, pp.18-24.

55. A. C. Moffat, 1986, “Clark's Isolation and Identification of Drugs,” The Pharmaceutical Press: London, 2nd ed.

56. Klotz, U.; Arzneimittelforschung, 2003, “Tramadol--the impact of its pharmacokinetic and pharmacodynamic properties on the clinical management of pain” Klotz U (1), Vol.53, pp. 681-687.

57. Richter, W.; Barth, H.; Flohe, L.; Giertz,H.; 1985, “Clinical investigation on the development of dependence during oral therapy with tramadol” Arzneimittelforschung Vol.35, pp. 1742-1744.

58. Babaei, A., Taheri, A. R., Afrasiabi, M., 2011, “A multi-walled carbon nanotube-modified glassy carbon electrode as a new sensor for the sensitive simultaneous determination of paracetamol and tramadol in pharmaceutical preparations and biological fluids” J. Braz. Chem. Soc. Vol. 22(8) pp. 1549-1558.

59. Epstein, D. H.; Preston, K. L.; Jasinski, D. R.; Biol. Psychol. 2006, “Abuse liability, behavioral pharmacology, and physical-dependence potential of opioids in humans and laboratory animals: lessons from tramadol” Biol Psychol. Vol. 73, pp.90-99.

60. Scott, L. J.; Perry, C. M.; 2000, “Tramadol: a review of its use in perioperative pain” Drugs Vol.60, pp. 139-176.

61. Tasis, D.; Tagmatarchis, N.; Bianco, A.; Prato, M.; 2006, “Chemistry of carbon nanotubes” Chem. Rev. Vol. 106, pp. 1105-1136.

62. Serp, P.; Corrias, M.; Kalck, P.; Appl. Catal., A, 2003,”Nanotechnology of catalysis” Appl. Catal. Vol.253, pp.337-358.

63. Sweetman, S. C.; Martindale: The Complete Drug Reference, 33rd ed.; Pharmaceutical Press: London, 2002.

64. Martin, F. L.; McLean, A. E.; 1998, “Pharmacology of tramadol” Drug Chem. Toxicol. Vol. 21, pp. 477-479.

65. Zhang, A. Q., Mitchell, S. C. and Smith, R. L., 1998, "Dimethylamine formation in the rat from various related amine precursors". Food Chem. Toxicol. Vol. 36 (11) pp. 923–927.

66. Neurath, G. B., 1977, "Primary and secondary amines in the human environment" Fd. Cosmet. Toxicol. Vol. 15 pp.275–282.

67. http://www.drhuang.com/science/chemistry/electrochemistry/polar.doc.htm.

68. D.A. Skoog, F.J. Holler and T.A. Nieman, 2007, “Principles of Instrumental Analysis”, Thomson Brooks/ Cole, 6th Ed., pp. 349-351.

69. Skoog, D. A., Holler, F. J. and Neiman, T. A., 2007, Principles of Instrumental Analysis, 6th edn, Thomson Brooks/Cole., pp. 169-173.

70. Zhao, H., Zhang, Y. Z. and Yuan, Z. B., 2002, “Mass transfer process in voltammetry” Electroanal., Vol. 14, pp. 1031-1035.

71. P.T. Kissinger and W.R. Heineman, 1996, “Laboratory Techniques in Electroanalytical Chemistry”, Marcel Dekker, Inc.

72. Wang G., Meng J., Liu H., Jiao S., Zhang W., Chen D. and Fang B., 2008, “Determination of uric acid in the presence of ascorbic acid with hexacyanoferrate lanthanum film modified electrode”, Electrochimica Acta, Vol. 53, pp. 2837-2843.

73. Yang G., Tan L., Shi Y., Wang S., Lu X., Bai H. and Yang Y., 2009, “Direct Determination of Uric Acid in Human Serum Samples Using Polypyrrole Nanoelectrode Ensembles”, Bull. Korean Chem. Soc., Vol. 30, pp. 454-458.

74. Sadikoglu M., Taskin G., Demirtas F. G., Selvi B., and Barut M., 2012, “Voltammetric Determination of UricAcid on Poly (p-Aminobenzene Sulfonic Acid)-Modified Glassy Carbon Electrode”, Int. J. Electrochem. Sci., Vol. 7, pp. 11550 – 11557.

75. Babaei, A., Reza, A. and Afrasiabi, M., 2011 “multi-walled carbon nanotube-modified glassy carbon electrode as a new sensor for the sensitive simultaneous determination of paracetamol and tramadol in pharmaceutical preparations and biological fluids” J.Braz.Chem.Soc.Vol.22.pp.8-12.

76. Garrett, j., Donard, J. and Babaei, A., 2010 “Selective Simultaneous Determination of Paracetamol and Uric Acid Using a Glassy Carbon Electrode Modified with Multiwalled Carbon Nanotube/Chitosan Composite” Electroanalysis, Vol. 22.pp. 1743.

77. S. Shahrokhian and H. R. Zare-Mehrjardi., 2009 “Electrochemical synthesis of polypyrrole in the presence of congo red; application to selective voltammetric determination of paracetamol in the presence of ascorbic acid,”Electroanalysis, Vol. 21. pp. 157–164.

78. Yuehua, Z., Lei.,W., Yujuan, X., Xifeng, X and Qingli, H., 2016 “Simultaneous Detection of Dopamine and Uric Acid Using a Poly(L-lysine)/Graphene Oxide Modified Electrode” Nanomaterials, Vol.6. pp. 178-186.

79. Nie, T., Limin, L., Ling, B. and Jingkun, X., 2013 “Simultaneous Determination of Folic Acid and Uric Acid under Coexistence of L-Ascorbic Acid Using a Modified Electrode Based on Poly (3, 4-Ethylenedioxythiophene) and Functionalized Single-Walled Carbon Nanotubes Composite” Electrochem. Sci., Vol. 8. pp. 7016 – 7029.

80. Chitravathi, S. and Munichandraiah, N., 2016 “ Voltammetric determination of paracetamol, Tramadol and Caffeine using Poly (Nile blue) modified glassy carbon electrode” Journal of Electroanalytical Chemistry, Vol. 764. pp. 93–103.

81. Ghorbani, F. Shahrokhiana, S. Mohammadid, A. and Dinarvand, R. 2010 “Simultaneous voltammetric determination of tramadol and acetaminophen using carbon nanoparticles mmodified glassy carbon electrode” Electrochimica Acta, Vol. 55. pp. 2752–2759.

82. Tao, N., Limin, L and Ling, B, 2011 “Determination of Folic Acid and Uric Acid under Coexistence of L-Ascorbic Acid Using a Modified Electrode Based on Poly (3, 4-Ethylenedioxythiophene) and Functionalized Single-Walled Carbon Nanotubes Composite” Electrochem. Sci., Vol. 8, pp. 7016 – 7029.

83. Hathoot, A. and Fahmy, M. 2013 “Electrooxidation and determination of tramadol in the presence of dopamine at poly 1, 8-diaminonaphthalene derivative modified platinum electrode” International Journal of Chemistry and Material Science, Vol. 1(3), pp. 45-54.

84. A. Ensafi, H. Karimi-Maleh and S. Mallakpour, 2011, “N-(3, 4-Dihydroxyphenethyl)-3, 5-dinitrobenzamide-Modified Multiwall Carbon Nanotubes Paste Electrode as a Novel Sensor for Simultaneous Determination of Penicillamine, Uric acid, and Tryptophan” Electroanalysis, Vol.6. pp. 1478–1487.

85. Shoup, D. and Szabo, A., 1982, “Chronoamperometric current at finite disk electrodes,” Journal of Electroanalytical Chemistry, Vol. 140, pp. 237-245.

86. Ikeuchi, H. and Kanakubo, M., 2000, Electrochemical sensor for amino acids and glucose based on glassy carbon electrodes modified with multi-walled carbon nanotubes and copper microparticles dispersed in polyethylenimineJournal of Electroanalytical Chemistry, Vol. 493, pp. 93-98.

87. Gavaghan, D.J. and Rollett, J.S., 1990, Quantitative analysis of steady-state currents of reversible redox species at a microdisk array electrode embedded in surface electrode," Journal of Electroanalytical Chemistry, Vol. 295, pp. 25-40.

88. Qian, W., Jin, B., Diao, G., Zhang, Z. and Shi, H., 1996, "Finite analytic method and its applications" Journal of Electroanalytical Chemistry, Vol. 414, pp. 17-33.

89. Skoog, D. A., Holler, F. J. and Neiman, T. A., 2007, Principles of Instrumental Analysis, 6th Ed., Thomson Brooks/Cole., pp. 169-173.

90. Bland, J.M. and Altman, D.G., 1996, "Statistics notes: measurement error", BMJ, Vol. 312, pp. 1654-1657.

91. M. Whitfield, and D. Jagner,, 1981, Marine electrochemistry: A practical introduction, John Wiley &Sons Inc.

92. Jr. D.K. Gosser, 1993, "Cyclic Voltammetry (Simulation and analysis of reaction mechanisms)", Wiley-VCH, Inc.

93. C.M.A. Brett and A.M.O. Brett, 1998, "Electroanalysis", Oxford University Press.

94. S. P. Kounaves, 1997, "Voltammetric Techniques" in Handbook of Instrumental Techniques for Analytical Chemistry, Upper saddle river, NJ.

95. Armada, P. G., Losada, J. and Perez, S. V., 1996, "Cation analysis scheme by differential pulse polarography", Electroanalysis, Vol. 73(6), pp. 544-546.

96. http://www.mayoclinic.org/diseases-conditions/gout/basics/definition/con-20019400.

97. http://www.mayoclinic.org/symptoms/high-uric-acid-level/basics/definition/sym-20050607.